

**ANALYSIS AND COMPUTER SIMULATION  
OF  
OPTIMAL ACTIVE VIBRATION CONTROL**

A Thesis

Submitted to the College of Graduate Studies and Research

in Partial Fulfillment of the Requirements

for the Degree of

Master of Science

in the

Department of Mechanical Engineering

University of Saskatchewan

Saskatoon, Saskatchewan

Canada

By

Nitin Ratnakar Dhotre

## **PERMISSION TO USE**

In presenting this thesis in partial fulfillment of the requirements for a Master's degree from the University of Saskatchewan, the author has agreed that the libraries of this University may make it freely available for inspection. The author further agrees that permission for copying of this thesis in any manner, in whole or in part, for scholarly purposes may be granted by the professor or professors who supervised my thesis work or, in their absence, by the Head of Department or the Dean of the College in which my thesis work was done. It is understood that any copying or publication or use of this thesis or parts thereof for financial gain shall not be allowed without the author's written permission. It is also understood that due recognition shall be given to the author and to the University of Saskatchewan in any scholarly use which may be made of any material in my thesis.

Requests for permission to copy or to make other use of material in this thesis in whole or part should be addressed to:

Head of the Department of Mechanical Engineering  
University of Saskatchewan  
Saskatoon, Saskatchewan, Canada, S7N 5A9

## ABSTRACT

Methodologies for the analysis and computer simulations of active optimal vibration control of complex elastic structures are considered. The structures, generally represented by a large number of degrees of freedom (DOF), are to be controlled by a comparatively small number of actuators.

Various techniques presently available to solve the optimal control problems are briefly discussed. A Parametric optimization technique that is versatile enough to solve almost any type of optimization problems is found to give poor accuracy and is time consuming. More promising is the optimality equations approach, which is based on Pontryagin's principle. Several new numerical procedures are developed using this approach. Most of the problems in this thesis are analysed in the modal space. Even complex structures can be approximated accurately in the modal space by using only few modes. Different techniques have been first applied to the cases where the number of modes to control was the same as the number of actuators (*determined* optimal control problems), then to cases in which the number of modes to control is larger than the number of actuators (*overdetermined* optimal control problems).

The determined optimal control problems can be solved by applying the Independent Modal Space Control (IMSC) approach. Such an approach is implemented in the Beam Analogy (BA) method that solves the problem numerically by applying the Finite Element Method (FEM). The BA, which uses the ANSYS program, is numerically very efficient. The effects of particular optimization parameters involved in BA are discussed in detail. Unsuccessful attempts have been made to modify this method in order to make it applicable for solving overdetermined or underactuated problems.

Instead, a new methodology is proposed that uses modified optimality equations. The modifications are due to the extra constraints present in the overdetermined problems. These constraints are handled by time dependent Lagrange multipliers. The modified optimality equations are solved by using symbolic differential operators. The corresponding procedure uses the MAPLE programming, which solves overdetermined problems effectively despite of the high order of differential equations involved.

The new methodology is also applied to the closed loop control problems, in which constant optimal gains are determined without using Riccati's equations.

## **ACKNOWLEDGEMENTS**

I owe my sincere appreciation and deep sense of gratitude to my supervisor Dr. Walerian Szyszkowski, PhD, P.Eng., for his constant encouragement, meticulous supervision, and constructive criticism all of which was instrumental in the successful completion of this thesis.

Thanks are due to the members of advisory committee R. Fotouhi and R.T. Burton. My profound thanks go to all the other professors of the Mechanical Engineering Department, at the University of Saskatchewan for all the help rendered in the course of my study.

The author is thankful to the Engineering Computer Center staff for their assistance in computer software and system operations.

Special thanks are extended to the author's parents, Dr. R. S. Dhotre and Ms. G. R. Dhotre, wife, Ms. Padma N. Dhotre and all other family members for their constant encouragement and support in making this work a reality.

Financial support provided by the Natural Sciences and Engineering Research Council (NSERC) of Canada in the form of operating grant of Dr. W. Szyszkowski is gratefully acknowledged.

## **DEDICATION**

This thesis is dedicated to the author's parents

Dr. Ratnakar S. Dhotre

&

Ms. Godavari R. Dhotre

## TABLE OF CONTENTS

<b>PERMISSION TO USE</b> .....	<b>i</b>
<b>ABSTRACT</b> .....	<b>ii</b>
<b>ACKNOWLEDGEMENTS</b> .....	<b>iv</b>
<b>DEDICATION</b> .....	<b>v</b>
<b>TABLE OF CONTENTS</b> .....	<b>vi</b>
<b>LIST OF FIGURES</b> .....	<b>ix</b>
<b>LIST OF TABLES</b> .....	<b>xi</b>
<b>1. INTRODUCTION</b> .....	<b>1</b>
1.1 Outline of Thesis .....	4
<b>2. PROBLEM FORMULATION</b> .....	<b>5</b>
2.1 Introduction .....	5
2.2 Equations of Motion.....	8
2.3 Modal Analysis .....	9
2.4 Optimal control and optimality equations.....	12
<b>3. SOME SOLUTION TECHNIQUES</b> .....	<b>16</b>
3.1 Introduction .....	16
3.2 Overdetermined gantry crane problem by optimality equations.....	16
3.3 Some Limitations .....	21
3.3 Parametric optimization technique.....	22
3.3.1 A piecewise linearly varying force approximation .....	25
<b>4. BEAM ANALOGY</b> .....	<b>31</b>
4.1 Introduction .....	31
4.2 Example 1: Gantry crane controlled by two actuators .....	36

4.3 Example 2: Frame structure .....	39
4.4 Effect of $a_2$ on the performance of the system.....	42
4.5 Effect of parameter $b_1$ on the performance of a system .....	43
4.6 Effect of parameter $c_2$ on the actuator forces .....	45
4.7 Example 3: Suspension system .....	49
<b>5. APPLICATION OF LAGRANGE MULTIPLIERS – A NEW METHODOLOGY .....</b>	<b>55</b>
5.1 Introduction .....	55
5.2 Gantry crane problem by new methodology .....	55
5.3 Some generalization – the use of differential operators.....	59
5.3.1 Application to the gantry crane problem.....	62
5.3.2 Application to the suspension system problem.....	66
5.4 A general overdetermined problem.....	70
5.4.1 Example 1: Suspension system .....	72
5.4.2 Example 2: Triple pendulum.....	73
<b>6. CLOSED LOOP CONTROL AND OPTIMAL GAINS .....</b>	<b>83</b>
6.1 Introduction .....	83
6.2 Calculation of gains by the Lagrange Multiplier method .....	84
6.2.1 Example 1: Suspension system .....	85
6.2.2 Example 2: Pendulum .....	89
6.3 Estimation of errors in calculating gains.....	91
6.3.1 Error due to the selection of test points.....	91
6.3.2 Error due to the assumption of a finite time.....	92
6.3.3 Condition Number.....	94
<b>7. CONCLUSIONS AND FUTURE WORK .....</b>	<b>97</b>
<b>REFERENCES .....</b>	<b>100</b>



**APPENDIX A: MAPLE PROGRAM ..... 102**

## LIST OF TABLES

<b>Table 3.1:</b> Performance index for different number of forces.....	28
<b>Table 4.1:</b> $ F_{\max} $ values for $c_2$ .....	48
<b>Table 6.1:</b> Values of force and $\eta$ 's for different times .....	87
<b>Table 6.2:</b> $T_1$ and $\eta$ 's for time instances indicated in Fig 6.4 .....	90
<b>Table 6.3:</b> Condition numbers and gains for various time sets .....	95

## LIST OF FIGURES

<b>Figure 1.1:</b> Smart Bridge Structure .....	2
<b>Figure 1.2:</b> (a) Gemini Telescope; (b) Satellite arms.....	2
<b>Figure 2.1:</b> Two bay frame structure.....	5
<b>Figure 2.2:</b> Gantry crane .....	7
<b>Figure 3.1:</b> (a) Plot of $x$ (m) versus time(s); (b) Plot of $\theta$ (rad) versus time(s) .....	19
<b>Figure 3.2:</b> (a) Plot of $\eta_1$ versus time; (b) Plot of $\eta_2$ versus time.....	20
<b>Figure 3.3:</b> Plot of $F_{m1}$ (N) versus time (s).....	20
<b>Figure 3.4:</b> Suspension system.....	21
<b>Figure 3.5:</b> (a) $F_{m1}$ is constant in each division; (b) $F_{m1}$ changes linearly with time in each division .....	23
<b>Figure 3.6:</b> Flowchart for parametric optimization technique .....	24
<b>Figure 3.7:</b> Linearly varying force .....	25
<b>Figure 3.8:</b> Plot of $F_{m1}$ versus time.....	27
<b>Figure 3.9:</b> Plot of performance index $J$ versus number of division $n_d$ .....	28
<b>Figure 3.10:</b> Plot of $x$ versus time for different cases .....	29
<b>Figure 3.11:</b> Plot of $\theta$ (rad) versus time(s) for different cases.....	29
<b>Figure 4.1:</b> Beam on elastic foundation .....	33
<b>Figure 4.2:</b> Flow chart for beam analogy.....	36
<b>Figure 4.3:</b> (a) Plot of DOFs for gantry crane; (b) Actuator forces plot for gantry crane	38
<b>Figure 4.4:</b> BA for Frame structure (disturbance exaggerated) with two actuators .....	39
<b>Figure 4.5:</b> Force and displacement plots .....	41
<b>Figure 4.6:</b> Force and displacement plot for different values of $a_2$ .....	43
<b>Figure 4.7:</b> Force and displacement plot for different values of $b_1$ .....	45
<b>Figure 4.8:</b> Force and displacement plot for different values of $c_2$ .....	47
<b>Figure 4.9:</b> Plot of $ F_{\max} $ versus $1/c_2$ , when $a_2=1$ , $b_1=1$ .....	48
<b>Figure 4.10:</b> Suspension System .....	49
<b>Figure 4.11:</b> The results for suspension system with dampers ( $\xi_1 = \xi_2 = 0.15$ ).....	53
<b>Figure 4.12:</b> The results for suspension system without dampers .....	54

<b>Figure 5.1:</b> Flowchart of the <i>MAPLE</i> program .....	65
<b>Figure 5.2:</b> Suspension system .....	66
<b>Figure 5.3:</b> Modal variables and DOFs versus time(s) plots.....	68
<b>Figure 5.4:</b> Modal controls $u_1$ , $u_2$ and actuator's force $F_a$ versus time (s) plots .....	69
<b>Figure 5.5:</b> Triple Pendulum .....	73
<b>Figure 5.6:</b> Mode shapes .....	75
<b>Figure 5.7:</b> Modal variables .....	78
<b>Figure 5.8:</b> DOFs.....	78
<b>Figure 5.9:</b> Optimal torque.....	79
<b>Figure 5.10:</b> Pendulum configuration at different times .....	80
<b>Figure 5.11:</b> (a) $t_f = 2s$ , (b) $t_f = 4s$ , (c) $t_f = 20s$ .....	80
<b>Figure 5.12:</b> Triple pendulum controlled by two actuators.....	81
<b>Figure 6.1:</b> Actuator force plot indicating various time instances selected .....	86
<b>Figure 6.2:</b> Modal trajectory .....	88
<b>Figure 6.3:</b> Selection of points on hyperplane $S$ .....	88
<b>Figure 6.4:</b> Actuator torque plot indicating various time instances selected .....	89
<b>Figure 6.5:</b> Modal trajectory .....	91
<b>Figure 6.6:</b> Force and torque plot.....	92
<b>Figure 6.7:</b> Magnified torque plots for pendulum.....	93
<b>Figure 6.8:</b> Error versus condition number plot.....	96
<b>Figure 7.1:</b> Conceptual design for solving overdetermined problems by BA.....	98

## List of Abbreviations

Listed below are the symbols and abbreviations used most frequently in the text. Occasionally, the same symbol may have a different meaning defined in the text

$A, A_1, A_2, \hat{A}$	Matrices	$KE$	Kinetic energy
$\hat{A}_k, \tilde{A}_k$	Constants	$L$	Length of gantry crane
$a$	Distance	$L_1, L_2, L_3$	Lengths of pendulum
$a_1..a_3, b_1..b_3, c_1..c_3$	Weighting parameters	$L_a$	Variable in Lagrange equation
$B, b$	Matrices	$L_b$	Length of a beam
$\hat{B}_k, \tilde{B}_k$	Constants	$M$	Mass matrix
BC	Boundary condition	$M_o, M_f, \hat{M}$	Moments on elastic beam
$C$	Damping matrix	$m_1, m_2, m_3$	Masses
$\hat{C}$	Matrix	$n$	Number of DOFs
$C_1..C_{12}$	Integration constants	$n_a$	Number of actuator forces
$\hat{c}_1..c_3$	Damping coefficients	$n_m$	Number of modes
$D_1$	Matrix	$n_d$	Number of divisions
$\hat{D}, \tilde{D}$	Differential operators	ODE	Ordinary Differential Equation
DOF	Degree of freedom	$P$	Vector of costates
$d_1, d_2$	Constants	$P_1, P_2, P_3, P_4$	Costates
$E_i, \tilde{E}$	Differential operators	$P_a$	Axial forces on beam
$EI$	Bending stiffness	$P_e$	Penalty
$F, F_a, F_1, F_2, \hat{F}_2$	Forces	$p_1, p_2, p_3, p_4$	Constants
$F_{m1}, F_{m2}$	Forces	$p_d, p_v$	Costates related to displacement and velocity
$FEM$	Finite element method	$Q_d, Q_v, \hat{Q}_d, \hat{Q}_v$	Weighting matrices
FBC	Final boundary condition	$q_1, q_2, q_3, q_4$	Variables
$G$	Gain matrix	$\hat{q}$	Load
$g$	Gravity ( $9.81 \text{ m/s}^2$ )	$R, \hat{R}$	Weighting matrices
$g_1, g_2$	Constants	$r_i$	Roots of equation
$\hat{g}_{id}, \hat{g}_{iv}$	Modal gains for displacement and velocity	$\hat{S}$	Slope
$H, \hat{H}$	Hamiltonian	$S, \bar{S}$	Hyperplane
$I$	Identity matrix	$T_0, T_f, \hat{T}$	Shear forces
IBC	Initial boundary condition	$T_1$	Torque
$J, \hat{J}$	Performance index	$TE$	Target Error
$j$	Constant		
$K$	Stiffness matrix		
$k_f$	Stiffness of elastic foundation		

$t$	Time
$\Delta t$	Time interval
$u_1, u_2, u_3$	Modal forces
$V$	Potential energy
$v$	Lagrange multipliers
$W$	Work done
$X$	Response matrix
$x, x_m, \tilde{x}, \bar{x}$	Displacement
$Y$	Matrix of variables
$y$	Displacement
$z$	Vector of states
$\alpha, \beta, \alpha_k, \beta_k$	Constants
$\phi$	Matrix of modal shapes
$\phi_\omega$	Matrix
$\eta_i$	Modal variables
$\zeta_i$	Modal damping coefficient
$\xi_i$	Damping coefficients
$\theta_i, \bar{\theta}$	Angle
$\omega_i$	Natural frequencies
$\varepsilon_i$	Errors
$\Omega$	$\omega^2$
$\Delta$	Damping matrix ( $2\omega_i\zeta_i$ )
$\Gamma$	Optimization parameter for time

# 1. INTRODUCTION

Most physical processes which take place in technology can be realized by various means depending on the will of man. Then the question arises of finding the best or, as is said, the *optimal* way of realizing these processes. Mathematical optimization helps answering such questions.

Optimal control, a branch of mathematical optimization, deals with time and dynamic processes. It has variety of applications in automation, robotics, and other areas. In this thesis it is applied to active control of vibrations in continuous elastic structures. Typically such structures may be quite complex and, if modelled by Finite Element Method (FEM), may require very large number of degrees of freedom (DOF).

Undesired vibrations may be attenuated by applying passive or/and active damping devices. In passive approach the system's performance depends on built-in dampers which use natural damping characteristics of the material. In active approach the performance of the system depends on actuators which can be programmed or set up according to particular needs. For example, to reduce vibrations in a long span bridge (see Fig. 1.1), one may use passive friction based dampers and/or actuators that would generate forces attenuating the vibrations that might be caused by moving load or wind.

An active control has many advantages over the passive control, mainly better and more precise vibration controls and usually lighter designs. The latter is due to the fact that passive dampers, especially in tall buildings [1], might be quite massive which in turn necessitates stronger and heavier structures.

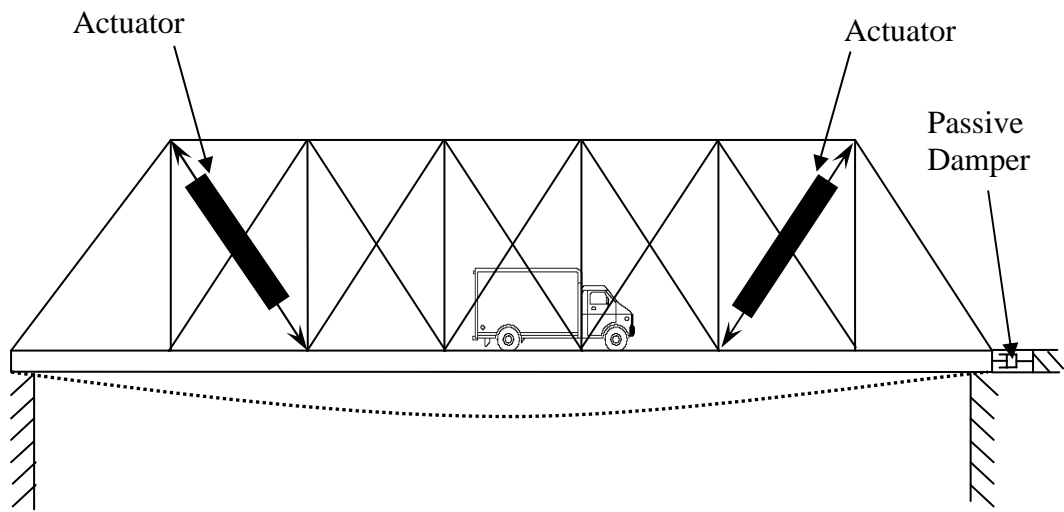
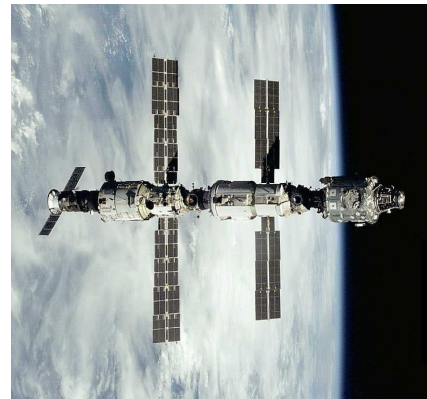


**Figure 1.1:** Bridge Structure

Active vibration control also plays a major role in controlling satellites and telescopes. A precise control of the movement is essential for a big telescope shown in Fig. 1.2-*a* [2]. Even very small vibrations are undesirable and must be effectively eliminated, which can be done only by active vibration control methods [3].



(*a*)



(*b*)

**Figure 1.2:** (a) Gemini Telescope; (b) Satellite arms

The solar cell panels or extended arms of a satellite shown in Fig. 1.2-*b* [4] need to rotate in a controlled manner to follow the Sun without exciting excessive vibrations. The disturbances imposed by the intermittent action of thrusters can be effectively attenuated by the quickly reacting actuators [5].



The main purpose of computer simulations of actively controlled structures is to predict the desired or expected optimal action of actuators, which then could be used either in designing a new damping system, or to improve an existing one. Such simulations could be based on the theory of elastic vibrations and the theory of optimal control. Separate software and techniques are presently available to analyse/simulate either the vibrations or the control problems.

The analysis of *vibration* can be efficiently performed by the FEM even for very complicated systems with a large number of DOFs. On the other hand, the *optimal control* techniques can handle systems with a limited number of DOFs (one preferable). That is why many real mechanical systems are simplified to a single or few DOFs models in control considerations.

On the other hand, most flexible bodies move in such a way that their motion is a combination of only several lower natural frequency modes. Also, motions of many structures that may need a large number of DOFs to model accurately in FEM can be approximated with fair precision by only one fundamental frequency mode. It indicates the practical importance and convenience of using modes instead of DOFs, therefore almost all the analysis presented in the thesis is done in the modal space.

There are two types of approaches to handle optimal active vibration control for multi modal systems. The *independent modal space control* (IMSC) approach controls the number of modes equal to the number of actuators [6]. Such systems will be referred to as the determined ones. If the number of modes to be controlled is greater than the number of actuators, such systems and the corresponding optimization problems will be referred to as the overdetermined optimal control problems (such problems are also referred to as the underactuated control problems).

Numerous techniques have been developed to solve IMSC problems, but very few techniques are available to solve overdetermined problems effectively. This research work is an attempt to find a better solution technique for optimal active vibration control of overdetermined problems.

## **1.1 Outline of Thesis**

An optimal control problem for the vibration attenuation is formulated in Chapter II. The dynamic systems are represented by the coupled equations of motion in terms of the DOFs, and then in terms of the modal variables in order to uncouple these equations. The objective of control, or the performance index, is also formulated in terms of DOFs and then in terms of modal variables. The performance is optimized by considering the constraints in the form of the equation of motion, the initial and final (target) boundary conditions.

Some general solution techniques that are available for optimal control problems are discussed in Chapter III. An overdetermined gantry crane problem is solved by various techniques to illustrate their pros and cons. The optimality equations approach and an iterative, gradient based parametric optimization technique are discussed in detail.

Beam Analogy (BA), a recently developed technique to solve complicated IMSC problems is studied in Chapter IV. The effects of various optimization parameters available in BA are discussed. This technique, which uses the FEM programme ANSYS, is found to be numerically very effective but is presently not applicable to the overdetermined problems.

A new technique to solve specifically overdetermined problems is developed in Chapter V. The Lagrange multipliers are used to handle the extra constraints generated in overdetermined problems. Gantry crane problem is solved initially and then the methodology is generalized for more complicated problems. The technique is programmed in MAPLE software to solve complex problems quickly.

Closed loop control is addressed in chapter VI by determining optimal gains for the time invariant problems. Obtaining gains accurately for the overdetermined problems becomes more difficult with more modes to control. An approach that uses the condition number to help finding acceptable solutions is presented.

Chapter VII contain conclusions and suggestions for the future research.

## 2. PROBLEM FORMULATION

### 2.1 Introduction

Extensive research has been done recently on active vibration control which aims on reducing the vibration level of a mechanical structure. Most of the techniques have been developed to control a given number of modes of vibrations by an equal number of actuators. This approach is referred to as an Independent Modal Space Control.

The structure may have a large number of DOFs and, hence, a large number of modes of vibrations. In IMSC approach, for example, actuators  $F1$  and  $F2$  acting on the structure shown in Fig. 2.1 can control only two modes of vibrations, leaving other modes uncontrolled. On the other hand, only lower modes may practically require some control [1]. This is because higher modes are usually damped out naturally due to the presence of internal and external friction in the system. Such a strategy should work well if the natural frequencies of the system are well separated and the frequencies of the uncontrolled modes are much higher than the controlled ones.

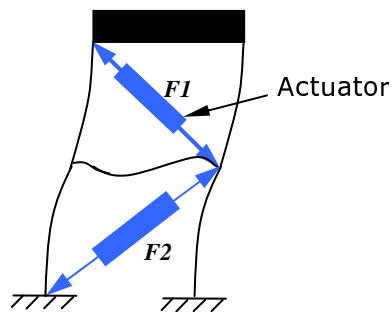


**Figure 2.1:** Two bay frame structure

In cases, where the natural frequencies are close to each other, it may be important to control a larger number of modes, for example, more than two modes in the

frame. Also there are cases (such as gantry crane in Fig. 2.2) where it would be advantageous for a certain number of actuators to control a number of modes that is greater than the number of actuators. Such problems are referred to as overdetermined problems.

The IMSC method is considered not applicable to the overdetermined problems. Instead, other methods, such as parametric optimization, optimality equations, etc. are applied. However, the application of such techniques is rather challenging from the computational point of view.

The main focus of this research work is to obtain better technique for the overdetermined problems. Similar to IMSC, such problems will be solved in modal space.

Many actively controlled mechanical systems can be represented by the equations of motion (Eq. 1.1) in the form

$$M\ddot{X} + C\dot{X} + KX = BF_a(t) = F \quad (2.1)$$

where  $M$ ,  $C$ ,  $K$  are constants matrices,  $C$  is Rayleighs damping matrix,  $F_a(t)$  is an actuation force vector,  $X$  is a vector representing  $n$  DOFs of the system,  $F$  is a corresponding force vector, matrix  $B$  assigns the actuator forces to DOFs.

Let the number of independent actuation forces be  $n_a$ . These forces are to control  $n$  number of DOFs, where  $n \gg n_a$ . Typically, not all matrices  $M$ ,  $C$  and  $K$  of Eq. (2.1) are diagonal, therefore the DOFs are coupled. The problem can be uncoupled by using modal space i.e. converting  $X$  variables into the modal variables  $\eta$ . The details of modal analysis are explained later. The modal variables and forces are related to the  $X$  variables and actuation forces as

$$X = \phi\eta, u = \phi^T BF_a \quad (2.2)$$

where  $\phi$  is a matrix of modal shapes.

Using these relations in Eq. (2.1), yields a new system of  $n$  uncoupled equations as

$$\ddot{\eta}_i + 2\zeta_i\omega_i\dot{\eta}_i + \omega_i^2\eta_i = u_i \quad (2.3)$$

where  $i=1..n$ ,  $\zeta_i$  is a modal damping coefficient and  $u_i$  is a modal force corresponding to  $i^{th}$  mode.

The above two formulations, Eq. (2.1) and (2.3), are mathematically equivalent as long as the number of modes in Eq. (2.3) is the same as the number of DOFs in Eq. (2.1). However, in Eq. (2.3) the higher the mode the less important it becomes in practise because of natural damping. Therefore, in order to obtain accurate solutions the number of modes,  $n_m$ , that need to be considered can be much smaller than the number of DOFs i.e.  $n_m \ll n$ . This property of the solution in modal space is used in the IMSC in which  $n_m$  is set to be equal to  $n_a \ll n$ .

If  $n_m > n_a$  the problem becomes overdetermined. Such problem is explained in detail on the gantry crane example (Fig. 2.2), which was analysed in [7] using different solution technique.

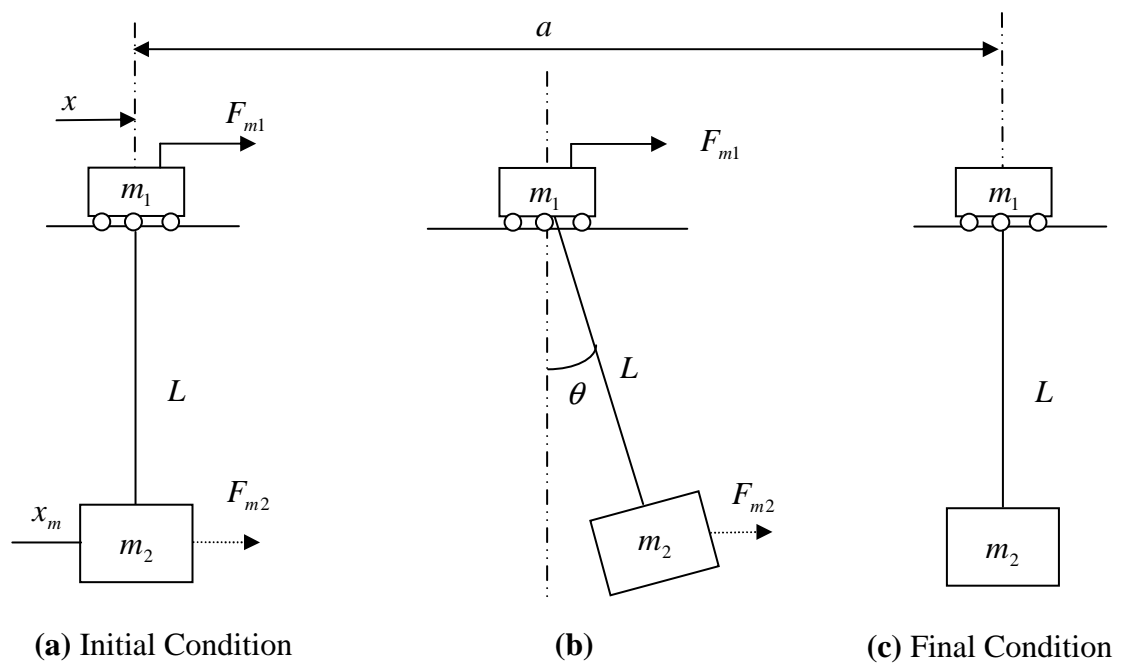


**Figure 2.2:** Gantry crane

The gantry crane example is selected as a test problem because of its simplicity. Its two DOFs, corresponding to the motion of mass  $m_1$  and motion of mass  $m_2$ , can be controlled by two actuators, one at mass  $m_1$  and other at mass  $m_2$ . This is a determined problem and can be converted into two modes problem to solve by IMSC approach. The

system can also be controlled by only one actuator, acting on  $m_1$ , for example. Such problem obviously becomes overdetermined with  $n_a = 1$ ,  $n_m = 2$  and can not be solved by IMSC.

The following is a detailed formulation of the overdetermined gantry crane problem. The control force  $F_{m1}$  is applied to move the system. It is required that masses  $m_1$  and  $m_2$  should start from the rest, travel a given distance 'a' and should stop without any oscillations when arriving to its final destination. The optimum value of force  $F_{m1}(t)$  and the corresponding displacement and velocity trajectories are to be determined.

The equations of motion for this system using the DOFs and then the modal space are discussed next.

## 2.2 Equations of Motion

Two forces  $F_{m1}$  and  $F_{m2}$  are considered for generality. The control problem will be made overdetermined by setting  $F_{m2} = 0$ . The damping effect is neglected. Lagrange's equations of motion are obtained as follows.

Let the displacement of mass  $m_1$  is  $x$ , and that of mass  $m_2$  is  $x_m$ .

Assuming  $\theta \ll 1$ , the displacement of mass  $m_2$  can be written as

$$x_m = x + L\theta$$

The velocity of mass  $m_1$  is  $\dot{x}$  and that of mass  $m_2$  is  $\dot{x}_m = \dot{x} + L\dot{\theta}$

Thus  $x$  and  $\theta$  can be used as DOFs of this system.

Kinetic Energy of the system is

$$KE = \frac{1}{2} m_1 (\dot{x})^2 + \frac{1}{2} m_2 (\dot{x} + L\dot{\theta})^2 \quad (2.4)$$

Potential Energy of the system is

$$V = m_2 g L \frac{\theta^2}{2} \quad (2.5)$$

Virtual work by forces  $F_{m1}$  and  $F_{m2}$  is

$$\delta W = F_{m1} \delta x + F_{m2} (\delta x + L\delta\theta) = (F_{m1} + F_{m2}) \delta x + (LF_{m2}) \delta\theta \quad (2.6)$$

Lagrange's Equations for the system are

$$\frac{d}{dt} \left( \frac{\partial L_a}{\partial \dot{x}} \right) - \frac{\partial L_a}{\partial x} = F_{m1} + F_{m2} \quad (2.7)$$

$$\frac{d}{dt} \left( \frac{\partial L_a}{\partial \dot{\theta}} \right) - \frac{\partial L_a}{\partial \theta} = LF_{m2} \quad (2.8)$$

where  $L_a = KE - V$ .

The right hand side of the above equations are the forces corresponding to the virtual displacements  $\delta x_1$  and  $\delta \theta$  respectively in Eq. (2.6).

Substituting Eq. (2.4) and (2.5) and differentiating one obtains

$$\begin{aligned} m_1 \ddot{x} + m_2 (\ddot{x} + L\ddot{\theta}) &= F_{m1} + F_{m2} \\ m_2 (\ddot{x} + L\ddot{\theta}) + m_2 g \theta &= F_{m2} \end{aligned}$$

These equations of motion can be expressed in the matrix form as

$$\begin{bmatrix} (m_1 + m_2) & m_2 \\ m_2 & m_2 \end{bmatrix} \begin{bmatrix} \ddot{x} \\ L\ddot{\theta} \end{bmatrix} + \begin{bmatrix} 0 & 0 \\ 0 & m_2 g / L \end{bmatrix} \begin{bmatrix} x \\ L\theta \end{bmatrix} = \begin{bmatrix} 1 & 1 \\ 0 & 1 \end{bmatrix} \begin{bmatrix} F_{m1} \\ F_{m2} \end{bmatrix} \quad (2.9)$$

Comparing with Eq (2.1), the matrices in Eq. (2.9) are

$$\begin{aligned} M &= \begin{bmatrix} (m_1 + m_2) & m_2 \\ m_2 & m_2 \end{bmatrix}, & C &= 0, & K &= \begin{bmatrix} 0 & 0 \\ 0 & m_2 g / L \end{bmatrix}, \\ B &= \begin{bmatrix} 1 & 1 \\ 0 & 1 \end{bmatrix}, & X &= \begin{bmatrix} x \\ L\theta \end{bmatrix}, & F_a &= \begin{bmatrix} F_{m1} \\ F_{m2} \end{bmatrix} \end{aligned} \quad (2.10)$$

The initial and final boundary conditions for these equations are

$$X^T(0) = [0 \ 0], \quad X^T(t_f) = [a \ 0] \quad \text{and} \quad \dot{X}^T(0) = \dot{X}^T(t_f) = 0 \quad (2.11)$$

The final boundary condition (for  $t = t_f$ ) will also be referred to as target condition. Eq. (2.9) are coupled equations in terms of  $x$  and  $\theta$ . The modal analysis is performed to uncouple these equations.

### 2.3 Modal Analysis

Modal analysis solves the eigenvalue problem to determine the frequencies  $\omega$  at which vibration naturally occurs, and the corresponding modal shapes  $\phi_\omega$ , the vibrating

system assumes [8]. Natural frequencies or the eigen values of the system with no damping can be obtained by substituting

$$x = \bar{x} \sin(\omega t), \theta = \bar{\theta} \sin(\omega t)$$

$$\text{or } X = \phi_{\omega} \sin(\omega t) \quad (2.12)$$

where  $\phi_{\omega}^T = [\bar{x} \quad L\bar{\theta}]$  and  $F = 0$  into equations of motion (2.9) to obtain

$$\begin{bmatrix} -\omega^2 & g - L\omega^2 \\ -\omega^2(m_1 + m_2) & -\omega^2 m_2 L \end{bmatrix} \begin{bmatrix} \bar{x} \\ \bar{\theta} \end{bmatrix} = 0 \quad (2.13)$$

Solving Eq. (2.13) for eigenvalues, the natural frequencies of the system are

$$\omega_1^2 = 0 \quad (2.14)$$

$$\omega_2^2 = (1 + m_2 / m_1) g / L \quad (2.15)$$

The first value indicates a rigid body mode of motion. Substituting  $\omega_1$  in Eq. (2.13) and requiring that  $\phi_1^T M \phi_1 = 1$ , the first normalized mode is obtained as

$$\phi_1 = \begin{bmatrix} 1 / \sqrt{m_1 + m_2} \\ 0 \end{bmatrix} \quad (2.16)$$

Similarly, for the second mode, substituting  $\omega_2$  into Eq. (2.13) and normalizing one obtains

$$\phi_2 = \begin{bmatrix} \sqrt{m_2 / m_1 (m_1 + m_2)} \\ -\sqrt{(m_1 + m_2) / m_1 m_2} \end{bmatrix} \quad (2.17)$$

The modal matrix  $\phi$  is defined as  $\phi = [\phi_1 \quad \phi_2]$  or

$$\phi = \begin{bmatrix} 1 / (\sqrt{m_1 + m_2}) & \sqrt{m_2 / m_1 (m_1 + m_2)} \\ 0 & -\sqrt{(m_1 + m_2) / m_1 m_2} \end{bmatrix} \quad (2.18)$$

Also, it can be verified that

$$\phi^T M \phi = I \quad \text{and} \quad \phi^T K \phi = \begin{bmatrix} \omega_1^2 & 0 \\ 0 & \omega_2^2 \end{bmatrix} = \Omega$$

where  $\Omega$  is a diagonal matrix of eigenvalues (square of frequencies).

Let  $\eta^T = [\eta_1 \quad \eta_2]$  be the modal variables such that

$$X = \phi \eta \quad (2.19)$$



Substituting Eq. (2.19) in (2.9) and pre-multiplying by  $\phi^T$  one obtains

$$I\ddot{\eta} + \Omega\eta = u \quad (2.20)$$

Modal forces are defined as

$$u = \begin{bmatrix} u_1 \\ u_2 \end{bmatrix} = \phi^T B F_a = \frac{1}{\sqrt{m_1 + m_2}} \begin{bmatrix} 1 & 1 \\ \sqrt{m_2/m_1} & -\sqrt{m_1/m_2} \end{bmatrix} \begin{bmatrix} F_{m1} \\ F_{m2} \end{bmatrix} \quad (2.21)$$

Note that, the matrix  $\phi^T B$  in the above equation is a square matrix if the number of modes equals number of actuator forces. In such cases it is possible to take inverse of this matrix, which allows conversion of modal controls  $u$  into the actuator forces  $F_a$ .

For overdetermined problems,  $\phi^T B$  is not square and such operation is not possible.

Eq. (2.20) for the gantry crane takes the form

$$\ddot{\eta}_1 + 0\eta_1 = u_1 \quad (2.22a)$$

$$\ddot{\eta}_2 + \omega_2^2 \eta_2 = u_2 \quad (2.22b)$$

The initial and final boundary conditions for these equations are

$$\eta^T(0) = [0 \ 0], \quad \eta^T(t_f) = [\eta_{t_f} \ 0] \quad \text{and} \quad \dot{\eta}^T(0) = \dot{\eta}^T(t_f) = 0$$

These modal BCs are obtained from the BCs for the DOFs, by making use of Eq. (2.19).

The Eq. (2.22) are uncoupled equations of motion and can be solved independently if the modal controls  $u_1$  and  $u_2$  are known.

In order to control the two modes of this system by one force, let  $F_{m2} = 0$ . Then from Eq. (2.21) one obtains

$$u_1 = F_{m1} / \sqrt{(m_1 + m_2)} \quad (2.23)$$

$$u_2 = F_{m1} \sqrt{m_2/m_1} / \sqrt{(m_1 + m_2)} \quad (2.24)$$

Both the modal controls depend on one force  $F_{m1}$ . It can be noted from Eq. (2.23) and (2.24) that the modal controls are not independent and satisfy the equation

$$u_1 - u_2 \sqrt{m_1/m_2} = 0 \quad (2.25)$$

Thus for this system, an extra constraint (2.25) that is imposed on modal control has to be considered. That is why this problem is referred as an overdetermined problem. To analyse it in the modal space one has to solve Eq. (2.22) that is additionally constrained by the condition (2.25) and BCs.

In control theory, one would be interested in finding a force  $F_{m1}$  that would satisfy the equation of motion and the target conditions. An infinite number of solutions may be possible.

In *optimal* control, the best force can be obtained by assuming a certain objective referred to as the *performance index*. Various optimization techniques to minimize the objective and to solve optimal control problems are briefly presented in coming sections.

## 2.4 Optimal control and optimality equations

This methodology is based on Pontryagin's maximum principle [9] and is capable of providing exact solutions. First the theory of optimal control is briefly described followed by the analysis of gantry crane example in the next chapter.

The optimal control problem for  $n$  DOF system is formulated as below. The cost function or the performance index is assumed as

$$J = \frac{1}{2} \int_0^{t_f} [X^T Q_d X + \dot{X}^T Q_v \dot{X} + F^T R F + \Gamma] dt \rightarrow \text{minimum} \quad (2.26)$$

where  $Q_d$ ,  $Q_v$  and  $R$  are positive definite weighting matrices.

In particular, the term  $\frac{1}{2} X^T Q_d X$  represents elastic energy of the system if  $Q_d = K$ .

The term  $\frac{1}{2} \dot{X}^T Q_v \dot{X}$  represents kinetic energy of the system if  $Q_v = M$ .

The term  $\frac{1}{2} F^T R F$  represents work done by external force, if  $R = K^{-1}$ .

The term  $\Gamma$  represents contribution of maneuver time. Optimal maneuver time, if not known, can be calculated by assigning weightage to  $\Gamma$ . If the maneuver time is already known then  $\Gamma = 0$ .

The objective function is minimized subject to the equation of motion (2.1)

$$M\ddot{X} + C\dot{X} + KX = BF_a(t) = F$$

The initial and final boundary conditions for the controlled maneuver are

$$\begin{aligned} \text{IBC: } X(0) &= X_0 & \text{FBC: } \dot{X}(t_f) &= \dot{X}_f \\ \dot{X}(0) &= \dot{X}_0 & X(t_f) &= X_f \end{aligned} \quad (2.27)$$

The purpose of optimal control is to determine  $F_a(t)$ ,  $X(t)$ ,  $t_f$  that satisfies Eq. (2.1), conditions (2.27) and minimizes the performance index (2.26).

The problem is now written in the form that uses the state variables and is solved by the optimal control methodology [9]. The state variables represent the system's displacements and velocities. For  $n$  DOF system there are  $2n$  state variables defined as

$$z = \begin{bmatrix} X \\ \dot{X} \end{bmatrix} \quad (2.28)$$

In terms of the state variables the performance index (2.26) is

$$J = \int_0^{t_f} f(z, F) dt = 1/2 \int_0^{t_f} [z^T Q z + F^T R F + \Gamma] dt \rightarrow \min \quad (2.29)$$

The state variables  $z$  and controls  $F$  must satisfy the equation of motion (2.20) which can be rewritten as  $2n$  of first order state equations in the form

$$\dot{z} = A_1 z + A_2 F \quad (2.30)$$

and  $4n$  boundary conditions

$$z(0) = z_0 \quad z(t_f) = z_f \quad (2.31)$$

where  $A_1 = \begin{bmatrix} 0 & 1 \\ -M^{-1}K & -M^{-1}C \end{bmatrix}_{2n \times 2n}$   $A_2 = \begin{bmatrix} 0 \\ M^{-1} \end{bmatrix}_{2n \times n}$  (2.32-33)

Formally, the objective (2.29) with the constraints (2.30-31) defines a constrained optimization problem, which can be solved by applying general optimization methods. The necessary conditions for  $z$  and  $F$  to minimize  $J$  and satisfy all the constraints can be derived from Pontryagin's principle. These conditions are in the form of differential equations and are referred to as the optimality equations. In order to apply Pontryagin's principle, the Hamiltonian is defined as

$$H = -f(z, F) + P^T (A_1 z + A_2 F) = H(z, P, F) \quad (2.34)$$

where  $P$  is a vector of costates.

For optimal motion  $H$  should be stationary in terms of  $z$ ,  $P$  and  $F$ . According to Pontryagin's principle the costates must satisfy the equation

$$-\frac{\partial H}{\partial z} = \dot{P} = Qz - A_1^T P \quad (2.35)$$

The state equation is

$$\frac{\partial H}{\partial P} = \dot{z} = A_1 z + A_2 F \quad (2.36)$$

Costate and state are  $4n$  of first order differential equations. The extremum of Hamiltonian with respect to control gives

$$\frac{\partial H}{\partial F} = -RF + A_2^T P = 0 \quad (2.37)$$

From the above equation, optimal control force is specified as

$$F = R^{-1} A_2^T P \quad (2.38)$$

The Hamiltonian must also satisfy the target equation

$$H(t_f) \delta \alpha_f = 0 \quad (2.39)$$

If  $t_f$  is given, this equation is automatically met. Otherwise  $H(t_f) = 0$  is used to determine the optimal maneuver time  $t_f$ . Eq. (2.35 – 2.38) constitute the set of optimality equations that must be satisfied by the optimal maneuver. It should be noted that formally the functions  $z$ ,  $P$  and  $F$  will be determined in terms of time. It implies that the actuator forces will also be known functions of time, constituting an open loop control problem.

If the modal space is used then  $X \rightarrow \eta$ ,  $M \rightarrow I$ ,  $K \rightarrow \Omega$ ,  $F \rightarrow u$ .

The problem defined by Eqs. (2.29 – 2.39) can also be analyzed using the Riccati equation derived as follows.

$$\text{Let } P = \hat{C}(t)z \quad (2.40)$$

where  $\hat{C}$  is a symmetric matrix of dimension  $2n$ .

Substituting back into Eq. (2.35) one obtains

$$\dot{\hat{C}}z + \hat{C}\dot{z} = -Qz - A_1^T \hat{C}z \quad (2.41)$$

Substituting Eq. (2.40) into Eq. (2.38)

$$F = R^{-1} A_2^T \hat{C}z \quad (2.42)$$

Substituting Eq. (2.36) and (2.42) into (2.41)

$$\dot{\hat{C}}z + \hat{C}A_1 z + \hat{C}A_2 R^{-1} A_2^T \hat{C}z + Qz + A_1^T \hat{C}z = 0$$

Since this equation must be satisfied for any  $z(t) \neq 0$ , the matrix  $\hat{C}(t)$  must satisfy the equation

$$\dot{\hat{C}} + \hat{C}A_1 + \hat{C}A_2R^{-1}A_2^T\hat{C} + Q + A_1^T\hat{C} = 0 \quad (2.43)$$

This equation is referred to as the Riccati equation. The boundary conditions for this equation can be derived from the target equation. The solution of the Riccati equation provides the matrix  $\hat{C}$  that can be substituted back to get controls, costates and trajectories of the optimal maneuver. Since the equation is non-linear due to the multiplication of matrices  $\hat{C}$  in the third term, it is generally difficult to solve.

It can be shown that  $\hat{C} \rightarrow \text{constant}$  if  $t_f \rightarrow \infty$  (and  $\Gamma = 0$ ) in Eq. (2.29). Then Eq. (2.43) becomes the algebraic Riccati equation in the form

$$\hat{C}A_1 + A_1^T\hat{C} + \hat{C}A_2R^{-1}A_2^T\hat{C} + Q = 0 \quad (2.44)$$

This equation solves the so-called time invariant optimal control problem. However, the Riccati equations are generally difficult to solve, as discussed in [10].

Eq. (2.42), which represents the relationship between forces and states, can be rewritten as

$$F = -G \cdot z \text{ where } G = -R^{-1}A_2^T\hat{C} \quad (2.45)$$

If matrix  $G$ , to be referred to as gain matrix, is known then the current controls (input) can be defined upon the knowledge of the states (output). This allows for a closed loop control with the optimal gains determined either from Eq. (2.44) or by directly minimizing the performance

$$J = 1/2 \int_0^{\infty} [z^T Q z + F^T R F] dt = \frac{1}{2} \int_0^{\infty} z^T (Q + G^T R G) z \cdot dt \quad (2.46)$$

Subject to  $\dot{z} = A_1 z + A_2 F = (A_1 - A_2 G)z$

A method of finding the optimal gains from the latter approach will be discussed in Chapter VI.

## 3. SOME SOLUTION TECHNIQUES

### 3.1 Introduction

Solution techniques for the optimal control problems defined in chapter II can generally be divided into two categories, analytical which attempt to solve the optimality equations, and parametric optimization that tries to minimize the performance index directly. An analytical technique can provide exact solutions but complicates quickly with the number of DOFs. Parametric optimization can theoretically handle more complicated problems but the convergence and sufficient accuracy is difficult to obtain. These techniques are briefly discussed in the coming sections.

### 3.2 Overdetermined gantry crane problem by optimality equations

Due to the simplicity, overdetermined gantry crane problem can be solved analytically. An exact solution of the crane controlled by the actuator  $F_{m1}$  is determined first for the comparison purposes. Results obtained by applying different methodologies will be verified against this solution.

$$\text{Let } u = \frac{F_{m1}}{\sqrt{m_1 + m_2}} \text{ and } j = \sqrt{m_2 / m_1} \quad (3.1\text{-a,b})$$

Eq. (2.22) can be rewritten as

$$\dot{\eta}_1 + 0\eta_1 = u \quad (3.2)$$

$$\ddot{\eta}_2 + \omega_2^2 \eta_2 = ju \quad (3.3)$$

As can be seen, the two modes of the gantry crane motion are controlled by one modal control  $u$ .

Let,

$$z_1 = \eta_1 \quad z_3 = \eta_2 \quad (3.4)$$

$$z_2 = \dot{\eta}_1 \quad z_4 = \dot{\eta}_2 \quad (3.5)$$

Equations of motion (3.2-3) can be written in the form of state equations as

$$\begin{aligned} \dot{z}_1 &= z_2 & \dot{z}_3 &= z_4 \\ \dot{z}_2 &= u & \dot{z}_4 &= -\omega_2^2 z_3 + uj \end{aligned} \quad (3.6)$$

Similarly as in [7], assume that the work done by actuators should be minimized in the maneuver executed in a given time  $t_f$ . The corresponding performance index is

$$J = \frac{1}{2} \int_0^{t_f} u^2 dt \quad (3.7)$$

Hamiltonian (Eq. (2.34)) can be written as,

$$H = -\frac{1}{2}u^2 + P_1 z_2 + P_2 u + P_3 z_4 + P_4 (-\omega_2^2 z_3 + uj) \quad (3.8)$$

The costates equations (2.35) are

$$\frac{\partial H}{\partial z_1} = -\dot{P}_1, \quad \dot{P}_1 = 0 \quad (3.9)$$

$$\frac{\partial H}{\partial z_2} = -\dot{P}_2, \quad \dot{P}_2 = -P_1 \quad (3.10)$$

$$\frac{\partial H}{\partial z_3} = -\dot{P}_3, \quad \dot{P}_3 = \omega_2^2 P_4 \quad (3.11)$$

$$\frac{\partial H}{\partial z_4} = -\dot{P}_4, \quad \dot{P}_4 = -P_3 \quad (3.12)$$

Note that for this particular case, the costate equations are independent of the states. A more generalized case is discussed later.

From Eq. (3.9-3.12) one can write

$$\ddot{P}_2 = 0 \quad (3.13)$$

$$\ddot{P}_4 + \omega_2^2 P_4 = 0 \quad (3.14)$$

The control equation (2.37) is

$$\frac{\partial H}{\partial u} = 0 \rightarrow u = P_2 + jP_4 \quad (3.15)$$

For this problem Eq. (3.13) can be independently integrated to obtain

$$P_2 = C_1 t + C_2 \quad (3.16)$$

Similarly integrating Eq. (3.14)

$$P_4 = C_3 \sin(\omega_2 t) + C_4 \cos(\omega_2 t) \quad (3.17)$$

Substituting Eq. (3.16) and (3.17) in (3.15)

$$u = C_1 t + C_2 + C_3 j \sin(\omega_2 t) + C_4 j \cos(\omega_2 t) \quad (3.18)$$

Substituting Eq. (3.18) into (3.2)

$$\dot{\eta}_1 = C_1 t + C_2 + C_3 j \sin(\omega_2 t) + C_4 j \cos(\omega_2 t)$$

Integrating above equation twice

$$\eta_1 = C_1 \frac{t^3}{6} + C_2 \frac{t^2}{2} - C_3 j \frac{\sin(\omega_2 t)}{\omega_2^2} - C_4 j \frac{\cos(\omega_2 t)}{\omega_2^2} + C_5 t + C_6 \quad (3.19)$$

Now substituting Eq. (3.18) into (3.3) and integrating

$$\eta_2 = \frac{1}{\omega_2^2 \sqrt{2}} [2C_1 t + 2C_2 + C_4 j (\cos(\omega_2 t) + \omega_2 t \sin(\omega_2 t)) - C_3 j \omega_2 t \cos(\omega_2 t)] + C_7 \sin(\omega_2 t) + C_8 \cos(\omega_2 t) \quad (3.20)$$

The solution is obtained in terms of eight integration constants  $C_1..C_8$ . These constants can be determined from the following boundary conditions.

$$\begin{aligned} \eta_1(0) &= 0 & \eta_1(t_f) &= a\sqrt{M+m} \\ \dot{\eta}_1(0) &= 0 & \dot{\eta}_1(t_f) &= 0 \\ \eta_2(0) &= 0 & \eta_2(t_f) &= 0 \\ \dot{\eta}_2(0) &= 0 & \dot{\eta}_2(t_f) &= 0 \end{aligned} \quad (3.21)$$

Let,  $m_1 = 1000Kg$ ,  $m_2 = 2000Kg$ ,  $L = 2m$ ,  $t_f = 4.515s$  (maneuver time),  $a=4m$ ,

$$\omega_2 = 3.836rad / s$$

Using above values, the integration constants can be calculated (using Maple software) as

$$\begin{aligned} C_1 &= -30.01979 & C_5 &= -2.231477 \\ C_2 &= 67.7727 & C_6 &= -0.55804 \\ C_3 &= -8.5599 & C_7 &= 0.3407816 \\ C_4 &= -8.211489 & C_8 &= -6.118878 \end{aligned} \quad (3.22)$$

Substituting these constants in Eq. (3.19) and (3.20)



$$\eta_1 = -5.00384t^3 + 33.888t^2 + 0.5814\sin(\omega_2 t) + 0.5581\cos(\omega_2 t) - 2.230t - 0.5581 \quad (3.23)$$

$$\eta_2 = -2.885t + 6.514 - 6.514\cos(\omega_2 t) - 1.514\sin(\omega_2 t) \cdot t + 1.577\cos(\omega_2 t) \cdot t + 0.341\sin(\omega_2 t) \quad (3.24)$$

The above modal variables are converted into  $x$  and  $\theta$  variables by using Eq. (2.19)

$$x = \frac{1}{\sqrt{M+m}}\eta_1 + \sqrt{\frac{m}{M(M+m)}}\eta_2 \quad (3.25)$$

$$L\theta = -\sqrt{\frac{M+m}{Mm}}\eta_2 \quad (3.26)$$

Substituting all constants, one can write,

$$x = -0.091347t^3 + 0.618677t^2 + \sin(\omega_2 t)\{0.01942 - 0.03908t\} + \cos(\omega_2 t)\{-0.15798 + 0.04074t\} - 0.11523t + 0.1579887 \quad (3.27)$$

$$L\theta = 0.1117406t - 0.252265 + \cos(\omega_2 t)\{0.252265 - 0.0611115t\} + \sin(\omega_2 t)\{0.058624t - 0.0131984\} \quad (3.28)$$

Plots of  $x(t)$  and  $\theta(t)$  are shown in Fig. 3.1. Some angular positions are also indicated in the graph.

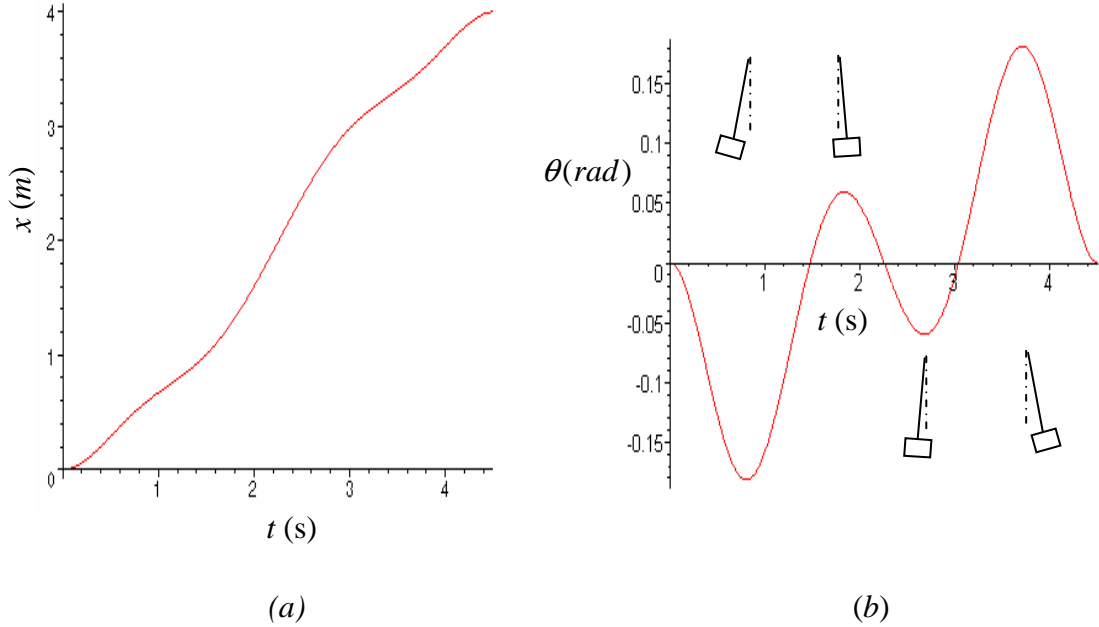


**Figure 3.1:** (a) Plot of  $x$  (m) versus time(s); (b) Plot of  $\theta$ (rad) versus time(s)

Fig. 3.2 represents the variation of modal variables  $\eta_1$  and  $\eta_2$

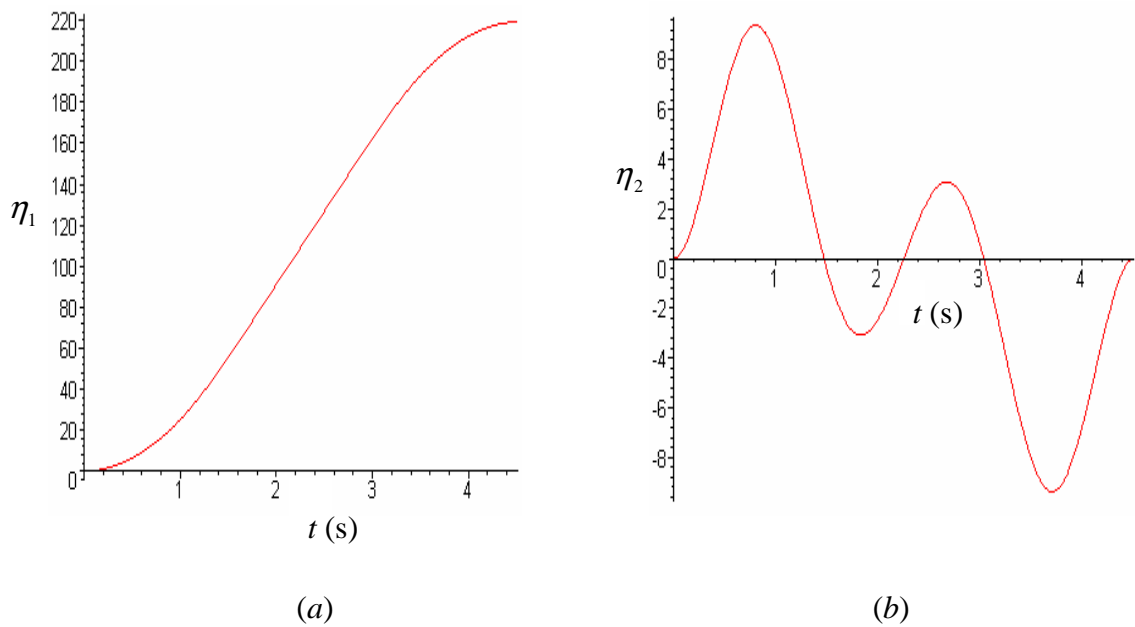


**Figure 3.2:** (a) Plot of  $\eta_1$  versus time; (b) Plot of  $\eta_2$  versus time

The optimal actuator force now can be calculated from Eq. (3.1-2) and equals to

$$F_{m1} = -1644.2519t + 3712.0632 - 468.8475 \sin(\omega_2 t) - 449.7618 \cos(\omega_2 t) \quad (3.29)$$

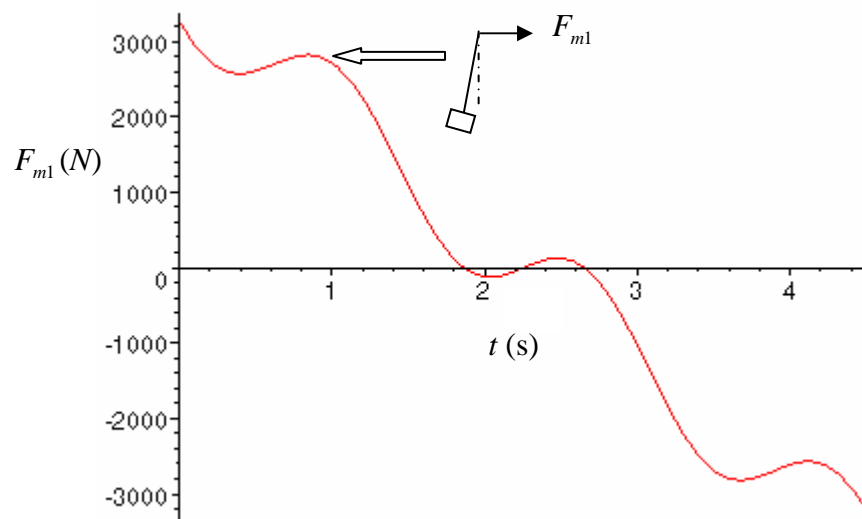


**Figure 3.3:** Plot of  $F_{m1}$  (N) versus time (s)

This force is plotted in Fig. 3.3. It can be noted that the  $F_{m1}$  changes within about  $\pm 3000N$ . Starting from the high positive value, the force is reduced to zero in the first half and then the same way it attains the high negative value in the later half. The force is zero after  $t = t_f$ . The optimal value of  $J_{opt} = 9.8 \times 10^6$  is calculated for the comparison purpose.

### 3.3 Some Limitations

It should be emphasised again that the analytical solution for the above overdetermined problem was possible because the costates in Eq. (3.9-12) were independent of states. It is not the case for most of the other control problems. For example, a suspension system shown in Fig. 3.4 (analysed in chapter V) with one actuator force to control two modes would be very difficult to solve by this technique.

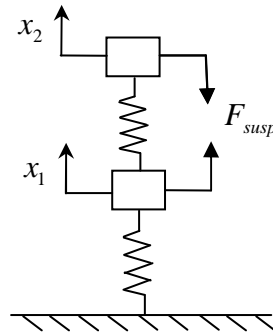


**Figure 3.4:** Suspension system

The problem with this case is that the costate equation takes the following form

$$\begin{aligned}
 \dot{P}_1 &= a_2 z_1 \omega_1^2 + P_2 \omega_1^2 \\
 \dot{P}_2 &= b_1 z_2 - P_1 \\
 \dot{P}_3 &= a_2 z_3 \omega_2^2 + P_4 \omega_2^2 \\
 \dot{P}_4 &= b_1 z_4 - P_3
 \end{aligned} \tag{3.30-a,b,c,d}$$

Unlike the costates (Eq. (3.9-12)) of gantry crane, these costates are coupled with the states  $z_1, z_2, z_3, z_4$ . The state equations for the problem in Fig. 3.4 are somewhat similar to Eq. (3.6), and takes the form

$$\begin{aligned}
\dot{z}_1 &= z_2 \\
\dot{z}_2 &= u - \omega_1^2 z_1 \\
\dot{z}_3 &= z_4 \\
\dot{z}_4 &= ju - \omega_2^2 z_3
\end{aligned} \tag{3.31-a,b,c,d}$$

In order to solve the problem defined by Eq. (3.30–31) it is important to uncouple the costates from the states. It would be possible if the boundary conditions were available for the costates, but in this case those are available only for the states. Hence, these type of problems are very difficult to solve. Various other techniques to tackle such more general problems are discussed in coming chapters.

### 3.3 Parametric optimization technique

This technique attempts to directly minimize the performance index (such as defined by (2.26), for example). A gradient based numerical procedure for unconstrained optimization problems will be used to solve the overdetermined gantry crane problem. The constraint optimization problem may be converted into unconstrained one by using a penalty function. If  $P_e$  is a penalty then the objective function could be the sum of a positive definite performance index and  $P_e$  times a positive definite constraints equation. Note that the costates do not need to be considered.

In order to solve gantry crane problem by parametric optimization, the force  $F_{m1}(t)$  may be approximated by a piecewise constant or linear functions as shown in Fig. 3.5. The total time span  $t_f$  is broken into  $n_d$  equal divisions. The optimum value of forces at the start and at the end of each division is to be obtained by optimization. To be consistent with the analytical solution in the section 3.2, the objective function includes summation of square of forces.

$$J = \sum_{n_d} \int_{t_i}^{t_{i+1}} F(t)^2 \cdot dt = J(F_1..F_{n_d+1}) \rightarrow \min$$

The procedure is explained with the help of flowchart shown in Fig. 3.6. The values of forces  $F_i$  at the starting point are assumed. Using IBCs at the start ( $t=0$ ) and the applied forces on the first division, the FBCs at the end of the first division are

calculated from analytical solution explained in the next section. These FBCs become IBCs for the second division which in turn yields the FBCs for second division. The loop is repeated for  $n_d$  divisions. The values of all variables at the end of last division are obtained and are compared with the required FBC values. The target error ( $TE$ ) is defined as

$$TE = \sum_i (\eta_i(t_f) - \eta_{i_f})^2 + (\dot{\eta}_i(t_f) - \dot{\eta}_{i_f})^2$$

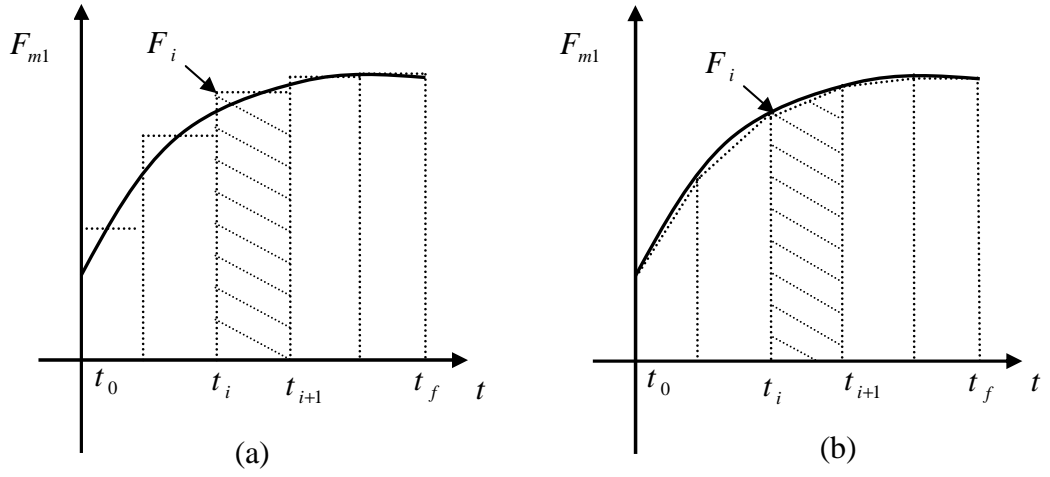


**Figure 3.5:** (a)  $F_{m1}$  is constant in each division; (b)  $F_{m1}$  changes linearly with time in each division

Any combination of forces  $F_i$  that eliminates this error solves the control problem. The combination that gives the minimum value of the performance index is considered optimal. In each iteration new forces are calculated by minimizing the objective function

$$\hat{J} = J + P_e \cdot (TE)$$

The Davidon-Fletcher-Powell (DFP) optimization procedure is used to minimize  $\hat{J}$ . The objective function includes forces and the penalty ( $P_e$ ) times error. The procedure is terminated if the target error is sufficiently small ( $TE < \varepsilon_1$ ) and the objective function between two consecutive iteration steps is smaller than user defined  $\varepsilon_2$ .

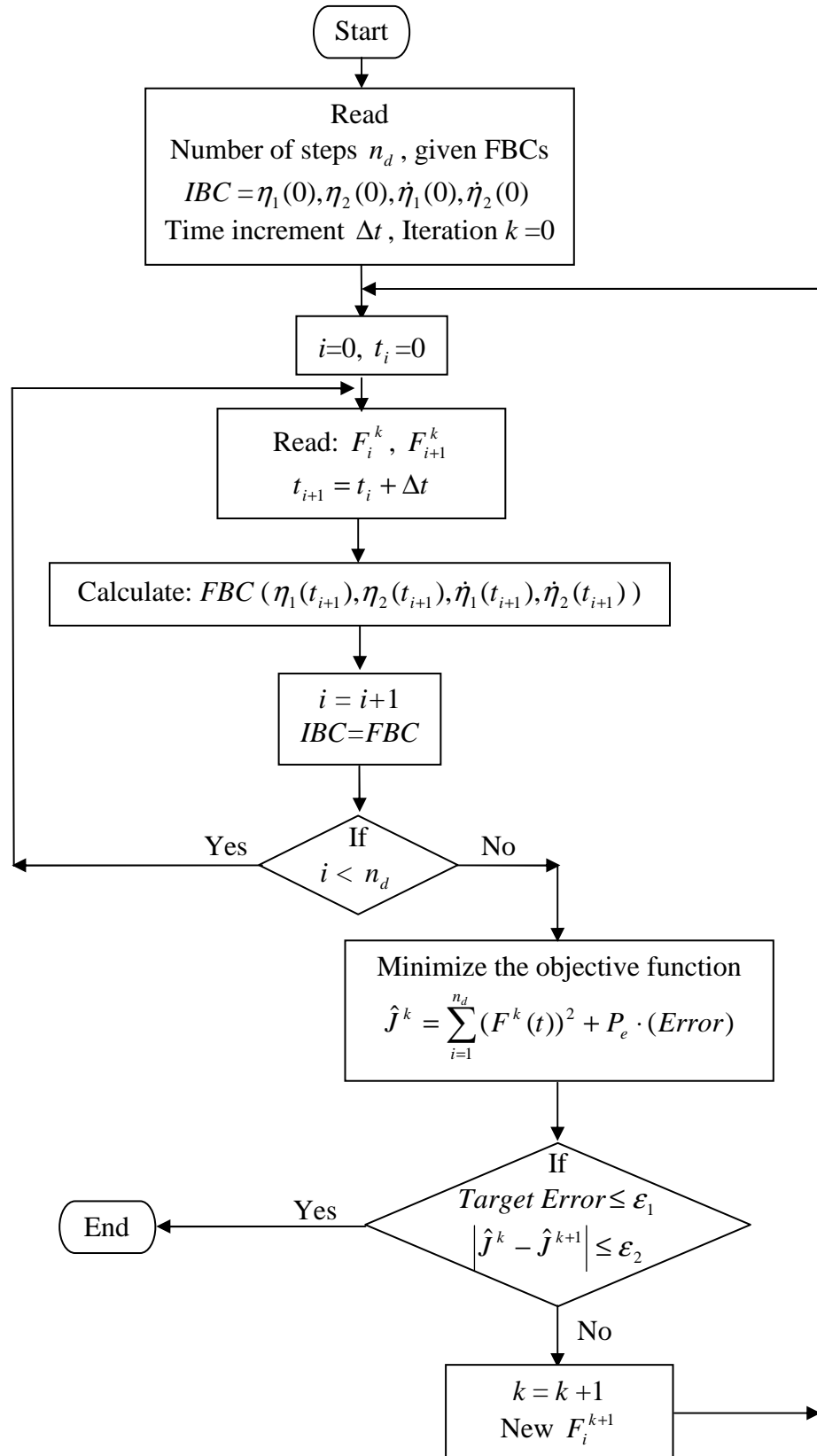


**Figure 3.6:** Flowchart for parametric optimization technique

In order to develop the programming codes, the analytical solution to obtain FBC is derived for a linearly varying force.

### 3.3.1 A piecewise linearly varying force approximation

Linearly varying forces are used as they give closer approximation to the actual forces than the constant value forces. The analytical solution for a division is obtained. The force applied on mass  $m_1$  for  $t_1 < t < t_2$  is shown in Fig. 3.7.

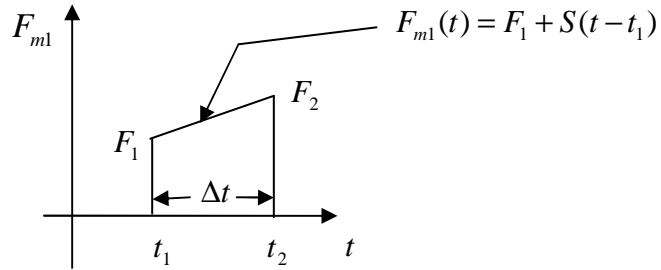


**Figure 3.7:** Linearly varying force

The force can be expressed as

$$F_{m1} = F_1 + \hat{S}(t - t_1) \quad (3.32)$$

where  $\hat{S} = slope = \frac{F_2 - F_1}{t_2 - t_1}$ .

The objective function  $J_i$  (where  $J = \sum_1^n J_i$ ) can be expressed as

$$J_i = \int_{t_1}^{t_2} F_{m1}(t)^2 \cdot dt = \frac{1}{3}(F_1^2 + F_1F_2 + F_2^2)\Delta t$$

From Eq. (2.23)

$$u_1 = q_1t + q_2 \quad (3.33)$$

$$u_2 = q_3t + q_4 \quad (3.34)$$

where  $q_1 = \frac{\hat{S}}{\sqrt{m_1 + m_2}}$   $q_2 = \frac{F_1 - \hat{S}t_1}{\sqrt{m_1 + m_2}}$

$$q_3 = \hat{S} \sqrt{\frac{m_2/m_1}{m_1 + m_2}} \quad q_4 = \sqrt{\frac{m_2/m_1}{m_1 + m_2}} (F_1 - \hat{S}t_1)$$

Let the initial boundary conditions for a time step be

$$\eta_1(t_1), \eta_2(t_1), \dot{\eta}_1(t_1), \dot{\eta}_2(t_1) \quad (3.35)$$

From equation (2.21)

$$\ddot{\eta}_1 = q_1 t + q_2 \quad (3.36)$$

Integrating with respect to  $t$ ,

$$\eta_1 = q_1 t^3 / 6 + q_2 t^2 / 2 + C_1 t + C_2 \quad (3.37)$$

$$\dot{\eta}_1 = q_1 t^2 / 2 + q_2 t + C_1 \quad (3.38)$$

$C_1$  and  $C_2$  are integration constants to be found from boundary conditions.

From Equation (2.22)

$$\ddot{\eta}_2 + \omega_2^2 \eta_2 = u_2 = q_3 t + q_4 \quad (3.39)$$

Integrating with respect to  $t$ ,

$$\eta_2 = C_3 \cos(\omega_2 t) + C_4 \sin(\omega_2 t) + q_3 t / \omega_2^2 + q_4 / \omega_2^2 \quad (3.40)$$

$$\dot{\eta}_2 = -C_3 \omega_2 \sin(\omega_2 t) + C_4 \omega_2 \cos(\omega_2 t) + q_3 / \omega_2^2 \quad (3.41)$$

$X$  variables are obtained using  $X = \phi \eta$

$$\begin{bmatrix} x \\ L\theta \end{bmatrix} = \begin{bmatrix} 1/(\sqrt{m_1 + m_2}) & \sqrt{m_2/m_1(m_1 + m_2)} \\ 0 & -\sqrt{(m_1 + m_2)/m_1 m_2} \end{bmatrix} \begin{bmatrix} \eta_1 \\ \eta_2 \end{bmatrix} \quad (3.42)$$

$C_1, C_2, C_3, C_4$  are integration constants and can be found from the initial boundary conditions (3.35). For numerical purposes the time scale is shifted so that for each division  $t_1 = 0$  and  $t_2 = \Delta t$ . Then from Eq. (3.37-38) and Eq. (3.40-41) one obtains

$$C_1 = \dot{\eta}_1(t_1)$$

$$C_2 = \eta_1(t_1)$$

$$C_3 = \eta_2(t_1) - q_4 / \omega_2^2 \quad (3.43-a,b,c,d)$$

$$C_4 = [\dot{\eta}_2(t_1) - q_3 / \omega_2^2] / \omega_2$$

The FBCs or the values of all functions at time  $t_2$  can be obtained by substituting all the constants in Eq. (3.37-38-40-41) and  $t = \Delta t$ .



The DFP program is used to solve the optimization problem. For a specific objective function, all the derivatives and increments of the variables (forces  $F_i$ ) are calculated numerically. The case of four forces i.e.  $n_d = 3$  is considered first, as it yields four unknowns which can be calculated directly from the four equations of boundary condition. In this case the target error criterion is met by only one set of forces. These forces can be obtained quickly by setting the penalty  $P_e$  high enough to eliminate the target error. For  $n_d > 3$ , the number of unknown forces is greater than the number of equations available and the optimization procedure has to simultaneously minimize the objective  $J$  and eliminate the target error.

In some cases, the target error corresponding to positions and velocities are several orders different, making it difficult to satisfy the target boundary condition. It is required to exaggerate those error functions by applying bigger penalty. As the value of penalty changes, the forces and error values changes almost randomly. The values of penalty functions become more and more difficult to predict when the number of steps and the number of  $F_i$ 's increases.

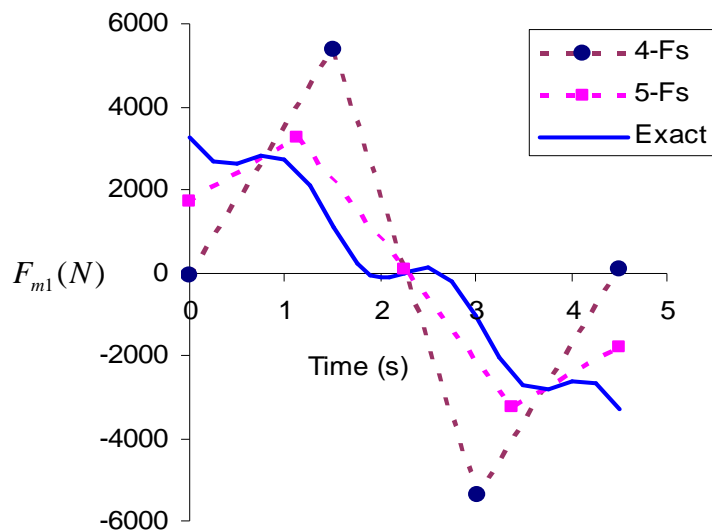


**Figure 3.8:** Plot of  $F_{m1}$  versus time

It can be concluded that the parametric optimization can be used to solve any type of problem but it is very difficult to obtain satisfactory convergence. The results of

DFP program for 4 forces and 5 forces are plotted in Fig. 3.8. The exact plot is also shown for comparison.

In order to illustrate how the performance index is optimized its values for these cases are listed in Table 3.1. The exact value is also shown.

Number of forces	$J$
4	2153E04
5	1125E04
Exact	988E04

**Table 3.1:** Performance index for different number of forces

It can be noted from Fig. 3.9 that the performance index improves drastically as the number of division  $n_d$  increases from three to four.

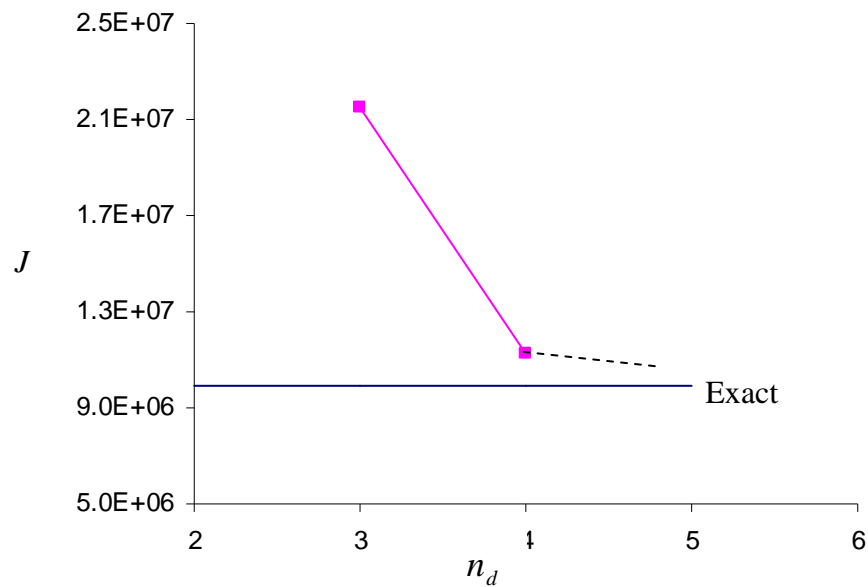


**Figure 3.9:** Plot of performance index  $J$  versus number of division  $n_d$

The dashed line shows that the performance index should reach the exact value if the number of divisions is increased. But in practise it is very difficult to handle the cases having four divisions or more.

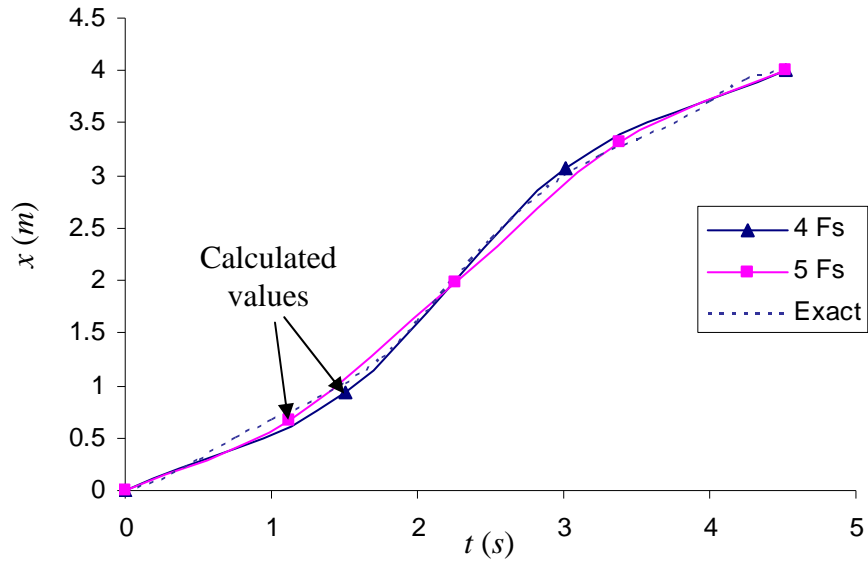


**Figure 3.10:** Plot of  $x$  versus time for different cases

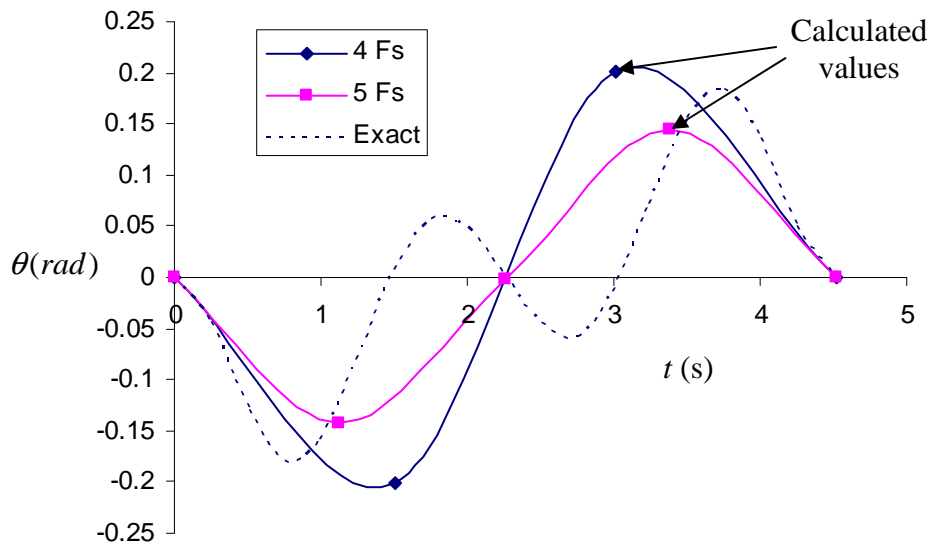


**Figure 3.11:** Plot of  $\theta$  (rad) versus time(s) for different cases

The displacement  $x(t)$  for these three cases is shown in Fig. 3.10. All the linear displacements resemble each other closely unlike the angular displacement  $\theta$  which is plotted in Fig. 3.11. In the plots, the calculated values at  $t_i$  were connected by cubic spline lines for convenience. The exact lines should be plotted using Eq. (3.37-42).

## 4. BEAM ANALOGY

### 4.1 Introduction

The two general solution methods mentioned before, optimality equations and parametric optimization can be used effectively to solve optimal control problems with a small number of DOFs to control. Both of these methods complicate quickly with the increase in the number of DOFs.

A new technique called *Beam Analogy (BA)* based on optimality equations has been developed in [11] to obtain the solutions for problems with large number of DOFs by using the IMSC approach. The technique eliminates the costates and uses the analogy between optimality equations for control and the deflection of a beam on elastic foundation. The optimality equations problem is converted into fourth order beam deflection problem and solved efficiently with the help of FEM as a boundary value problem.

The standard first order optimality equations (2.35 – 2.37) can be combined to eliminate the costate and to obtain the second order equations of optimal states as [11]

$$\ddot{z} + (D_1 A_1^T D_1^{-1} - A_1) \dot{z} - (D_1 A_1^T D_1^{-1} A_1 + D_1 Q) z = 0 \quad (4.1)$$

$$\text{where } D_1 = A_2 R^{-1} A_2^T \quad (4.2)$$

Eq. (4.1) together with boundary conditions (Eq. (2.31)), constitutes a boundary value problem of second order. Formally, this problem is suitable for handling by the finite element method. However, for the mechanical system defined by Eq. (2.1), matrix  $D_1$  is singular. The singularity may be removed if the costates related to the displacement ( $P_d$ ), are considered separately from the costates related to the velocity ( $P_v$ ). The costate vector may be decomposed into

$$P = \begin{bmatrix} P_d \\ P_v \end{bmatrix} \quad (4.3)$$

Now, using the degree of freedom  $X(t)$ , instead of the costates  $z$ , the costate equation (2.35) can be written in the form

$$\dot{P} = \begin{bmatrix} \dot{P}_d \\ \dot{P}_v \end{bmatrix} = -\frac{\partial H}{\partial X} = \begin{bmatrix} Q_d X + (M^{-1}K)P_v \\ Q_v \dot{X} - P_d + (M^{-1}C)P_v \end{bmatrix} \quad (4.4)$$

The optimal control force from Eq.(2.38) becomes

$$F = R^{-1}M^{-1}P_v \quad (4.5)$$

Note that the set of three equations comprising Eq. (2.1) and (4.4) contain three sets of variables  $X$ ,  $P_d$  and  $P_v$ . The costate  $P_d$  and  $P_v$  can be written in terms of  $X$  as [11]

$$P_d = Q_v \dot{X} - MR(M\ddot{X} + C\dot{X} + KX) + CR(M\ddot{X} + C\dot{X} + KX) \quad (4.6a)$$

$$P_v = MR(M\ddot{X} + C\dot{X} + KX) \quad (4.6b)$$

Finally, eliminating the costates, the equations for optimal DOFs are derived as [11]

$$MRM\ddot{\ddot{X}} + [2KRM - Q_v - CRC]\ddot{X} + [KRK + Q_d]X = 0 \quad (4.7)$$

It can be noted that the DOFs of Eq. (4.7) are coupled. Assuming that  $Q_d$ ,  $Q_v$  and  $R$  are linear combinations of matrices  $M$ ,  $C$  and  $K$

$$Q_d = a_1M + a_2K + a_3C$$

$$Q_v = b_1M + b_2K + b_3C \quad (4.8-a,b,c)$$

$$R^{-1} = c_1M + c_2K + c_3C$$

and using modal relations i.e.  $X = \phi\eta$  the optimality equations become uncoupled in the modal space and assume the following form [11]

$$\hat{R}\ddot{\ddot{\eta}} + (2\Omega\hat{R} - \hat{Q}_v - \hat{R}\Delta^2)\ddot{\eta} + (\hat{R}\Omega^2 + \hat{Q}_d)\eta = 0$$

$$\text{or} \quad \hat{R}_{ii}\ddot{\ddot{\eta}}_i + (2\omega_i^2\hat{R}_{ii} - \hat{Q}_{vii} - \hat{R}_{ii}\Delta_{ii}^2)\ddot{\eta}_i + (\hat{R}_{ii}\omega_i^4 + \hat{Q}_{dii})\eta_i = 0 \quad i = 1..n_m \quad (4.9)$$

where  $n_m$  is the number of modes to control, and matrices  $\hat{Q}_d$ ,  $\hat{Q}_v$  and  $\hat{R}$  are diagonal with the terms:

$$\hat{Q}_{dii} = a_1 + a_2\omega_i^2 + a_32\omega_i\zeta_i$$

$$\hat{Q}_{vii} = b_1 + b_2\omega_i^2 + b_32\omega_i\zeta_i \quad (4.10-a,b,c)$$

$$\hat{R}_{ii} = [c_1 + c_2\omega_i^2 + c_32\omega_i\zeta_i]^{-1}$$

$a_1, a_2, a_3, b_1, b_2, b_3, c_1, c_2, c_3$  are the optimization parameters.

The terms of diagonal modal damping matrix  $\Delta$  are  $\Delta_{ii} = 2\omega_i \zeta_i$

The Boundary Conditions in the modal space are

$$\eta(0) = \eta_0, \frac{d\eta}{dt}(0) = \dot{\eta}_0 \quad (4.11-a)$$

$$\eta(t_f) = \eta_f, \frac{d\eta}{dt}(t_f) = \dot{\eta}_f \quad (4.11-b)$$

Having solved Eq. (4.9) for optimal modal variables  $\eta_i$  the corresponding modal controls are calculated from  $u_i = \ddot{\eta}_i + 2\zeta_i \omega_i \dot{\eta}_i + \omega_i^2 \eta_i$ .

It should also be noted that Eq. (4.9) is the optimality equation for the optimization problem defined by the performance index (2.26) with the constraint (2.1). This optimization problem in the modal space is reformulated as

$$J = \frac{1}{2} \int_0^{t_f} (\eta^T \hat{Q}_d \eta + \dot{\eta}^T \hat{Q}_v \dot{\eta} + u^T \hat{R} u + \Gamma) dt \quad \rightarrow \text{Minimize} \quad (4.12)$$

where the variables  $\eta$  and  $u$  satisfy the equation of motion ( $I\ddot{\eta} + \Delta\dot{\eta} + \Omega\eta = u$ ) and  $\hat{Q}_d, \hat{Q}_v$  and  $\hat{R}$  are diagonal matrices defined above (see Eq. (4.10)).

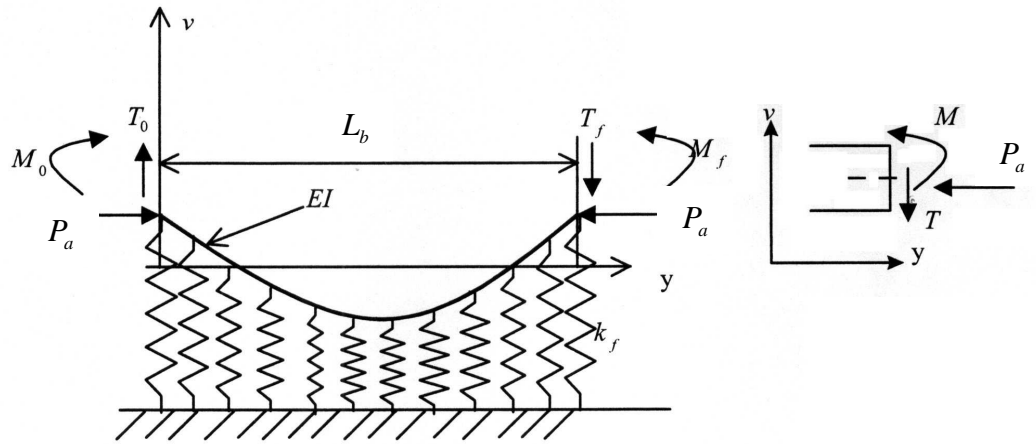


**Figure 4.1:** Beam on elastic foundation

The optimal control problem defined by Eq. (4.9-4.12) is analogous to the static beams problem shown in Fig. 4.1. The beam of a length  $L_b$  and bending stiffness  $EI$  supported on elastic foundations of stiffness  $k_f$  is loaded only at the ends by bending moment  $M_0$  and  $M_f$ , shear forces  $T_0$  and  $T_f$  and the axial forces  $P_a$  (compressive force is assumed positive). Small deflections in the beam are governed by the well-known fourth order differential equation [12]

$$EI_i v_i'''' + P_{a_i} v_i'' + k_{f_i} v_i = 0 \quad (4.13)$$

where,  $i$  is a beam number,  $v$  is a vertical deflection and  $v'_i = \frac{dv_i}{dy}$

For each mode to control there is one optimality equation and hence one analogous beam. The geometrical boundary conditions are assumed in the form

$$v_i(0) = v_{i0}, \frac{dv_i}{dy}(0) = \theta_{i0} \quad v_i(L_i) = v_{if}, \frac{dv_i}{dy}(L_i) = \theta_{if} \quad (4.14)$$

Using the sign conventions indicated in the Fig. 4.1, the bending moment and shear forces in the beam are

$$\hat{M} = EI \frac{d^2 v}{dy^2} \quad (4.15)$$

$$\hat{T} = EI \frac{d^3 v}{dy^3} \quad (4.16)$$

The analogy between the boundary value problem for control (Eq. (4.9-4.12)) and the boundary value problem for a structural beam (Eq. (4.13-4.14)) gives the following correspondence

$$EI_i \equiv \frac{1}{c_1 + c_2 \omega_i^2 + c_3 2\omega_i \zeta_i} \quad (4.17)$$

$$P_{a_i} \equiv 2\omega_i^2 \frac{1}{c_1 + c_2 \omega_i^2 + c_3 2\omega_i \zeta_i} - (b_1 + b_2 \omega_i^2 + b_3 2\omega_i \zeta_i) + \left( 4\zeta_i^2 \omega_i^2 \frac{1}{c_1 + c_2 \omega_i^2 + c_3 2\omega_i \zeta_i} \right) \quad (4.18)$$



$$k_{f_i} \equiv \left[ \omega_i^4 \frac{1}{c_1 + c_2 \omega_i^2 + c_3 2\omega_i \zeta_i} + (a_1 + a_2 \omega_i^2 + a_3 2\omega_i \zeta_i) \right] \quad (4.19)$$

The equivalent variables are

$$y_i \equiv t_i \quad v_i(y) \equiv \eta_i(t) \quad (4.20)$$

The numerical values of  $L_b$  and  $t_f$  can be assumed to be identical. The modal functions in time domain are analogous to the beam variables as follows

$$\eta_i(t) \equiv v_i(y) \quad \dot{\eta}_i \equiv \theta_i \quad \ddot{\eta}_i \equiv \frac{M_i}{EI_i} \quad \dot{\dot{\eta}}_i \equiv \frac{T_i}{EI_i} \quad (4.21)$$

The modal force can be derived in terms of the beam parameter as

$$u_i(t) \equiv \frac{M_i}{EI_i} + 2\omega_i \zeta_i \theta_i + \omega_i^2 v_i \quad (4.22)$$

Thus all the parameters of optimality equations problem are converted into analogous beams problem. It should be emphasized that the beams are fictitious and each beam represents the time response of one mode of the vibrating structure considered. These fictitious beams are then solved by FEM and the results are converted back to the solution of optimal control problem. The flowchart detailing the procedure is shown in Fig 4.2. The FEM related calculations such as the modal analysis and solution of the analogous beams are done by ANSYS. The details of operations of the BA procedure are explained in [13, 14]. Here the procedure is first applied to the gantry crane problem with two DOFs and then to the frame structure that has a much larger number of DOFs and finally to determine optimal solutions for a suspension system.

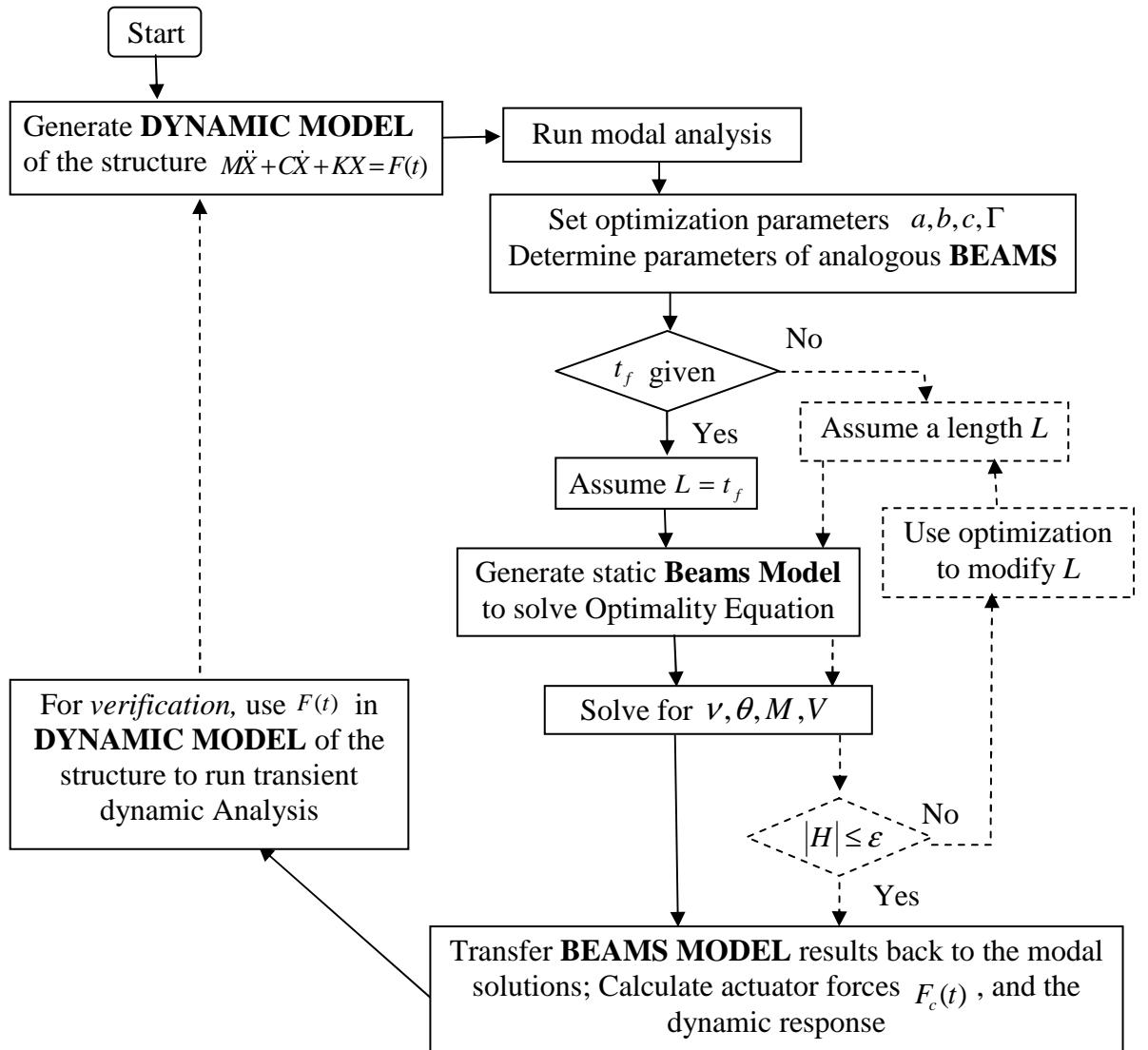


**Figure 4.2:** Flow chart for beam analogy

## 4.2 Example 1: Gantry crane controlled by two actuators

The gantry crane is modeled by two DOFs converted into two modes of motion. The IMSC methodology and the *BA* can only be used if two actuators are to control these two modes.

Let the performance index be

$$J = \frac{1}{2} \int_0^{t_f} (u_1^2 + u_2^2) dt \quad (4.23)$$

where the modal controls  $u_1$  and  $u_2$  in terms of forces  $F_{m1}$  and  $F_{m2}$  are given by Eq. (2.21).

Comparing this performance index with the Eq. (2.26), one obtains the weighting matrices defined by Eq. (4.8) as

$$Q_d = 0$$

$$Q_v = 0$$

$$R^{-1} = 1$$

$$\Gamma = 0 \text{ since the final time is given.}$$

This corresponds to the values of the parameters in the Eq. (4.8) being zero with the exception of  $c_1 = 1$ . Let, as before, the crane travel 4m distance starting from  $x(0) = -4m$  to  $x(t_f) = 0$  then the boundary conditions in the modal variables are

$$\text{IBCs: } \eta_1(0) = -219.089, \dot{\eta}_1(0) = \eta_2(0) = \dot{\eta}_2(0) = 0$$

$$\text{FBCs: } \eta_1(t_f) = \dot{\eta}_1(t_f) = \eta_2(t_f) = \dot{\eta}_2(t_f) = 0$$

Following the procedure through (4.1) to (4.9), the modal equations of the gantry crane take the form

$$\ddot{\eta}_1 = 0 \tag{4.24}$$

$$\ddot{\eta}_2 + 2\omega_2^2 \dot{\eta}_2 + \omega_2^4 \eta_2 = 0 \tag{4.25}$$

Two independent fictitious analogous beams are constructed for the above two equations (identical set of beams will be used to solve the frame problem shown in Fig. 4.4). For the first beam, comparing Eq. (4.24) with (4.13), the parameters are

$$EI_1 \equiv 1$$

$$P_{a1} \equiv 0 \tag{4.26}$$

$$k_{f1} \equiv 0$$

and the BCs are  $v_1(0) \equiv -219.089, \dot{v}_1(0) \equiv v_1(L) \equiv \dot{v}_1(L) \equiv 0$

Similarly, comparing (4.24) with (4.13) the second beam is formed.

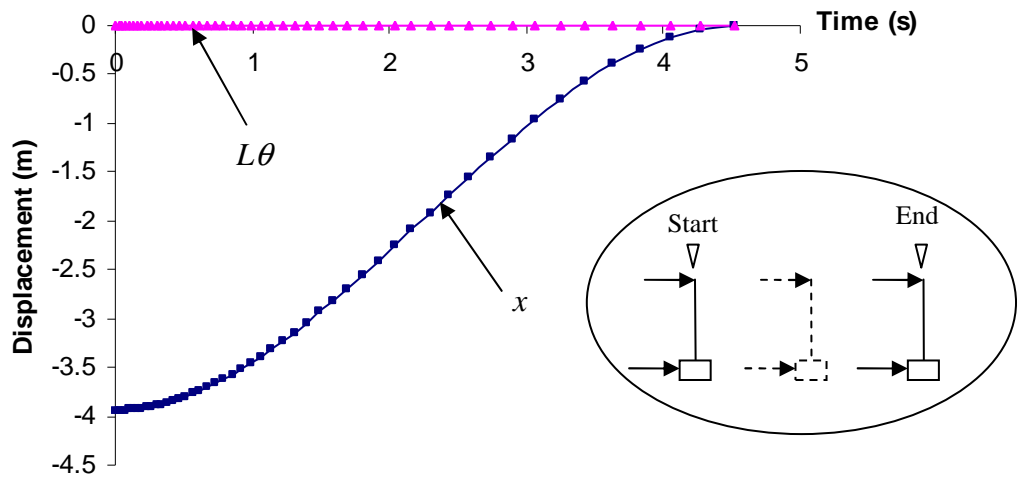
$$EI_2 \equiv 1$$

$$P_{a2} \equiv 2\omega_2^2 \tag{4.27}$$

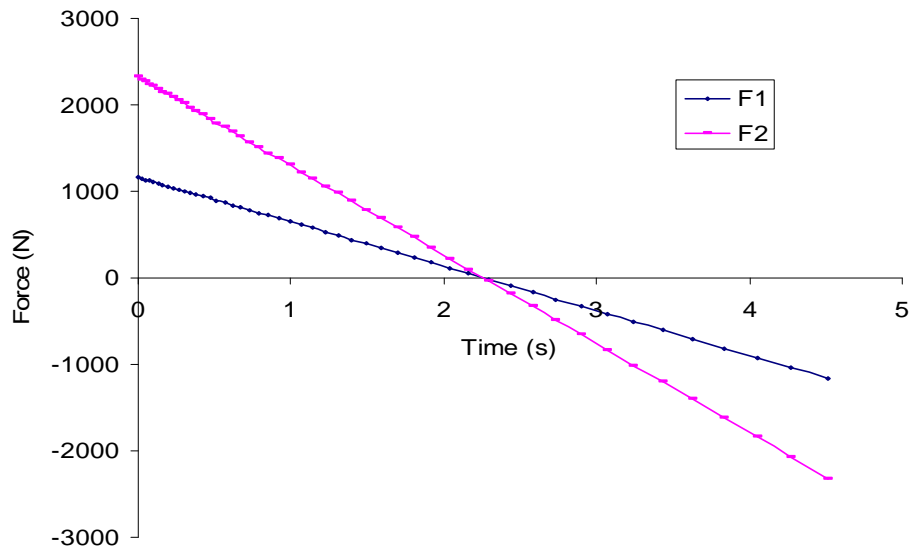
$$k_{f_2} \equiv \omega_2^4$$

and the BCs are  $v_2(0) \equiv \dot{v}_2(0) \equiv v_2(L) \equiv \dot{v}_2(L) \equiv 0$

Let the final time  $t_f = 4.51524 \text{ s}$  which means that  $L = 4.51524 \text{ m}$



(a)



(b)

**Figure 4.3:** (a) Plot of DOFs for gantry crane; (b) Actuator forces plot for gantry crane

These two fictitious beams are analyzed separately by FEM using forty eight beam elements to obtain  $v$ ,  $\theta$ ,  $M$  and shear force  $V$ . The results are converted back to the original case by using Eq. (4.20-22). The DOFs for gantry crane and the actuation forces are plotted in Fig. (4.3). The dots indicate the values calculated at the nodal points of the fictitious beams.

The gantry problem controlled by two forces is somewhat trivial. The optimal solution requires that two forces are applied on two masses in such a way that the angle  $\theta$  is always zero. In the first half of the maneuver, the masses accelerates while in second half decelerates to stop at  $t_f$ .

### 4.3 Example 2: Frame structure

A structure mentioned in section 2.1 (Fig. 2.1) is solved to illustrate the application of  $BA$  to a more complicated problem. More details of the frame are indicated in Fig. 4.4. The whole structure is modeled by about thirty real beam elements, mass element and ninety DOFs. The locations of some nodes are indicated in figure.

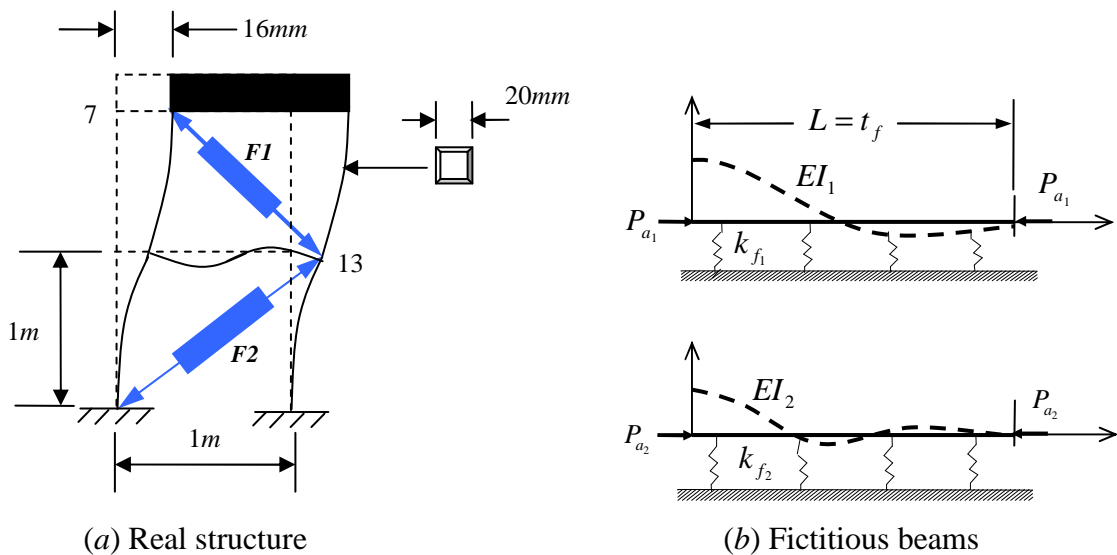


**Figure 4.4:**  $BA$  for Frame structure (disturbance exaggerated) with two actuators

A frame of  $20 \times 20 \text{mm}$  square tube with  $2 \text{mm}$  wall thickness is made up of aluminium and supports a mass of  $100 \text{Kg}$  on the top. In an initial disturbed configuration the node 7 is displaced by  $16 \text{mm}$ . Two actuators configured as shown and generating forces  $F1$  and

$F_2$  are applied to bring the structure to the rest. The modal analysis of frame is done by ANSYS. The first three modal frequencies are

$$\omega_1 = 4.736 \text{rad/s}, \omega_2 = 171.79 \text{rad/s} \text{ and } \omega_3 = 232.509 \text{rad/s}$$

This case was extensively analyzed in [13]. It was shown that it is sufficient to control only first two modes of vibrations. The initial deflections can be transformed into the initial boundary condition in the modal space for the two modes as

$$\eta_1(0) = 0.1604 \text{ and } \eta_2(0) = 0.0036$$

The performance index to be minimized is as follows

$$J = \frac{1}{2} \int_0^{t_f} [X^T Q_d X + \dot{X}^T Q_v \dot{X} + F^T R F + \Gamma] dt \quad (4.28)$$

To represent the energies the following weighting matrices are used.

$$\begin{aligned} Q_d &= a_2 K \\ Q_v &= b_1 M \\ R^{-1} &= c_2 K \end{aligned} \quad (4.29)$$

The optimal maneuver time will be obtained for  $\Gamma = 0.5$ .

Note that all the optimization parameters in the Eq. (4.8) equal to zero except  $a_2$ ,  $b_1$  and  $c_2$ . This way the terms in Eq. (4.28) have simple interpretation of the strain energy, elastic energy and the work of external forces respectively. Substituting the values of these parameters in Eq. (4.17-19), two fictitious beams can be formed with the following properties.

$$\begin{aligned} EI_i &\equiv \frac{1}{c_2 \omega_i^2} \\ P_{ai} &\equiv \frac{2}{c_2} - b_1 \\ k_{fi} &\equiv \left[ \omega_i^2 \frac{1}{c_2} + (a_2 \omega_i^2) \right] \end{aligned} \quad (4.30)$$

Where the values of  $a_2$ ,  $b_1$  and  $c_2$  have to be assumed.

Let these optimization parameters be

$$a_2 = 1, b_1 = 1, c_2 = 0.01$$

This implies that the following performance index is minimized.

$$J = \frac{1}{2} \int_0^{t_f} [X^T KX + \dot{X}^T M\dot{X} + 100F^T K^{-1}F + 0.5] dt \quad (4.31)$$

The optimum forces and displacement response are plotted in Fig. 4.5 (a) and (b) respectively. The actuation forces oscillates relatively fast for almost first half of the maneuver time. This can be attributed to the attempts of eliminating the vibrations of the second mode.

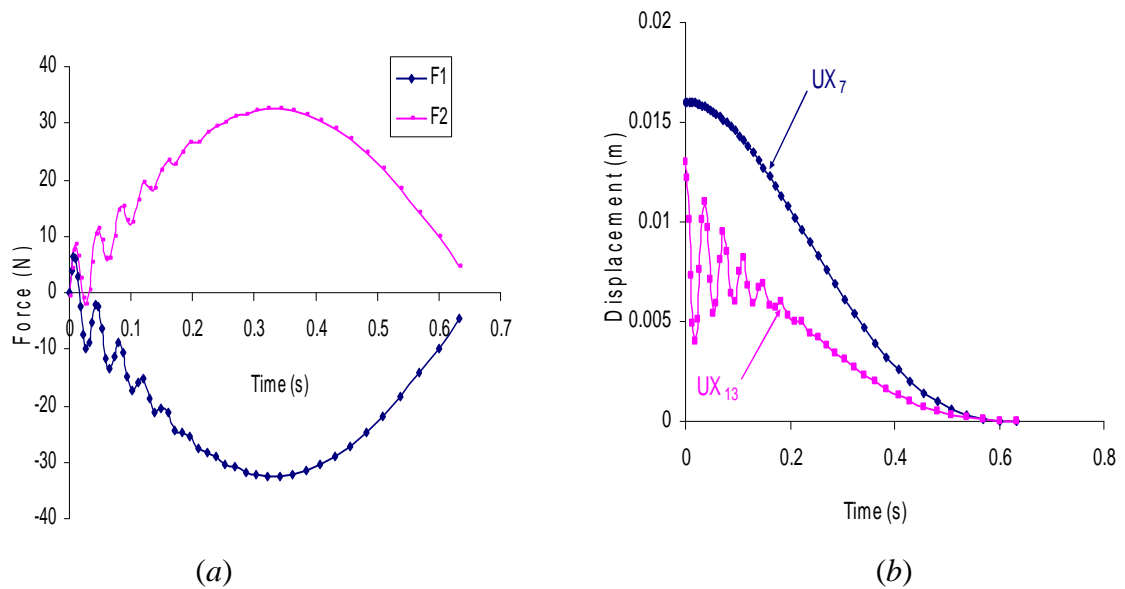


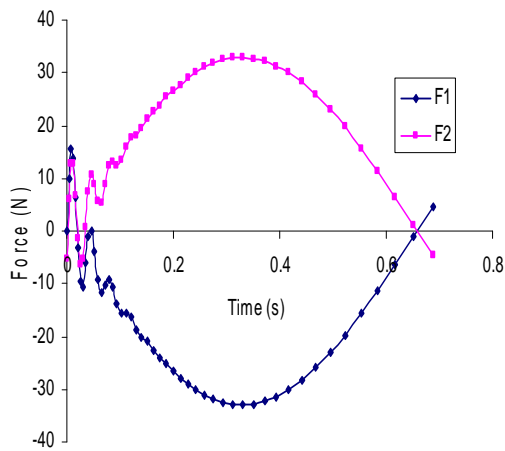
**Figure 4.5:** Force and displacement plots

The values of these optimization parameters can be changed to achieve different effects. The influences of  $a_2$ ,  $b_1$  and  $c_2$  on the performance of two bay frame structure are discussed one by one by changing the value of one parameter and keeping others constant. It should help to understand sensitivity of the system's optimal response to the values of these parameters.

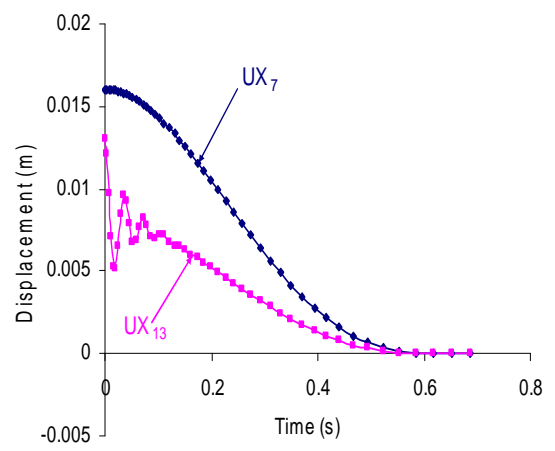
#### 4.4 Effect of $a_2$ on the performance of the system

This parameter controls the level of strain energy in the frame. Effects of increasing the value of  $a_2$  can be observed in Fig. 4.6.

**Case 1:**  $a_2=10$ ,  $b_1=1$ ,  $c_2=0.01$

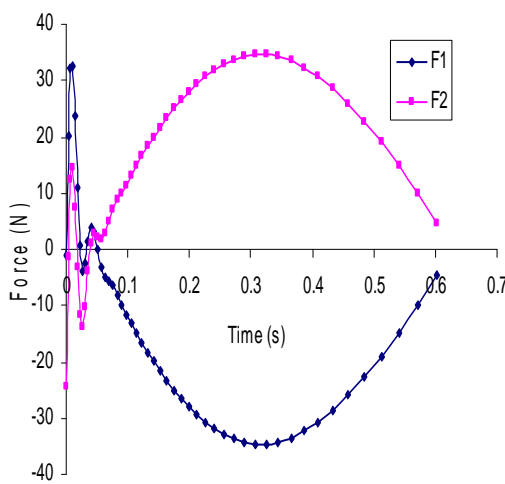


(a)

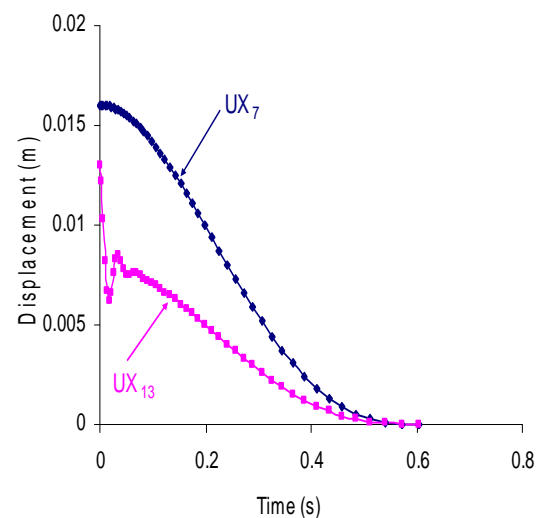


(b)

**Case 2:**  $a_2=50$ ,  $b_1=1$ ,  $c_2=0.01$



(c)



(d)



**Case 3:**  $a_2=100$ ,  $b_1=1$ ,  $c_2=0.01$

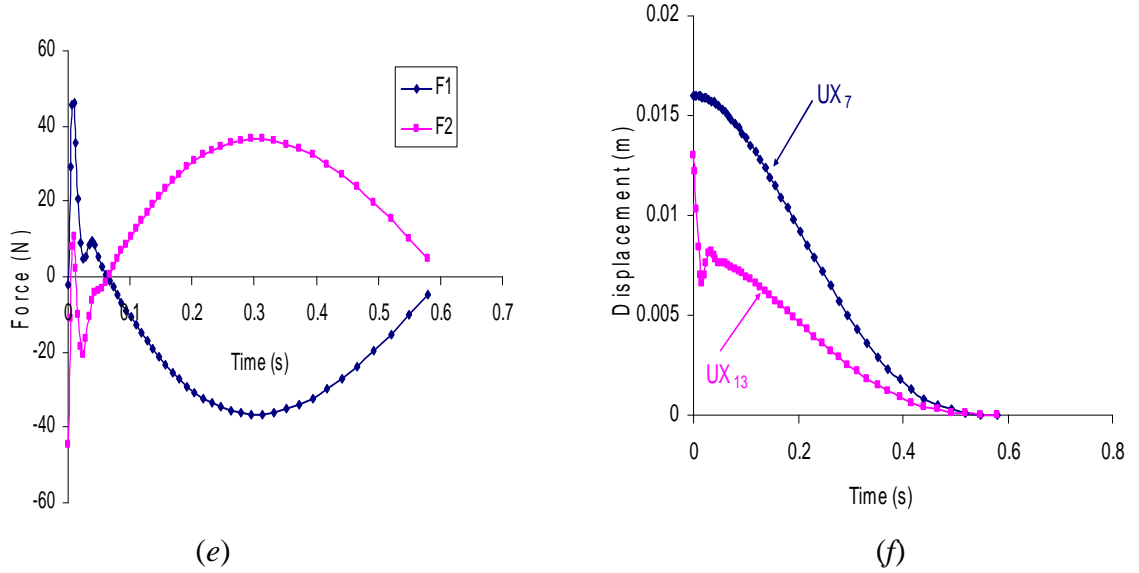


**Figure 4.6:** Force and displacement plot for different values of  $a_2$

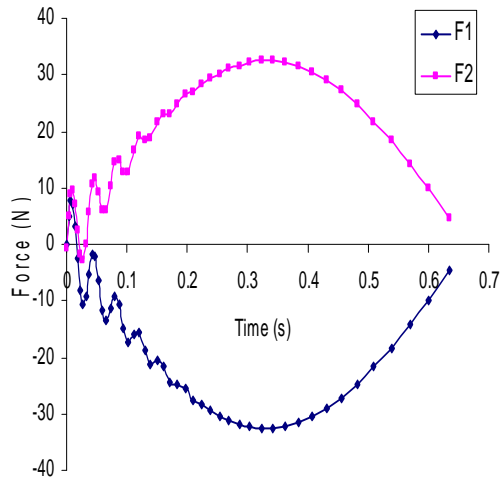
It can be noted that as  $a_2$  increases, the vibrations of the second mode are eliminated faster, the actuation forces oscillates less (their maximum value remains almost unaltered) and the value of final time reduces.

#### 4.5 Effect of parameter $b_1$ on the performance of a system

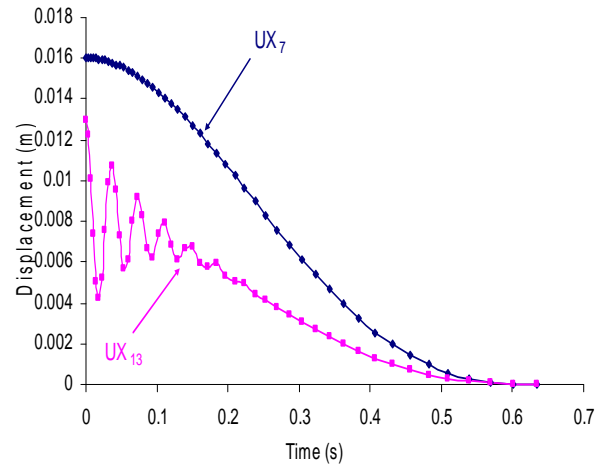
This parameter controls the level of kinetic energy in the frame. Effects of increasing the value of  $b_1$  can be observed in Fig. 4.7. It can be noted that as the value of  $b_1$  increases, the vibration (peaks at the start of  $UX_{13}$ ) in the second mode reduces rapidly. If the value of  $b_1$  is bigger the optimization process try to reduce the kinetic energy of a system faster.

As the kinetic energy and the elastic energy in the vibration system are correlated to each other, the effect of  $a_2$  and  $b_1$  on the system is almost the same.

**Case 1:**  $b_1=2, a_2=1, c_2=0.01$

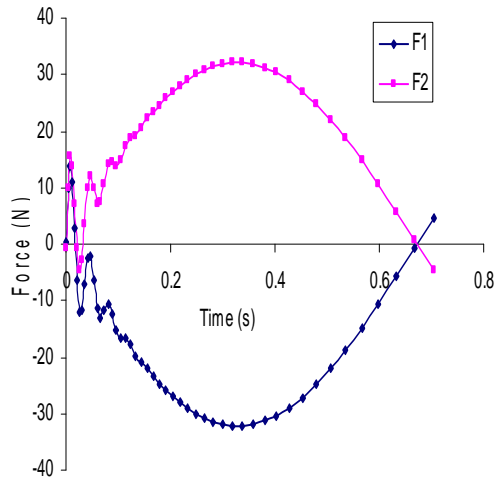


(a)

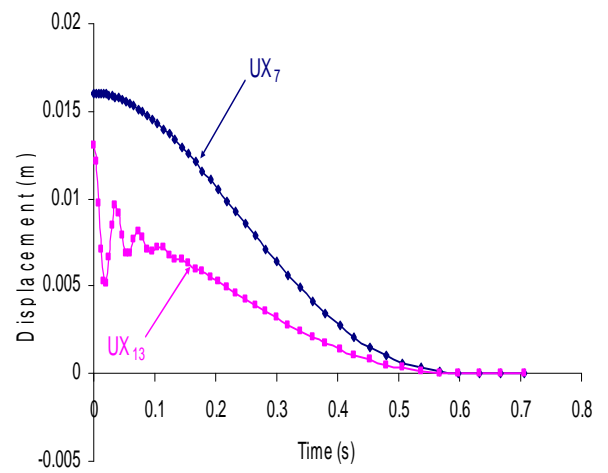


(b)

**Case 2:**  $b_1=10, a_2=1, c_2=0.01$



(c)



(d)

**Case 3:**  $b_1 = 30$ ,  $a_2 = 1$ ,  $c_2 = 0.01$

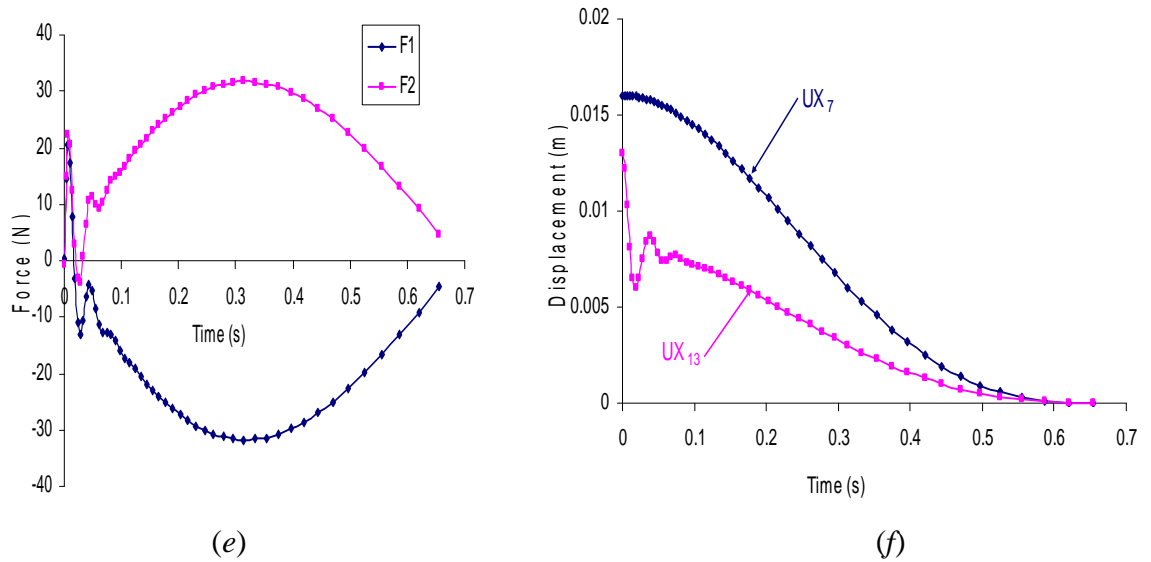
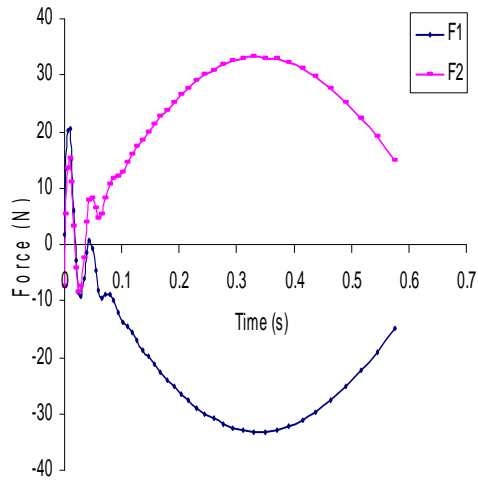


**Figure 4.7:** Force and displacement plot for different values of  $b_1$

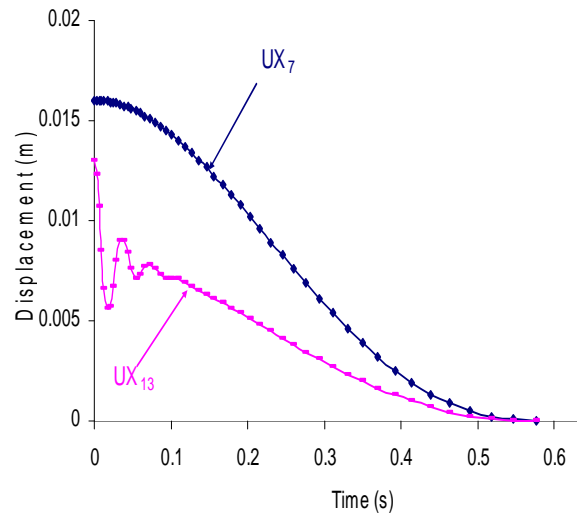
#### 4.6 Effect of parameter $c_2$ on the actuator forces

This parameter controls the work done by actuators and affects mostly the value of actuator forces. The effect of this parameter on the system is studied by changing the value of  $c_2$  and keeping  $a_2 = b_1 = 1$ . Various cases are compared by plotting forces and displacements in Fig. 4.8.

**Case 1:**  $c_2 = 0.1$ ,  $b_1 = 1$ ,  $a_2 = 1$

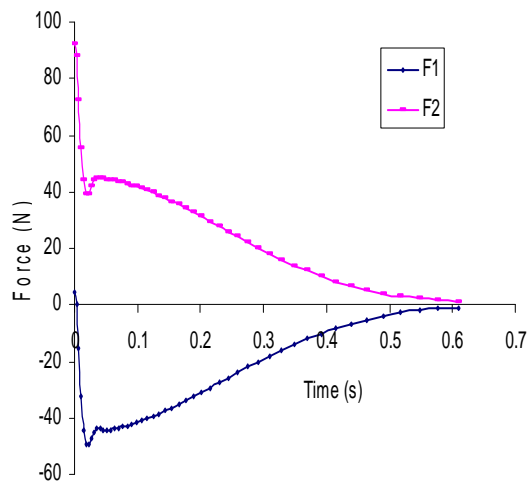


(a)

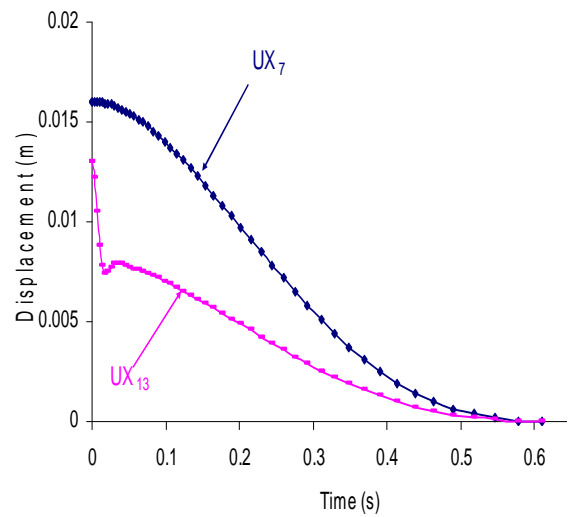


(b)

**Case 2:**  $c_2 = 1$ ,  $b_1 = 1$ ,  $a_2 = 1$

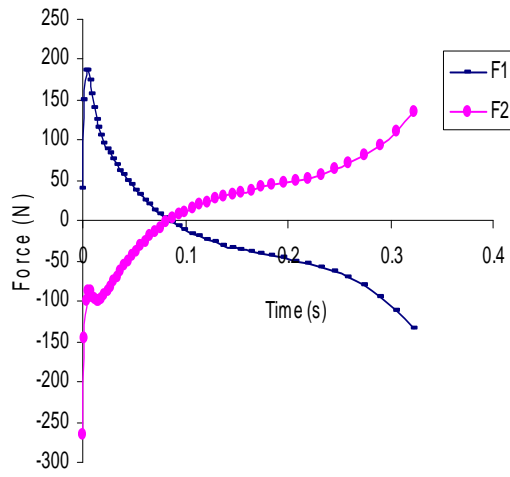


(c)

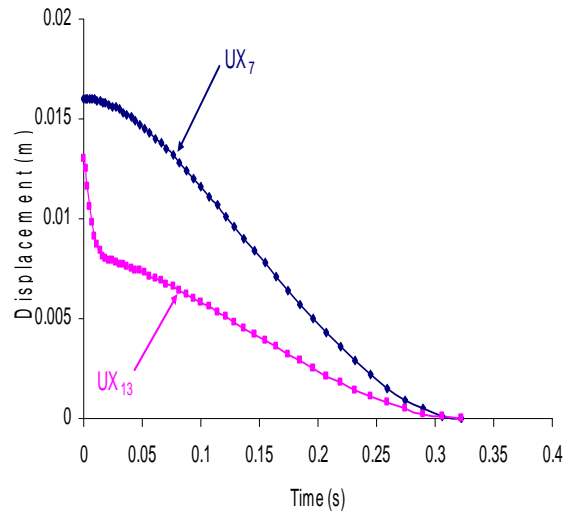


(d)

**Case 3:**  $c_2=8, b_1=1, a_2=1$

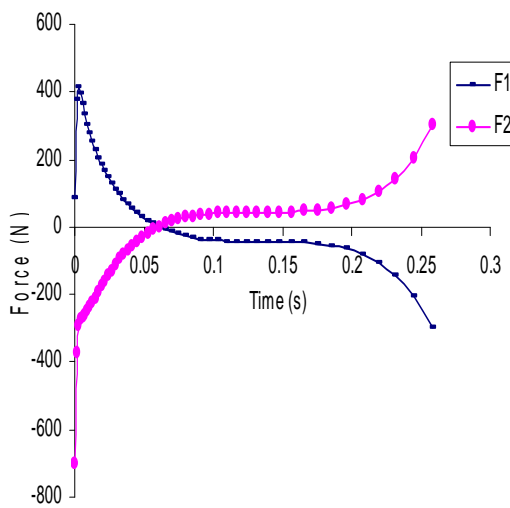


(e)

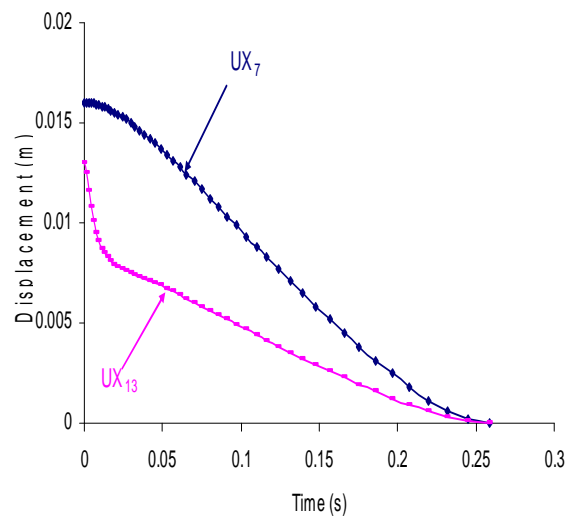


(f)

**Case 4:**  $c_2=40, b_1=1, a_2=1$



(g)



(h)

**Figure 4.8:** Force and displacement plot for different values of  $c_2$

The absolute maximum force  $|F_{\max}|$  (N) to be generated in either actuator for all the plots are tabulated in Table 4.1

$c_2$	$ F_{\max} $
0.1	33.138
1	92.213
4	167.23
8	265.61
15	393.22
40	699.03
80	1030.66

**Table 4.1:**  $|F_{\max}|$  values for  $c_2$

The tabulated values are plotted in Fig. 4.9 in terms of  $1/c_2$ .

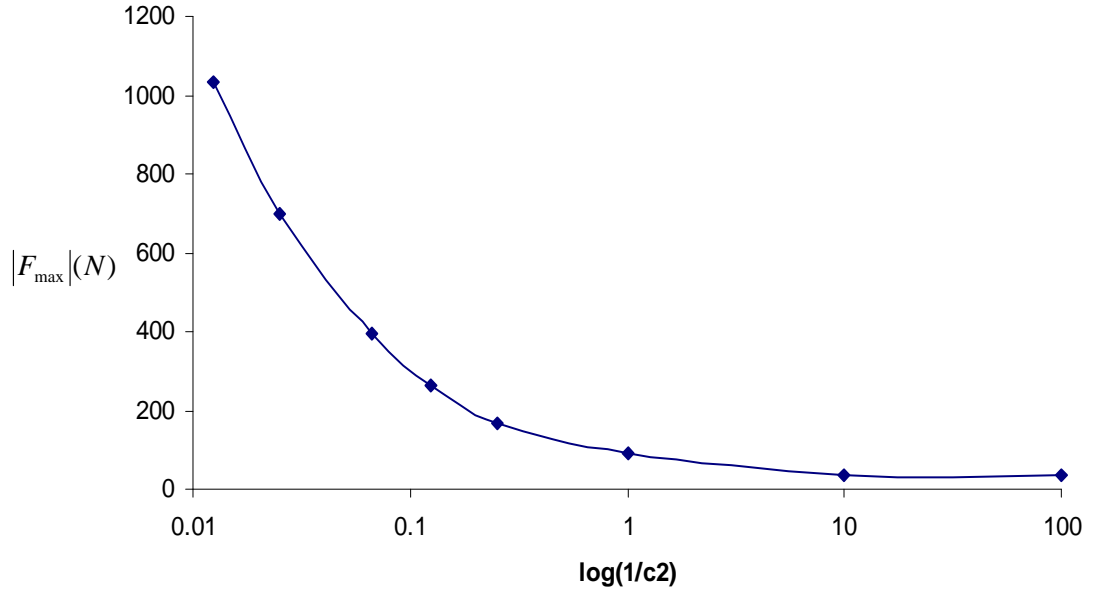


**Figure 4.9:** Plot of  $|F_{\max}|$  versus  $1/c_2$ , when  $a_2=1$ ,  $b_1=1$

As the value of  $1/c_2$  increases, it imposes bigger penalty on the force term, which results in smaller values of forces. For reduction of the actuator work, value of

$1/c_2$  should be bigger. The value of optimal time also reduces with the decrease in the value of  $1/c_2$ .

It can also be noted that the behavior of the forces changes with the change in  $c_2$  as seen in the Fig. 4.8-*a,c,e*. For  $c_2 = 0.1$  and  $0.01$ , the forces are relatively small initially which allows for the more oscillations of the system (examine the plots of  $UX_{13}$ ).

The vibrations are attenuated without any oscillations for  $c_2 \geq 8$ . Thus, for the problem considered, the actuators will provide undercritical active damping if  $c_2 < 8$ , while the damping will be overcritical for  $c_2 > 8$ .

### 4.7 Example 3: Suspension system

A suspension system shown in the Fig. 4.10 is one of the simplest vibrating systems which can be controlled passively and actively by applying one actuator as well as two actuators. Such a system is routinely used to represent the suspension of a car (see [15] for example).

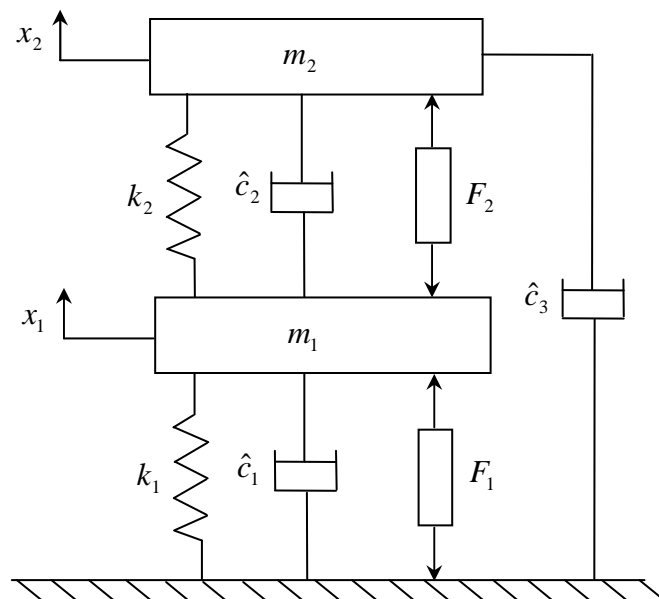


**Figure 4.10:** Suspension System

Mass  $m_2$  is to represent a quarter of the car's mass, while  $m_1$  the mass of one wheel with attachments. Usually,  $k_1$  corresponds to the tire stiffness and  $k_2$  to the stiffness of a spring in the shock absorber installed. Therefore, typically  $m_2 \gg m_1$  and  $k_2 \ll k_1$ . Optimal actuator forces are to be calculated to control the vibrations when system is released from the initial disturbed position. In this chapter the *BA* is used to solve the problem with two actuators. The overdetermined problem with one actuator will be solved in the next chapter.

Formally, Rayleigh's damping can be used here if the third viscous damper is added in parallel to other two dampers.

The equations of motion for such a system can be written as,

$$\begin{bmatrix} m_1 & 0 \\ 0 & m_2 \end{bmatrix} \begin{bmatrix} \ddot{x}_1 \\ \ddot{x}_2 \end{bmatrix} + \begin{bmatrix} \hat{c}_1 + \hat{c}_2 & -\hat{c}_2 \\ -\hat{c}_2 & \hat{c}_2 + \hat{c}_3 \end{bmatrix} \begin{bmatrix} \dot{x}_1 \\ \dot{x}_2 \end{bmatrix} + \begin{bmatrix} k_1 + k_2 & -k_2 \\ -k_2 & k_2 \end{bmatrix} \begin{bmatrix} x_1 \\ x_2 \end{bmatrix} = \begin{bmatrix} 1 & -1 \\ 0 & 1 \end{bmatrix} \begin{bmatrix} F_1 \\ F_2 \end{bmatrix} \quad (4.32)$$

Let the data for suspension system be

$m_1 = 40kg$  ,  $m_2 = 200kg$  ,  $k_1 = 235440N/m$  ,  $k_2 = 39240N/m$  and the internal damping of 15% (damping coefficients  $\xi_1 = \xi_2 = 0.15$ ).

The modal analysis is done the same way as performed in chapter II. The natural frequencies are

$$\omega_1 = 12.94105rad/s , \omega_2 = 83.040527rad/s$$

Modal shape function is

$$\phi = \begin{bmatrix} 0.0103319 & 0.157776 \\ 0.0705596 & -0.0046204 \end{bmatrix}$$

$$\text{Let, } u = \phi^T F \quad (4.33)$$

$$\text{where } u = \begin{bmatrix} u_1 \\ u_2 \end{bmatrix} \text{ and } F = \begin{bmatrix} F_1 - F_2 \\ F_2 \end{bmatrix}$$

$$\text{Let, } x = \phi \eta \quad (4.34)$$

For Rayleigh's damping,

$$\hat{c}_i = \alpha M_i + \beta K_i \quad (4.35)$$

Substituting (4.34-35) in (4.32) and using modal properties one can write



$$\begin{bmatrix} \dot{\eta}_1 \\ \dot{\eta}_2 \end{bmatrix} + \begin{bmatrix} \alpha + \beta\omega_1^2 & 0 \\ 0 & \alpha + \beta\omega_2^2 \end{bmatrix} \begin{bmatrix} \eta_1 \\ \eta_2 \end{bmatrix} = \begin{bmatrix} u_1 \\ u_2 \end{bmatrix} \quad (4.36)$$

The values of constants  $\alpha$  and  $\beta$  can be obtained by solving following equation for  $i = 1, 2$

$$2\xi_i\omega_i = \alpha + \beta\omega_i^2 \quad (4.37)$$

Substituting values in Eq. (4.37),

$$\alpha = 3.358868$$

$$\beta = 0.0031255998$$

The values of  $\hat{c}_1, \hat{c}_2, \hat{c}_3$  can be obtained from following equation.

$$\phi^T C \phi = \begin{bmatrix} \alpha + \beta\omega_1^2 & 0 \\ 0 & \alpha + \beta\omega_2^2 \end{bmatrix}$$

solving above equation

$$\hat{c}_1 = 870.33726 N.s/m, \hat{c}_2 = 122.63361 N.s/m, \hat{c}_3 = 671.7959 N.s/m$$

Let, the performance index to be minimized is as follows

$$J = \frac{1}{2} \int_0^{t_f} [X^T Q_d X + \dot{X}^T Q_v \dot{X} + F^T R F + \Gamma] dt \quad (4.38)$$

As before, to represent the energies in performance index, the following weighting matrices are used.

$$Q_d = a_2 K$$

$$Q_v = b_1 M \quad (4.39-a,b,c)$$

$$R^{-1} = c_2 K$$

The optimal maneuver time is  $t_f = 2s$  and  $\Gamma = 0$ .

Note that as before, all the optimization parameters in the Eq. (4.8) are equal to zero except  $a_2$ ,  $b_1$  and  $c_2$ . Substituting the values of these parameters in Eq. (4.17-19), two analogous beams can be formed with the following properties.

$$EI_i \equiv \frac{1}{c_2 \omega_i^2}$$

$$P_{ai} \equiv \frac{2}{c_2} - b_1 + \frac{4\zeta_i^2}{c_2} \quad (4.40-a,b,c)$$

$$k_{fi} \equiv \omega_i^2 \left( \frac{1}{c_2} + a_2 \right) \quad i = 1,2$$

It can be noted that, the damping affects only the term  $P_{ai}$  and increases the axial force applied on the beam.

Let the optimization parameters be

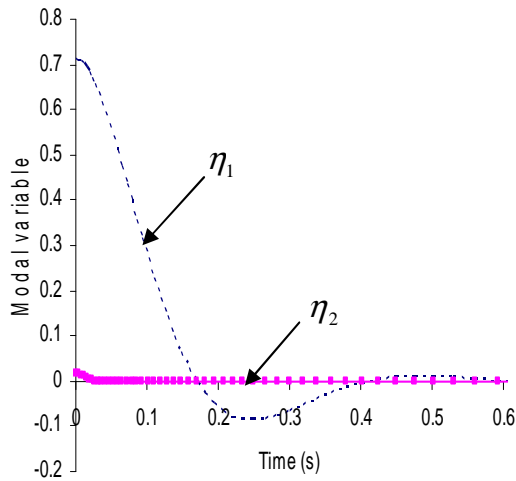
$$a_2 = 1, b_1 = 1, c_2 = 1$$

The boundary conditions are

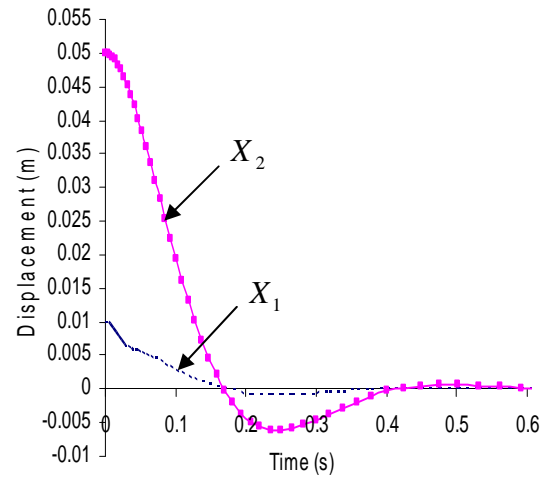
$$\text{IBC: } x_1(0) = 10\text{mm}, x_2(0) = 50\text{mm}, \dot{x}_1(0) = 0, \dot{x}_2(0) = 0$$

$$\text{FBC: } x_1(t_f) = 0, x_2(t_f) = 0, \dot{x}_1(t_f) = 0, \dot{x}_2(t_f) = 0$$

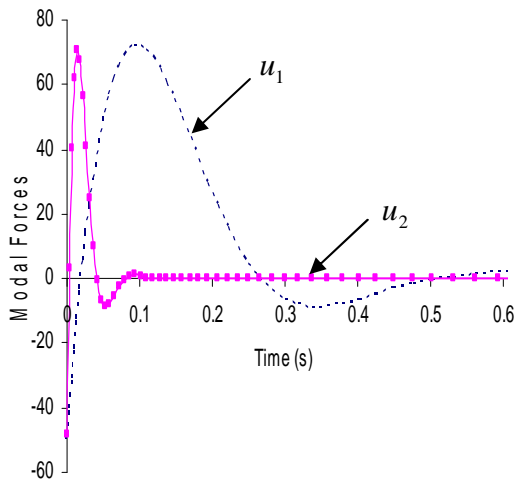
The displacements and optimum forces are plotted in Fig. 4.11 by running the *BA* program. For the better visibility, the plots are shown for a short period of 0.6s, as the system is almost at rest after around 0.6s.



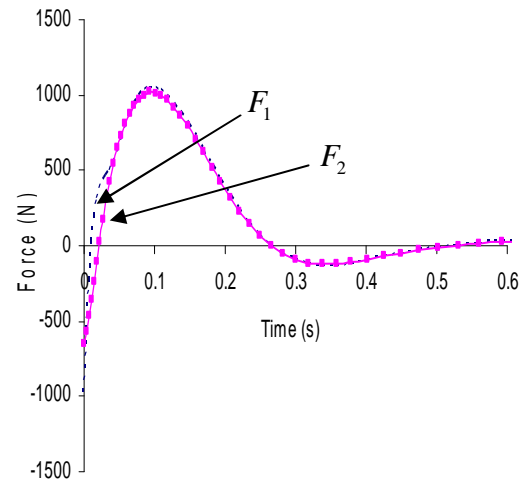
(a)



(b)



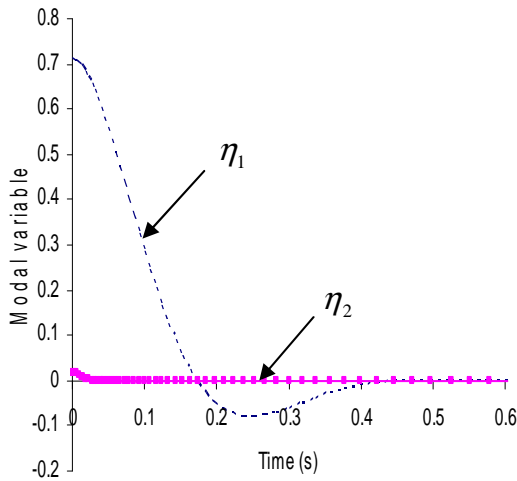
(c)



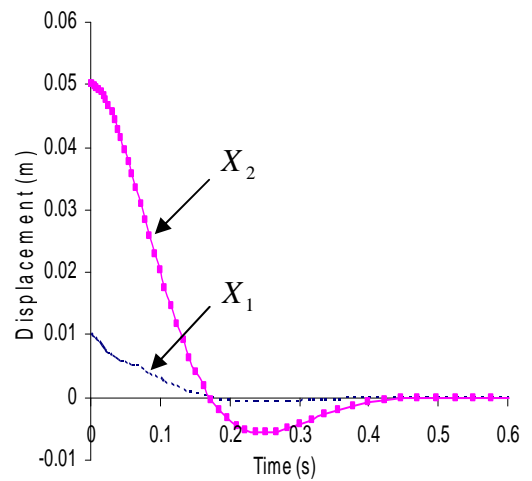
(d)

**Figure 4.11:** The results for suspension system with dampers ( $\xi_1 = \xi_2 = 0.15$ )

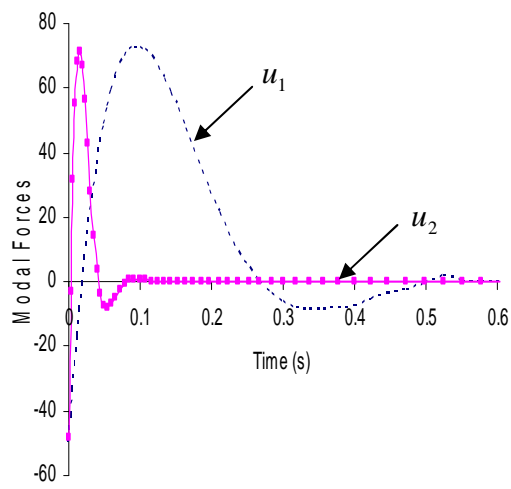
Such a fast vibration attenuation is essentially due to the action of actuators. For comparison purposes the *BA* analysis is repeated for the suspension system without dampers ( $\xi_1 = \xi_2 = 0$ ). The plots of zero damping case are presented in Fig 4.12.



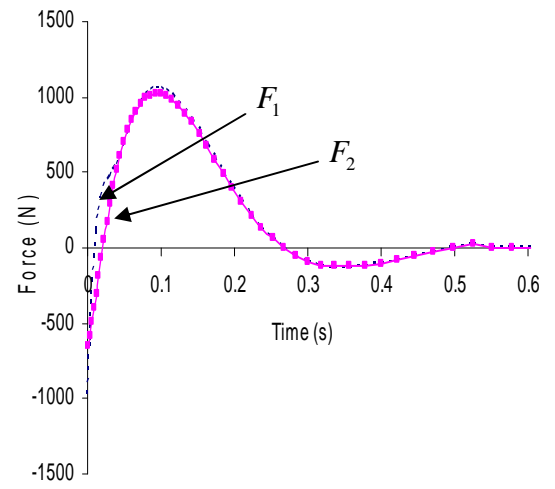
(a)



(b)



(c)



(d)

**Figure 4.12:** The results for suspension system without dampers

It can be noted that the difference between the two cases is negligible.

## 5. APPLICATION OF LAGRANGE MULTIPLIERS – A NEW METHODOLOGY

### 5.1 Introduction

The solution techniques of optimal control problem presented in the previous chapter allowed for decoupling the modes so that it was possible to solve each mode independently, including the modal controls. Such an approach, especially when combined with the  $BA$  is very efficient numerically, but can be applied only to the determined problems in which the number of actuators is the same as the number of modes to control. As shown in chapter II, the overdetermined problem can also be analysed in the modal space but then the number of extra constraints in the form of Eq. (2.25) must be imposed on the modal controls. Usually, in general optimization strategies, most of constraints can be handled by using constant Lagrange multipliers. In optimal control the extra constraints require the Lagrange multipliers that are functions of time. Here the modified optimality equations that include these time dependent Lagrange multipliers are derived and then solved. This method is first applied to the overdetermined gantry crane problem and then extended to more complicated problems.

### 5.2 Gantry crane problem by new methodology

Consider the gantry crane problem as a two mode problem governed by Eq. (2.22) with an extra constraint (2.25) imposed on the modal controls. The performance index for such a problem can formally be assumed as (see Eq. (3.7))

$$J = \frac{1}{2} \int_0^{t_f} (u_1^2 + u_2^2) dt \quad (5.1)$$

The constraint (2.25) can be written in the form

$$h(u_1, u_2) = u_1 - d_2 u_2 = 0 \quad (5.2)$$

where  $d_2 = \frac{1}{j} = \frac{1}{\sqrt{2}}$  for the gantry crane solved in chapter III.

Now instead of Hamiltonian given by Eq. (3.8), the augmented Hamiltonian has to be considered

$$\hat{H} = H + \nu h \quad (5.3)$$

where  $\nu$  is a Lagrange multiplier.

Substituting for  $H$  and  $h$  one obtains

$$\hat{H} = -\frac{1}{2}(u_1^2 + u_2^2) + P_1 z_2 + P_2 u_1 + P_3 z_4 + P_4(-\omega_2^2 z_3 + u_2) + \nu(u_1 - d_2 u_2) \quad (5.4)$$

The approach presented in chapter III will change only in this sense that now the optimal controls must satisfy the following equations (instead of Eq. (3.15)).

$$\frac{\partial \hat{H}}{\partial u_1} = \frac{\partial \hat{H}}{\partial u_2} = 0 \quad (5.5-a,b)$$

From Eq. (5.5-a,b) one obtains

$$\begin{aligned} u_1 &= P_2 + \nu \\ u_2 &= P_4 - d_2 \nu \end{aligned} \quad (5.6-a,b)$$

Substituting (5.6) into the state equations (3.2) and (3.3), one can express the costates in terms of the modal variables and the multiplier  $\nu$  as

$$\begin{aligned} P_2 &= \dot{\eta}_1 - \nu \\ P_4 &= \dot{\eta}_2 + \omega_2^2 \eta_2 + d_2 \nu \end{aligned} \quad (5.7-a,b)$$

Substituting (5.7) in the costate equations (3.13 - 3.14) gives the optimality equations in the form

$$\ddot{\eta}_1 - \ddot{\nu} = 0 \quad (5.8)$$

$$\ddot{\eta}_2 + 2\omega_2^2 \dot{\eta}_2 + \omega_2^4 \eta_2 + d_2(\ddot{\nu} + \omega_2^2 \nu) = 0 \quad (5.9)$$

Eq. (5.2), using the equation of motion, can be written in the form

$$\dot{\eta}_1 - d_2(\dot{\eta}_2 + \omega_2^2 \eta_2) = 0 \quad (5.10)$$

Eq. (5.8-10) constitute a set of three ordinary differential equations (ODE) with three unknown functions  $\eta_1$ ,  $\eta_2$  and  $\nu$ . These equations can be solved by eliminating variables. Differentiate Eq. (5.10) twice

$$\ddot{\eta}_1 - d_2(\ddot{\eta}_2 + \omega_2^2 \eta_2) = 0 \quad (5.11)$$

Next, substitute (5.10-11) into (5.9) to obtain

$$\ddot{\eta}_1 + d_2^2 \ddot{v} + \omega_2^2 (\ddot{\eta}_1 + d_2^2 v) = 0 \quad (5.12)$$

Then, substitute (5.8) in the above equation to obtain

$$\ddot{v} + d_2^2 \ddot{v} + \omega_2^2 (\ddot{\eta}_1 + d_2^2 v) = 0 \quad (5.13)$$

Finally, differentiating above equation twice and substituting  $\ddot{\eta}_1 = \ddot{v}$  from Eq. (5.8) one obtains

$$\ddot{v} + \omega_2^2 \ddot{v} = 0 \quad (5.14)$$

Note that, four differentiation operations were performed, which means that the solution will have four more integration constants than the original problem.

Eq. (5.14) is only in terms of  $v$  and can be integrated to obtain

$$v = C_1 + C_2 t + C_3 \cos(\omega_2 t) + C_4 \sin(\omega_2 t) \quad (5.15)$$

Differentiating twice and substituting into Eq. (5.8) one obtains

$$\ddot{\eta}_1 = -C_3 \omega_2^2 \cos(\omega_2 t) - C_4 \omega_2^2 \sin(\omega_2 t) \quad (5.16)$$

Integrating the above equation we have

$$\eta_1 = \frac{1}{6\omega_2^2} \left\{ -6C_3 \cos(\omega_2 t) - 6C_4 \sin(\omega_2 t) + \omega_2^2 (C_5 t^3 + 3C_6 t^2 + 6C_7 t + 6C_8) \right\} \quad (5.17)$$

Similarly, substituting (5.15) in (5.9) and integrating one obtains

$$\eta_2 = -\frac{C_2 t + C_1}{\omega_2^2} d_2 + C_9 \cos(\omega_2 t) + C_{10} \sin(\omega_2 t) + C_{11} \cos(\omega_2 t)t + C_{12} \sin(\omega_2 t)t \quad (5.18)$$

Eq. (5.15,17,18) contain twelve integration constants. These constants must satisfy four equations that can be obtained by comparing the terms of Eq. (5.10) when  $\eta_1$  and  $\eta_2$  are substituted. This equation takes the form

$$2d_2 C_{12} \omega_2 \cos(\omega_2 t) - 2d_2 C_{11} \omega_2 \sin(\omega_2 t) - d_2^2 C_2 t - d_2^2 C_1 = C_3 \cos(\omega_2 t) + C_4 \sin(\omega_2 t) + C_5 t + C_6 \quad (5.19)$$

To have identical coefficients on both the RHS and LHS terms the following is required

$$\begin{aligned}
C_3 &= \sqrt{2}C_{12}\omega_2 \\
C_4 &= -\sqrt{2}C_{11}\omega_2 \\
C_5 &= -\frac{C_2}{2} \\
C_6 &= -\frac{C_1}{2}
\end{aligned} \tag{5.20-a,b,c,d}$$

Substituting back into Eq. (5.15,17,18), one obtains the following functions containing eight integration constants.

$$\begin{aligned}
v &= C_1 + C_2t + \sqrt{2}\omega_2[C_{12}\cos(\omega_2t) - C_{11}\sin(\omega_2t)] \\
\eta_1 &= \frac{1}{6\omega_2^2} \left\{ -\frac{\omega_2^2 t^2 (3C_1 + C_2 t)}{2} + 6\omega_2^2 (C_7 t + C_8) - 6\sqrt{2}\omega_2 [C_{12}\cos(\omega_2t) - C_{11}\sin(\omega_2t)] \right\} \\
\eta_2 &= -\frac{C_2 t + C_1}{\omega_2^2} d_2 + C_9 \cos(\omega_2t) + C_{10} \sin(\omega_2t) + C_{11} \cos(\omega_2t)t + C_{12} \sin(\omega_2t)t \quad (5.21-a,b,c)
\end{aligned}$$

These eight constants can be determined from the eight boundary conditions for the modal variables, which can be written as

$$\begin{aligned}
\eta_1(0) &= 0 & \eta_1(t_f) &= a\sqrt{M+m} = 219.089 \\
\dot{\eta}_1(0) &= 0 & \dot{\eta}_1(t_f) &= 0 \\
\eta_2(0) &= 0 & \eta_2(t_f) &= 0 \\
\dot{\eta}_2(0) &= 0 & \dot{\eta}_2(t_f) &= 0
\end{aligned} \tag{5.21-d}$$

The numerical values of constants are

$$\begin{aligned}
C_1 &= -135.554 & C_9 &= -6.51388 \\
C_2 &= 60.0461 & C_{10} &= 0.341089 \\
C_7 &= -2.23025 & C_{11} &= 1.57702 \\
C_8 &= -0.55816 & C_{12} &= -1.51398
\end{aligned} \tag{5.21-e}$$

Substituting into Eq. (5.21) one obtains

- the Lagrange multiplier function

$$v = -135.554 + 60.0461t - 8.21326\cos(\omega_2t) - 8.55523\sin(\omega_2t) \tag{5.22}$$

- the modal variables



$$\eta_1 = -0.55816 - 2.23024t + 33.888t^2 - 5.0038t^3 + 0.5582 \cos(\omega_2 t) + 0.5814 \sin(\omega_2 t) \quad (5.23)$$

$$\eta_2 = 6.5138 - 2.885t + (1.577 \cdot t - 6.51388) \cos(\omega_2 t) + (0.3411 - 1.514 \cdot t) \sin(\omega_2 t) \quad (5.24)$$

Note that Eq. (5.23-24) are the same as Eq. (3.23-24) that were obtained in chapter III without using Lagrange multipliers. It can also be noted that, for this particular gantry crane problem, Eq. (5.8-10) are simple enough to be solved by eliminating variables. However, this procedure might not be feasible to use for more complicated problems. A generalized procedure that applies the Lagrange multipliers is derived in the next section.

### 5.3 Some generalization – the use of differential operators

The above method is first generalized to an arbitrary two modal frictionless system controlled by one actuator, and finally to a general overdetermined system. Also, in this chapter differential operators are introduced. The performance index for a two modal system can be written in the form

$$J = \frac{1}{2} \int_0^{t_f} \sum_{i=1}^2 (\hat{Q}_{dii} \eta_i^2 + \hat{Q}_{vii} \dot{\eta}_i^2 + \hat{R}_{ii} u_i^2 + \Gamma) dt \quad (5.25)$$

where  $\hat{Q}_{dii}$ ,  $\hat{Q}_{vii}$  and  $\hat{R}_{ii}$  are defined in chapter IV (see Eq. (4.10)).

The modal variables and controls satisfy the equations of motion

$$\ddot{\eta}_i + \omega_i^2 \eta_i = u_i \quad i = 1, 2 \quad (5.26)$$

and the constraint

$$h(u_1, u_2) = g_1 u_1 + g_2 u_2 = 0 \quad (5.27)$$

where  $g_i$  are known constants.

As before, the augmented Hamiltonian is defined as

$$\begin{aligned} \hat{H} = & -\frac{1}{2} \left\{ \sum_{i=1}^2 (\hat{Q}_{dii} \eta_i^2 + \hat{Q}_{vii} \dot{\eta}_i^2 + \hat{R}_{ii} u_i^2 + \Gamma) \right\} + P_1 \dot{\eta}_1 \\ & + P_2 [u_1 - \omega_1^2 \eta_1] + P_3 \dot{\eta}_2 + P_4 [u_2 - \omega_2^2 \eta_2] + v h \end{aligned} \quad (5.28)$$

The optimal control must satisfy

$$\frac{\partial \hat{H}}{\partial u_1} = \frac{\partial \hat{H}}{\partial u_2} = 0 \quad (5.29)$$

Now, one can proceed similarly as with  $\hat{H}$  defined by Eq. (5.4). Using the above equations first the costates (see (5.7)) and then modal controls (see (5.6)) can be eliminated. The optimality equations in terms of the modal variables  $\eta_1$ ,  $\eta_2$  and the multiplier  $v$  takes the form (instead of (5.8-9))

$$\begin{aligned} \hat{R}_{11}\ddot{\eta}_1 + (2\hat{R}_{11}\omega_1^2 - \hat{Q}_{v11})\dot{\eta}_1 + (\hat{R}_{11}\omega_1^4 + \hat{Q}_{d11})\eta_1 - g_1(\ddot{v} + \omega_1^2 v) &= 0 \\ \hat{R}_{22}\ddot{\eta}_2 + (2\hat{R}_{22}\omega_2^2 - \hat{Q}_{v22})\dot{\eta}_2 + (\hat{R}_{22}\omega_2^4 + \hat{Q}_{d22})\eta_2 - g_2(\ddot{v} + \omega_2^2 v) &= 0 \end{aligned} \quad (5.30-a,b)$$

The constraint (5.27) can be rewritten as

$$g_1(\ddot{\eta}_1 + \omega_1^2 \eta_1) + g_2(\ddot{\eta}_2 + \omega_2^2 \eta_2) = 0 \quad (5.30-c)$$

Eq. (5.30) represent a general form of the set (5.8-10) that was solved by direct elimination of variables in the previous section. However, it could be much more difficult to apply this approach to solve Eq. (5.30). Instead, the solution to these differential equations can be formalized using the symbolic differential operator defined as

$$D^n = \frac{d^n}{dt^n}$$

For example, Eq. (5.30-a) can be written in the form

$$\left[ \hat{R}_{11}D^4 + (2\hat{R}_{11}\omega_1^2 - \hat{Q}_{v11})D^2 + (\hat{R}_{11}\omega_1^4 + \hat{Q}_{d11}) \right] \eta_1 - g_1(D^2 + \omega_1^2)v = 0 \quad (5.31)$$

or in short

$$E_1 \eta_1 - g_1(D^2 + \omega_1^2)v = 0 \quad (5.32)$$

where

$$E_1 = \hat{R}_{11}D^4 + (2\hat{R}_{11}\omega_1^2 - \hat{Q}_{v11})D^2 + (\hat{R}_{11}\omega_1^4 + \hat{Q}_{d11}) \quad (5.33)$$

is a fourth order differential operator containing a linear combination of operators  $D^n$ .

Eq. (5.30-b) can be written in a similar form with  $E_1$  replaced by  $E_2$  (with indices “1” replaced by “2”). The above notation allows writing the set (5.30) in the short form as

$$\begin{aligned} E_1 \eta_1 - g_1(D^2 + \omega_1^2)v &= 0 \\ E_2 \eta_2 - g_2(D^2 + \omega_2^2)v &= 0 \end{aligned} \quad (5.34-a,b,c)$$

$$g_1(D^2 + \omega_1^2)\eta_1 + g_2(D^2 + \omega_2^2)\eta_2 = 0$$

Applying the operators  $E_1$  and  $E_2$  on Eq. (5.34-c) one obtain

$$g_1(D^2 + \omega_1^2)E_2E_1\eta_1 + g_2(D^2 + \omega_2^2)E_1E_2\eta_2 = 0$$

then substituting for the operations  $E_1\eta_1$  and  $E_2\eta_2$  from (5.34-a,b) we have

$$[g_1^2(D^2 + \omega_1^2)^2 E_2 + g_2^2(D^2 + \omega_2^2)^2 E_1]v = 0$$

$$\text{or } \tilde{E}v = 0 \tag{5.35}$$

where the operator

$$\tilde{E} = g_1^2(D^2 + \omega_1^2)^2 E_2 + g_2^2(D^2 + \omega_2^2)^2 E_1 \tag{5.36}$$

is of eighth order. Note that sixteen differentiation operations were performed while deriving Eq. (5.35).

Interestingly, if the variables  $\eta_2$  and  $v$  are eliminated from the set (5.34) then one obtains

$$[g_1^2(D^2 + \omega_1^2)^2 E_2 + g_2^2(D^2 + \omega_2^2)^2 E_1]\eta_1 = \tilde{E}\eta_1 = 0 \tag{5.37}$$

If, in turn, the variables  $\eta_1$  and  $v$  are eliminated, then one obtains again

$$\tilde{E}\eta_2 = 0 \tag{5.38}$$

Thus the optimality equations (5.30, 34) can be written in the short form as

$$\tilde{E}\eta_1 = \tilde{E}\eta_2 = \tilde{E}v = 0 \tag{5.39}$$

where  $\tilde{E}$  is a differential operator that can be specified for the system considered.

The general solution to each of Eq. (5.39) is in the exponential form,  $e^{rt}$  [16], where eight roots  $r_1..r_8$  can be derived from the characteristic polynomial equation of eighth order for operator  $\tilde{E}$ . The roots are in the form  $\pm\alpha_k \pm i\beta_k$  ( $k = 1,2$ ), where  $\alpha_k$  and  $\beta_k$  are real numbers. Once the roots are known, the set of eight independent solution functions can be obtained. For example, if  $\alpha_k$  and  $\beta_k$  are positive and non-multiple then each pair generates the solutions  $e^{\pm\alpha_k t} \sin(\beta_k t)$  and  $e^{\pm\alpha_k t} \cos(\beta_k t)$

### 5.3.1 Application to the gantry crane problem

As an illustration, the above methodology is reapplied to the gantry crane problem for which  $\hat{R}_{11} = \hat{R}_{22} = 1$ ,  $\omega_1 = 0$ ,  $\hat{Q}_{dii} = \hat{Q}_{vii} = 0$ ,  $g_1 = 1$ ,  $g_2 = -d_2$

Substituting into (5.30) one obtains

$$\begin{aligned}\ddot{\eta}_1 - \ddot{v} &= 0 \\ \ddot{\eta}_2 + 2\omega_2^2\ddot{\eta}_2 + \omega_2^4\eta_2 + d_2(\ddot{v} + \omega_2^2v) &= 0 \\ \dot{\eta}_1 - d_2(\dot{\eta}_2 + \omega_2^2\eta_2) &= 0\end{aligned}\tag{5.40-a,b,c}$$

which is same as the Eq. (5.8-10).

The fourth order operators (5.33) are  $E_1 = D^4$ ,  $E_2 = (D^2 + \omega_2^2)^2$  and the eighth order operator (5.36) is

$$\tilde{E} = (1 + d_2^2)(D^2 + \omega_2^2)^2 D^4\tag{5.41}$$

The characteristic equation for this operator is

$$(r^2 + \omega_2^2)^2 r^4 = 0\tag{5.41-a}$$

The roots of this equation are  $0,0,0,0, \pm i\omega_2, \pm i\omega_2$  and each of the solution of Eq (5.39) for  $v$ ,  $\eta_1$  and  $\eta_2$  will have the form

$$\begin{aligned}v &= C_1 + C_2t + C_3t^2 + C_4t^3 + (C_5 + C_7t)\sin(\omega_2t) + (C_6 + C_8t)\cos(\omega_2t) \\ \eta_1 &= A_1 + A_2t + A_3t^2 + A_4t^3 + (A_5 + A_7t)\sin(\omega_2t) + (A_6 + A_8t)\cos(\omega_2t) \\ \eta_2 &= B_1 + B_2t + B_3t^2 + B_4t^3 + (B_5 + B_7t)\sin(\omega_2t) + (B_6 + B_8t)\cos(\omega_2t)\end{aligned}\tag{5.42-a,b,c}$$

Since each operator is of 8<sup>th</sup> order, the above functions contain  $8 \times 3 = 24$  integration constants. When solving Eq. (5.39) it is convenient to denote the integration constants as  $C_1..C_8$ ,  $A_1..A_8$  and  $B_1..B_8$  instead of a sequential notation in the previous section (constants  $C_1..C_{12}$  in Eq. (5.15,17,18)).

Eq. (5.40 a) requires that  $D^4\eta_1 = D^2v$ . By grouping and comparing similar terms in this equation we obtain

$$\begin{aligned}C_3 &= C_4 = 0 \\ A_5 &= -C_5\end{aligned}\tag{5.43-a,b,c}$$

$$A_6 = -C_6$$

Similarly, comparing similar terms of Eq. (5.40 b) requires that  $(D^2 + \omega_2^2)^2 \eta_2 = d_2(D^2 + \omega_2^2)v$ , we obtain

$$C_8 = C_7 = 0$$

$$\omega_2^2 B_1 = -d_2 C_1 \quad (5.44-a,b,c)$$

$$\omega_2^2 B_2 = -d_2 C_2$$

Finally, comparing similar terms in Eq. (5.40 c) we have

$$B_3 = B_4 = A_7 = A_8 = 0$$

$$d_2 \omega_2^2 B_1 = 2A_3$$

$$d_2 \omega_2^2 B_2 = 6A_4 \quad (5.45-a,b,c,d,e)$$

$$2d_2 B_8 = \omega_2 A_5$$

$$2d_2 B_7 = -\omega_2 A_6$$

The above sixteen equations allow to reduce the number of independent integration constants from twenty-four to eight, that is to the number of the given boundary conditions imposed on the variables  $\eta_1$  and  $\eta_2$ . The solution functions are

$$v = C_1 + C_2 t + C_5 \sin(\omega_2 t) + C_6 \cos(\omega_2 t)$$

$$\eta_1 = A_1 + A_2 t - \frac{t^2 d_2^2}{6} (3C_1 - C_2 t) - C_5 \sin(\omega_2 t) - C_6 \cos(\omega_2 t) \quad (5.46-a,b,c)$$

$$\eta_2 = -\frac{d_2}{\omega_2^2} (C_1 + C_2 t) + B_5 \sin(\omega_2 t) + B_6 \cos(\omega_2 t) + \frac{\omega_2 t}{2d_2} (C_6 \sin(\omega_2 t) + C_5 \cos(\omega_2 t))$$

As can be seen the above functions are identical to the ones obtained in section 5.2 without using the differential operators. In this case the constants  $C_1, C_2, C_5, C_6, A_1, A_2, B_5$  and  $B_6$  corresponds to the constants  $C_1, C_2, C_7, C_8, C_9, C_{10}, C_{11}$  and  $C_{12}$  in Eq. (5.21) respectively.

The advantage of using the operators is that the whole procedure can be automated within the *MAPLE* program (see Appendix A). The flowchart is shown in Fig. 5.1. Once  $\tilde{E}$  is specified the roots of the corresponding characteristic equation can be obtained by ‘solve’ command. Grouping and comparison of the terms involved in the

differentiation of  $\eta_1$ ,  $\eta_2$  and  $v$  can be handled by ‘collect’ command. This operation renders the set of equations similar to Eq. (5.43-45). By adding the boundary conditions, such as given by Eq. (5.21-*d*), the complete set of integration constants is calculated. This, in turn, allows the determination of modal variables and modal controls and finally the optimal values of DOFs and actuator forces. More details of the program are discussed in the section that follows.

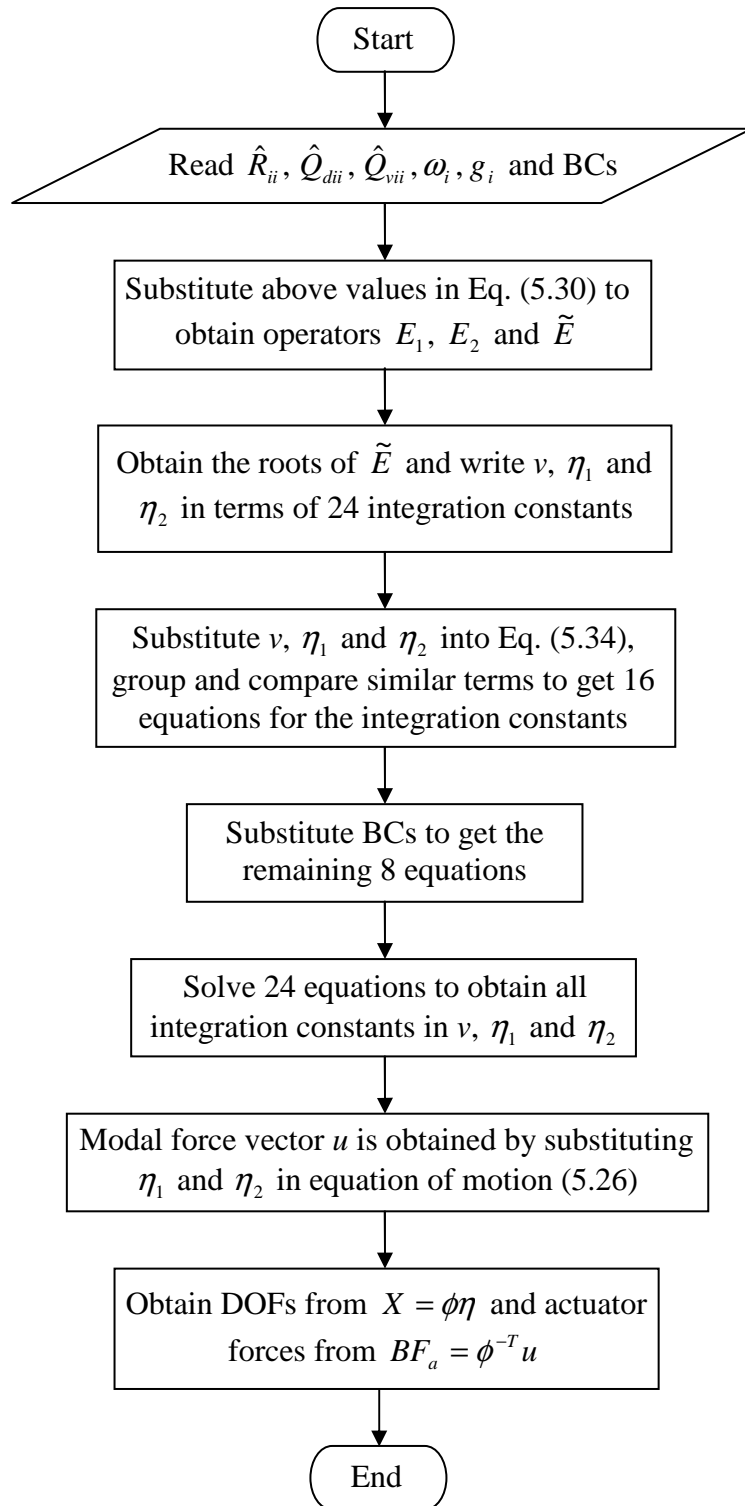


**Figure 5.1:** Flowchart of the *MAPLE* program

### 5.3.2 Application to the suspension system problem

The above methodology is applied to the suspension system problem considered in chapter IV, where two modes of vibrations were controlled by two actuators  $F_1$  and  $F_2$ . Here the system is to be controlled by only one actuator,  $F_2$ , which makes the problem overdetermined (see Fig. 5.2).

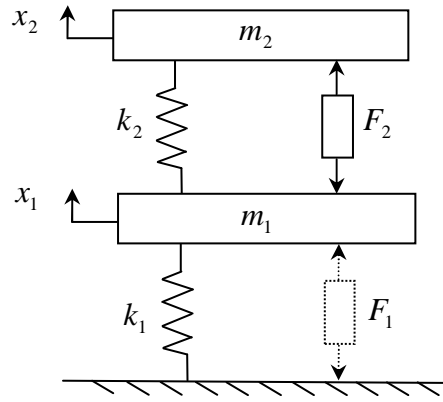


**Figure 5.2:** Suspension system

The optimization parameters in Eq. (4.8) are zero except  $a_2 = b_1 = c_2 = 1$  which yields the following values of the diagonal of the weighting matrices (4.10).

$$\hat{R}_{ii} = 1/\omega_i^2, \hat{Q}_{dii} = \omega_i^2, \hat{Q}_{vii} = 1, \Gamma = 0$$

As before the system was disturbed by assuming  $x_1(0) = 10mm$ ,  $x_2(0) = 50mm$  and should be brought to the rest by actuators in  $t_f = 2s$ .

$$\text{Since } F = \phi^{-T} u = \begin{bmatrix} 0.4133025 & 6.311674 \\ 14.11189 & -0.9242058 \end{bmatrix} \begin{bmatrix} u_1 \\ u_2 \end{bmatrix} = \begin{bmatrix} F_1 - F_2 \\ F_2 \end{bmatrix}$$

and  $F_1 = 14.525 \cdot u_1 + 5.38747 \cdot u_2 = 0$ , then  $u_1 + 0.37089 \cdot u_2 = 0$  and  $g_1 = 1$ ,  $g_2 = 0.37089$ .

The frequencies of the system are

$$\omega_1 = 12.94105 \text{ rad/s}, \omega_2 = 83.040527 \text{ rad/s}$$

The set (5.30) has the form



$$\begin{aligned}
\ddot{\eta}_1 + \omega_1^2 \dot{\eta}_1 + 2\omega_1^4 \eta_1 - g_1 \omega_1^2 (\ddot{v} + \omega_1^2 v) &= 0 \\
\ddot{\eta}_2 + \omega_2^2 \dot{\eta}_2 + 2\omega_2^4 \eta_2 - g_2 \omega_2^2 (\ddot{v} + \omega_2^2 v) &= 0 \\
g_1 (\dot{\eta}_1 + \omega_1^2 \eta_1) + g_2 (\dot{\eta}_2 + \omega_2^2 \eta_2) &= 0
\end{aligned} \tag{5.47-a,b,c}$$

The fourth order operators (5.33) are  $E_i = D^4 \omega_i^{-2} + D^2 + 2\omega_i^2$ , and the eighth order operator is

$$\tilde{E} = g_1^2 (D^2 + \omega_1^2)^2 E_2 + g_2^2 (D^2 + \omega_2^2)^2 E_1 \tag{5.48}$$

The roots of characteristic equation for the operator  $\tilde{E}$  are  $\pm \alpha_k \pm i\beta_k$  ( $k=1,2$ ), where

$$\alpha_1 = 7.5742, \alpha_2 = 22.3544, \beta_1 = 12.8185, \beta_2 = 82.8699 \tag{5.48-a}$$

Each of the variables  $v$ ,  $\eta_1$  and  $\eta_2$  will have the form (only  $\eta_1$  is shown)

$$\begin{aligned}
\eta_1 = e^{\alpha_1 t} [A_1 \cos(\beta_2 t) + A_2 \sin(\beta_2 t)] + e^{-\alpha_1 t} [A_3 \cos(\beta_2 t) + A_4 \sin(\beta_2 t)] \\
+ e^{\alpha_2 t} [A_5 \cos(\beta_1 t) + A_6 \sin(\beta_1 t)] + e^{-\alpha_2 t} [A_7 \cos(\beta_1 t) + A_8 \sin(\beta_1 t)]
\end{aligned} \tag{5.49}$$

It can be observed that  $\omega_1 \cong \beta_1$  and  $\omega_2 \cong \beta_2$

Twenty four equations in terms of integration constants can be obtained from boundary conditions and by substituting  $\eta_1$  and  $\eta_2$  into (5.47) and comparing the terms, similarly as it was done before.

Boundary Conditions are

$$\begin{aligned}
\eta_1(0) = 0.709734 & \quad \eta_1(2) = 0 \\
\eta_2(0) = 0.0169135 & \quad \eta_2(2) = 0 \\
\dot{\eta}_1(0) = 0 & \quad \dot{\eta}_1(2) = 0 \\
\dot{\eta}_2(0) = 0 & \quad \dot{\eta}_2(2) = 0
\end{aligned}$$

The set of constants  $A_1..A_8$  and  $B_1..B_8$  solved by Maple are (constants  $C_1..C_8$  are not shown since they are not needed for further manipulations)

$$\begin{aligned}
A_1 = 0.1356 \times 10^{-27} & \quad B_1 = -0.6171 \times 10^{-27} \\
A_2 = 0.7172 \times 10^{-28} & \quad B_2 = 0.5065 \times 10^{-27} \\
A_3 = -.2451 \times 10^{-2} & \quad B_3 = 0.3644 \times 10^{-2} \\
A_4 = -.2686 \times 10^{-3} & \quad B_4 = 0.1230 \times 10^{-1} \\
A_5 = -0.8533 \times 10^{-13} & \quad B_5 = -0.5486 \times 10^{-15}
\end{aligned}$$

$$A_6 = 0.3648 \times 10^{-13}$$

$$B_6 = -0.7474 \times 10^{-14}$$

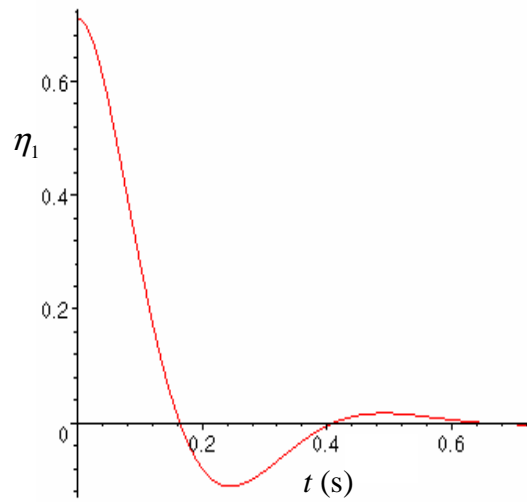
$$A_7 = 0.7122$$

$$B_7 = 0.01327$$

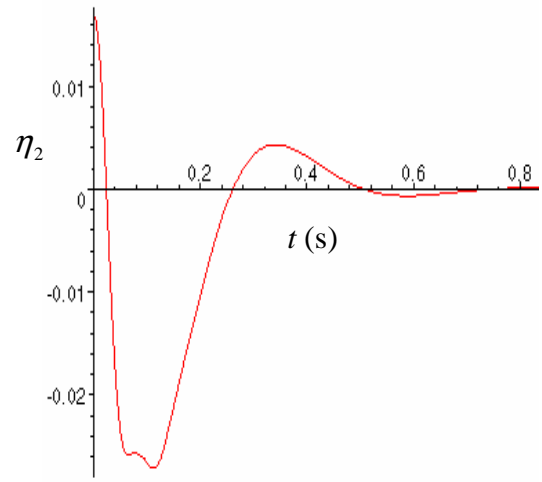
$$A_8 = 0.4182$$

$$B_8 = -0.0653$$

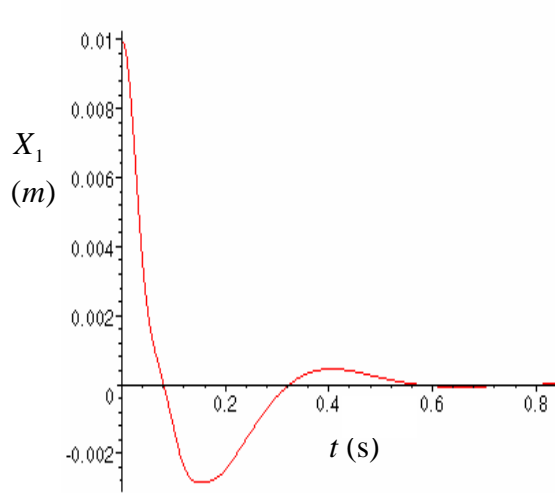
These constants may be substituted back to get the response plot shown in Fig. 5.3.



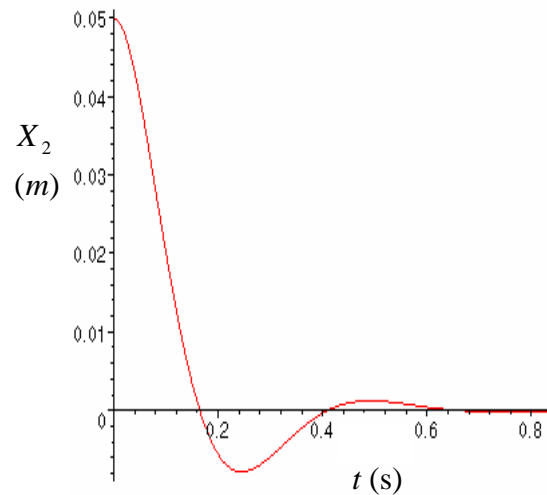
(a)



(b)



(c)



(d)

**Figure 5.3:** Modal variables and DOFs versus time(s) plots

The modal controls are plotted in Fig. 5.4-*a,b* and the corresponding actuator's force is shown in Fig. 5.4-*c*. Note that  $u_1 = -0.37089 \cdot u_2$  as it was imposed by an extra constraint (5.47-*c*). The actuator force  $F_a$  was determined from  $F_a = F_2 = 14.112 \cdot u_1 - 0.92395 \cdot u_2$ .

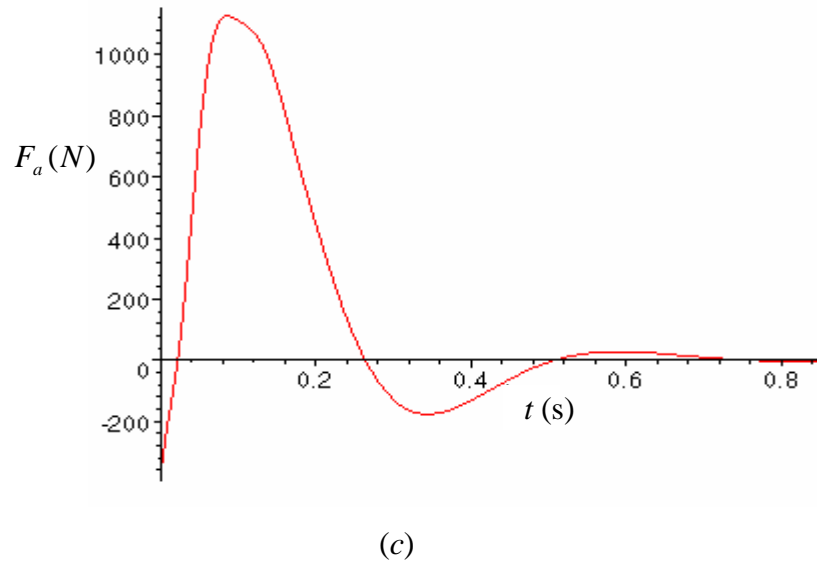
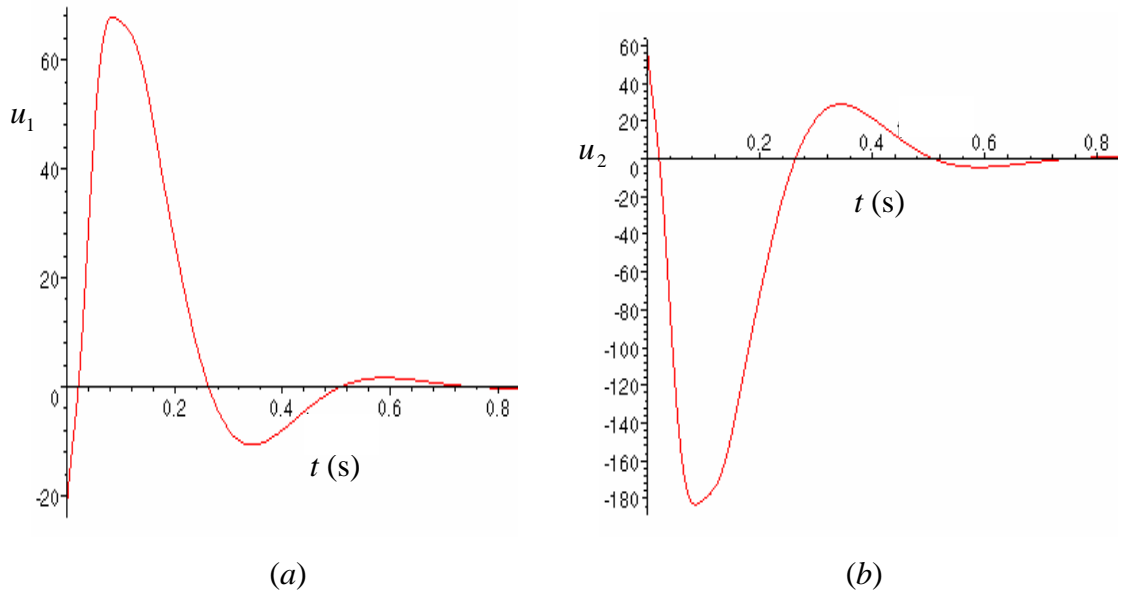


**Figure 5.4:** Modal controls  $u_1$ ,  $u_2$  and actuator's force  $F_a$  versus time ( $s$ ) plots



$$\dot{P}_v = -\frac{\partial H}{\partial \dot{\eta}} = \hat{Q}_v \dot{\eta} - P_d + \Delta P_v \quad (5.53-a,b)$$

while the new optimal control requires that

$$\frac{\partial H}{\partial u} = -\hat{R}u + P_v + Av = 0 \quad (5.54)$$

Above equation is a generalization of Eq. (5.6).

Eliminating the costates and modal control, the modified optimality equation becomes

$$\hat{R} \ddot{\eta} + (2\Omega \hat{R} - \hat{Q}_v - \hat{R} \Delta^2) \dot{\eta} + (\hat{R} \Omega^2 + \hat{Q}_d) \eta - (A\ddot{v} - \Delta A\dot{v} + \Omega Av) = 0 \quad (5.55)$$

This is a generalization of Eq. (5.30-a,b). Note that Eq. (5.55) contains  $n_m$  equations with  $n_m$  unknown components of modal variable  $\eta$ , and  $n_c$  components of Lagrange multipliers vector  $v$ .

Eq. (5.30-c) can be generalized by presenting the constraint equations (5.51) in the form

$$A^T u = A^T (I\dot{\eta} + \Delta\dot{\eta} + \Omega\eta) = 0 \quad (n_c \text{ equations}) \quad (5.56)$$

The sets (5.55-56) have  $(n_m + n_c)$  equations that contain  $n_m$  modal variables and  $n_c$  Lagrange multipliers and can be solved explicitly.

Eq. (5.55) using the differential operators can be written as

$$E_i \eta_i = \sum_{j=1}^{n_c} \hat{D}_{ij} v_j \quad i = 1..n_m \quad (5.57-a)$$

while Eq. (5.56) as

$$\sum_{i=1}^{n_m} \tilde{D}_{ij} \eta_i = 0 \quad j = 1..n_c \quad (5.57-b)$$

where the operators are

$$\begin{aligned} E_i &= \hat{R}_{ii} D^4 + (2\omega_i^2 \hat{R}_{ii} - \hat{Q}_{vii} - \hat{R}_{ii} \Delta_i^2) D^2 + (\hat{R}_{ii} \omega_i^4 + \hat{Q}_{dii}) \\ \hat{D}_{ij} &= g_{ji} (D^2 - \Delta_i D + \omega_i^2) \\ \tilde{D}_{ij} &= g_{ji} (D^2 + \Delta_i D + \omega_i^2) \end{aligned} \quad (5.58-a,b,c)$$

Note that  $\hat{D}_{ij} = \tilde{D}_{ij}$  for no damping case ( $\Delta_i = 0$ ).

The set of equations (5.57) can be written in the matrix form as

$$\begin{array}{c}
\left[ \begin{array}{ccc|ccc}
E_1 & \dots & 0 & -\hat{D}_{11} & \dots & -\hat{D}_{1n_c} \\
\dots & \dots & \dots & \dots & \dots & \dots \\
0 & \dots & E_{n_m} & -\hat{D}_{n_m 1} & \dots & -\hat{D}_{n_m n_c} \\
\hline
\tilde{D}_{11} & \dots & \tilde{D}_{n_m 1} & 0 & \dots & 0 \\
\dots & \dots & \dots & \dots & \dots & \dots \\
\tilde{D}_{1n_c} & \dots & \tilde{D}_{n_m n_c} & 0 & \dots & 0
\end{array} \right] \begin{array}{c} \eta_1 \\ \dots \\ \eta_{n_m} \\ v_1 \\ \dots \\ v_{n_c} \end{array} = 0 \\
\underbrace{\hspace{10em}}_{\bar{E}} \quad \underbrace{\hspace{2em}}_Y
\end{array} \tag{5.59}$$

Or  $\bar{E}_{n_t \times n_t} Y_{n_t \times 1} = 0$

where the size of matrix  $\bar{E}$  is  $n_t = n_c + n_m$  and  $Y$  contains all the modal variables and Lagrange multipliers.

It can be shown by applying the operators similarly as in Eq. (5.34), section 5.3, that each component of vector  $Y$  will satisfy the equation

$$\det \bar{E} \cdot Y_i = \tilde{E} \cdot Y_i = 0 \tag{5.60}$$

Note that each operator  $E_i$  is of fourth order and each operator  $\tilde{D}_{ij}$  or  $\hat{D}_{ij}$  is of second order. The order of the operator  $\tilde{E} = \det \bar{E}$  is  $4 \times n_m$  and its form can be always found by calculating the determinant of  $\bar{E}$  in Eq. (5.59). Once  $\tilde{E}$  is determined then the roots of the corresponding characteristic equation can be obtained, and the integration constants calculated similarly as in the previous section. The above approach is first verified on the suspension system solved before, and then applied to a triple pendulum problem.

### 5.4.1 Example 1: Suspension system

The general method is applied to the suspension system for verification purposes. For the system in Fig 5.2 in the previous section,  $n_m = 2$ ,  $n_c = 1$ ,  $n_t = 3$  and as before

$$\hat{R}_{ii} = 1/\omega_i^2, \hat{Q}_{dii} = \omega_i^2, \hat{Q}_{vii} = 1, \Gamma = 0 \text{ and } \Delta_i = 0$$

Eq. (5.57-a,b) are in the following form

$$E_1 \eta_1 = \hat{D}_{11} v_1$$

$$E_2 \eta_2 = \hat{D}_{21} v_1$$

$$\tilde{D}_{11}\eta_1 + \tilde{D}_{21}\eta_2 = 0$$

where  $E_i = D^4 \omega_i^{-2} + D^2 + 2\omega_i^2$ ,  $\hat{D}_{11} = \tilde{D}_{11} = g_1(D^2 + \omega_1^2)$  and  $\hat{D}_{21} = \tilde{D}_{21} = g_2(D^2 + \omega_2^2)$

$$\text{Matrix } \bar{E} \text{ has the form } \bar{E} = \begin{bmatrix} E_1 & 0 & -\hat{D}_{11} \\ 0 & E_2 & -\hat{D}_{21} \\ \tilde{D}_{11} & \tilde{D}_{21} & 0 \end{bmatrix} \quad (5.61)$$

and

$$\tilde{E} = \det \bar{E} = \tilde{D}_{21}\hat{D}_{21}E_1 + \tilde{D}_{11}\hat{D}_{11}E_2 = g_1^2(D^2 + \omega_1^2)^2 E_2 + g_2^2(D^2 + \omega_2^2)^2 E_1 \quad (5.61a)$$

which is the same as Eq. (5.48) obtained before.

### 5.4.2 Example 2: Triple pendulum

A triple pendulum with masses  $m_1, m_2, m_3$  and massless links  $L_1, L_2, L_3$  is shown in Fig. 5.5 in a disturbed initial position. Such a system has three DOFs or three modes of vibrations. All three modes are to be controlled by applying only one torque  $T_1$ , which makes the problem overdetermined.

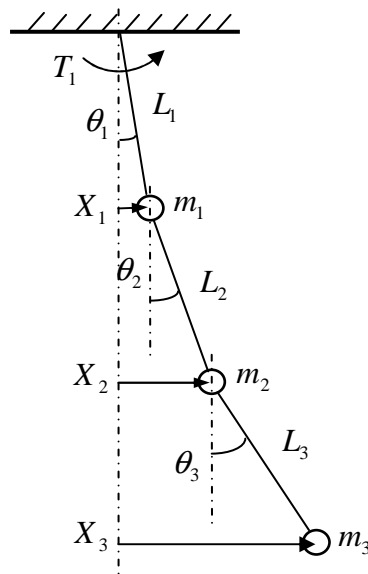


**Figure 5.5:** Triple Pendulum

Governing equations of motion are obtained by energy method.

Assuming small amplitude oscillations one may write

$$X_1 = L_1 \theta_1$$

$$X_2 = X_1 + L_2 \theta_2 = L_1 \theta_1 + L_2 \theta_2$$

$$X_3 = X_2 + L_3 \theta_3 = L_1 \theta_1 + L_2 \theta_2 + L_3 \theta_3$$

Kinetic Energy,

$$KE = \frac{1}{2} \left\{ m_1 L_1^2 \dot{\theta}_1^2 + m_2 \left( L_1 \dot{\theta}_1 + L_2 \dot{\theta}_2 \right)^2 + m_3 \left( L_1 \dot{\theta}_1 + L_2 \dot{\theta}_2 + L_3 \dot{\theta}_3 \right)^2 \right\}$$

Potential energy,

$$PE = g \left\{ m_3 \left[ L_1 \left( 1 - \theta_1^2 / 2 \right) + L_2 \left( 1 - \theta_2^2 / 2 \right) + L_3 \left( 1 - \theta_3^2 / 2 \right) \right] + m_2 \left[ L_1 \left( 1 - \theta_1^2 / 2 \right) + L_2 \left( 1 - \theta_2^2 / 2 \right) \right] \right. \\ \left. + g m_1 L_1 \left( 1 - \theta_1^2 / 2 \right) \right\}$$

and  $L = KE - PE$

Lagrange equations are

$$\frac{d}{dt} \left( \frac{\partial L}{\partial \dot{\theta}_1} \right) - \frac{\partial L}{\partial \theta_1} = T_1$$

$$\frac{d}{dt} \left( \frac{\partial L}{\partial \dot{\theta}_2} \right) - \frac{\partial L}{\partial \theta_2} = 0$$

$$\frac{d}{dt} \left( \frac{\partial L}{\partial \dot{\theta}_3} \right) - \frac{\partial L}{\partial \theta_3} = 0$$

After differentiation and grouping, the above three equations can be written in the matrix form as,

$$M \ddot{\theta} + K \theta = F \tag{5.62}$$

where,  $\theta^T = [\theta_1 \quad \theta_2 \quad \theta_3]$ ,  $F^T = [T_1 \quad 0 \quad 0]$

$$M = \begin{bmatrix} L_1^2 (m_1 + m_2 + m_3) & L_1 L_2 (m_2 + m_3) & L_1 L_3 m_3 \\ L_1 L_2 (m_2 + m_3) & L_2^2 (m_2 + m_3) & L_2 L_3 m_3 \\ L_1 L_3 m_3 & L_2 L_3 m_3 & L_3^2 m_3 \end{bmatrix}$$



$$K = \begin{bmatrix} L_1 g(m_1 + m_2 + m_3) & 0 & 0 \\ 0 & L_2 g(m_2 + m_3) & 0 \\ 0 & 0 & L_3 g m_3 \end{bmatrix}$$

Let,  $L_1 = 1m$ ,  $L_2 = 2m$ ,  $L_3 = 3m$

$m_1 = 1kg$ ,  $m_2 = 2kg$ ,  $m_3 = 3kg$

For the above data, the natural frequencies are

$\omega_1 = 1.373406rad/s$ ,  $\omega_2 = 3.778047rad/s$ ,  $\omega_3 = 9.362831rad/s$

The corresponding mode shape matrix is

$$\phi = \begin{bmatrix} 0.06932 & 0.2295 & 0.970836 \\ 0.08052 & 0.20861 & -0.570085 \\ 0.104673 & -0.27964 & 0.05863 \end{bmatrix} \quad (5.63)$$

The modes are shown in Fig 5.6

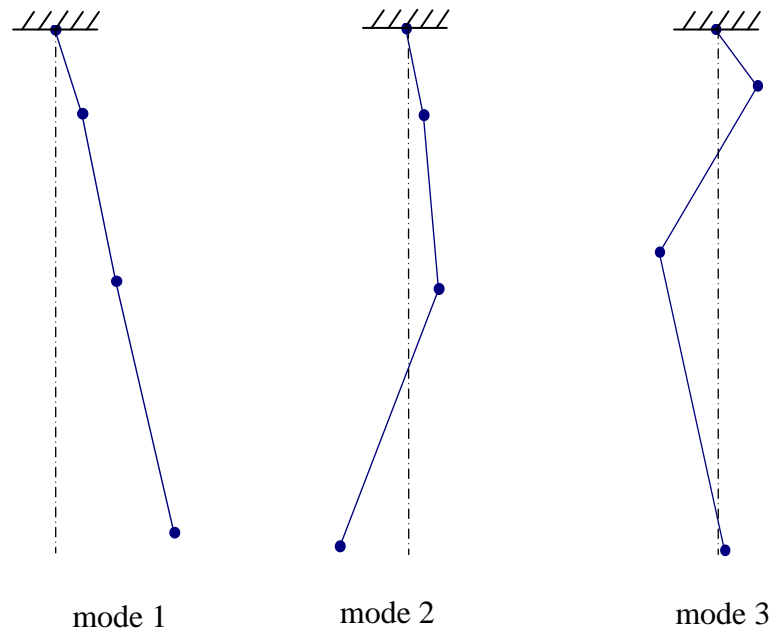


**Figure 5.6:** Mode shapes

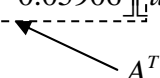
Modal equations of motion can be written in the following form

$$\ddot{\eta}_i + \omega_i^2 \eta_i = u_i \quad i = 1,2,3 \quad (5.64)$$

where  $\theta = \phi\eta$  and  $u = \phi^T F$ .

The second relation gives

$$F = \phi^{-T} u = \begin{bmatrix} 2.16324 & 0.94640 & 0.65185 \\ 4.18781 & 1.43379 & -0.63796 \\ 4.89945 & -1.72971 & 0.05906 \end{bmatrix} \begin{bmatrix} u_1 \\ u_2 \\ u_3 \end{bmatrix} = \begin{bmatrix} T_1 \\ 0 \\ 0 \end{bmatrix} \quad (5.65)$$


  
 $A^T$

Note that the bottom part of the matrix  $\phi^{-T}$  represents  $A^T$ , the matrix of constraints.

Eq. (5.65) also provides the equation for the actuator moment  $T_1$  as

$$T_1 = 2.16324 \cdot u_1 + 0.9464 \cdot u_2 + 0.65185 \cdot u_3 \quad (5.66-a)$$

The constraint equations are in the form

$$h_1 = 0 = 4.18781 \cdot u_1 + 1.43379 \cdot u_2 - 0.63796 \cdot u_3$$

$$h_2 = 0 = 4.89945 \cdot u_1 - 1.72971 \cdot u_2 + 0.05906 \cdot u_3 \quad (5.66-b,c)$$

Note that the constraint equations (5.66-b,c) are homogenous and can be further modified to obtain a simpler form.

Namely, eliminating  $u_3$  and  $u_1$  from (5.66-b) and (5.66-c) respectively gives

$$h_1 = u_1 - 0.30205u_2 = 0$$

$$h_2 = u_2 - 0.23639u_3 = 0 \quad (5.67-a,b)$$

Thus, instead of the full form of matrix  $A$  as defined by Eq. (5.66), this matrix can be modified to

$$A^T = \begin{bmatrix} 1 & g_{12} & 0 \\ 0 & 1 & g_{23} \end{bmatrix} \quad (5.68)$$

where  $g_{12} = -0.30205$  and  $g_{23} = -0.23639$ .

The form (5.68) is more convenient for further manipulations.

Similarly as in the suspension problem, let the optimization parameters in Eq. (4.8) be all zero except  $a_2 = b_1 = c_2 = 1$  which yields  $\hat{R}_{ii} = 1/\omega_i^2$ ,  $\hat{Q}_{dii} = \omega_i^2$ ,  $\hat{Q}_{vii} = 1$ , also  $t_f = 3s$ ,  $\Gamma = 0$  and  $\Delta_i = 0$  (no damping)

For this system,  $n_m = 3$ ,  $n_a = 1$ ,  $n_c = 2$ ,  $n_t = 5$

Eq. (5.57-a) can be written as

$$\begin{aligned}
E_1 \eta_1 &= \hat{D}_{11} v_1 + \hat{D}_{12} v_2 \\
E_2 \eta_2 &= \hat{D}_{21} v_1 + \hat{D}_{22} v_2 \\
E_3 \eta_3 &= \hat{D}_{31} v_1 + \hat{D}_{32} v_2
\end{aligned} \tag{5.69}$$

Eq. (5.57-b) can be written as

$$\begin{aligned}
\tilde{D}_{11} \eta_1 + \tilde{D}_{21} \eta_2 + \tilde{D}_{31} \eta_3 &= 0 \\
\tilde{D}_{12} \eta_1 + \tilde{D}_{22} \eta_2 + \tilde{D}_{32} \eta_3 &= 0
\end{aligned} \tag{5.70}$$

where  $E_i = D^4 \omega_i^{-2} + D^2 + 2\omega_i^2$  and  $\hat{D}_{ij} = \tilde{D}_{ij} = g_{ji}(D^2 + \omega_i^2)$ .

The coefficients  $g_{ji}$  are given by Eq. (5.68) as  $g_{11} = g_{22} = 1$ ,  $g_{12} = -0.30205$ ,  $g_{23} = -0.23639$  and  $g_{13} = g_{21} = 0$ .

Then  $\hat{D}_{11} = \tilde{D}_{11} = (D^2 + \omega_1^2)$ ,  $\hat{D}_{22} = \tilde{D}_{22} = (D^2 + \omega_2^2)$ ,  $\hat{D}_{21} = \tilde{D}_{21} = -0.30205(D^2 + \omega_2^2)$ ,  $\hat{D}_{32} = \tilde{D}_{32} = -0.23639(D^2 + \omega_3^2)$  and  $\hat{D}_{31} = \tilde{D}_{31} = \hat{D}_{12} = \tilde{D}_{12} = 0$

Now, matrix  $\bar{E}$  has a form

$$\bar{E} = \begin{bmatrix} E_1 & 0 & 0 & -\hat{D}_{11} & 0 \\ 0 & E_2 & 0 & -\hat{D}_{21} & -\hat{D}_{22} \\ 0 & 0 & E_3 & 0 & -\hat{D}_{32} \\ \tilde{D}_{11} & \tilde{D}_{21} & 0 & 0 & 0 \\ 0 & \tilde{D}_{22} & \tilde{D}_{32} & 0 & 0 \end{bmatrix} \tag{5.71}$$

and  $\tilde{E} = \det \bar{E} = \tilde{D}_{21} \hat{D}_{21} \tilde{D}_{32} \hat{D}_{32} E_1 + \tilde{D}_{32} \hat{D}_{32} \tilde{D}_{11} \hat{D}_{11} E_2 + \tilde{D}_{22} \hat{D}_{22} \tilde{D}_{11} \hat{D}_{11} E_3$ .

The order of operator  $\tilde{E}$  is twelve (2+2+2+2+4).

The roots of characteristic equation for the operator  $\tilde{E}$  can be obtained and each of the variables  $v$ ,  $\eta_1$  and  $\eta_2$  can be calculated by Maple. The roots are  $r_{1,2} = 0.2652 \pm 1.3777i$ ,  $r_{3,4} = -0.2652 \pm 1.3777i$ ,  $r_{5,6} = 0.8665 \pm 3.8262i$ ,  $r_{7,8} = -0.8665 \pm 3.8262i$ ,  $r_{9,10} = 5.0742 \pm 9.1881i$ ,  $r_{11,12} = -5.0742 \pm 9.1881i$ . The following boundary conditions are used.

$$\text{IBC: } \theta_1(0) = 5^\circ, \theta_2(0) = 10^\circ, \theta_3(0) = 15^\circ, \dot{\theta}_1(0) = 0, \dot{\theta}_2(0) = 0, \dot{\theta}_3(0) = 0$$

$$\text{FBC: } \theta_1(3) = 0, \theta_2(3) = 0, \theta_3(3) = 0, \dot{\theta}_1(3) = 0, \dot{\theta}_2(3) = 0, \dot{\theta}_3(3) = 0$$

The optimal variation of the modal variables is shown in Fig. 5.7.

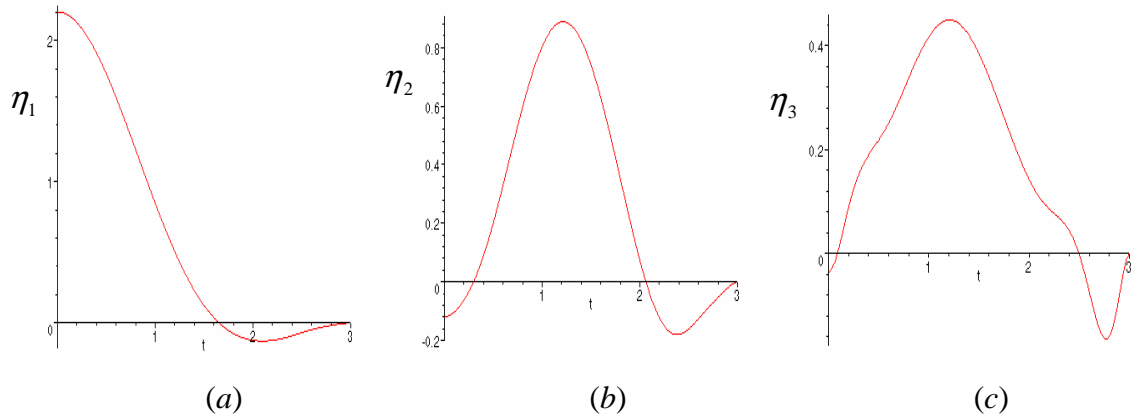


**Figure 5.7:** Modal variables versus  $t(s)$

The corresponding variation of the DOFs is presented in Fig 5.8.

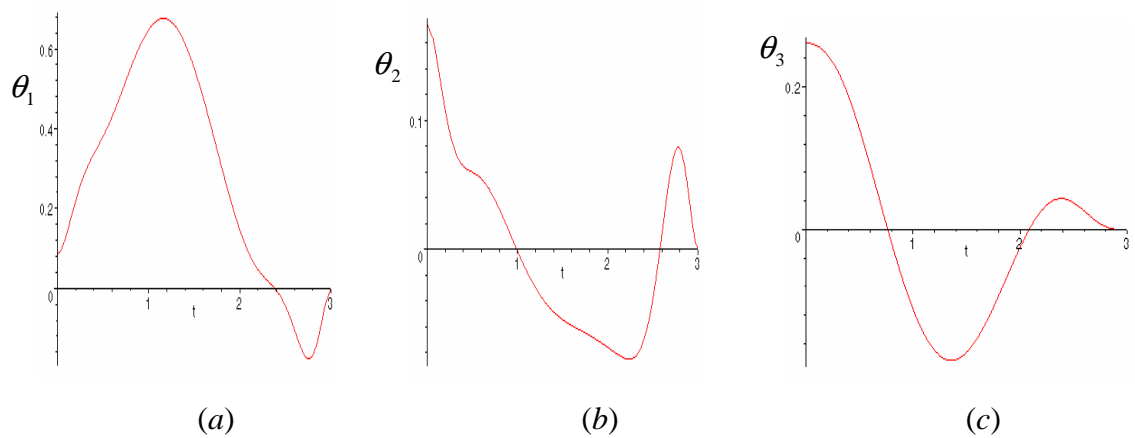


**Figure 5.8:** DOFs versus  $t(s)$

The optimal torque is shown in Fig. 5.9. It can be noted that the torque has positive value for most of the time and negative value at the end of time span. This can be attributed to the fact that mass  $m_3 > m_2 > m_1$  and also to the time span which is short. The pendulum configurations at  $t = 0, 0.5, 1, 1.5, 2, 2.5, 3$ , indicated by dots in Fig. 5.9, are shown in Fig. 5.10.

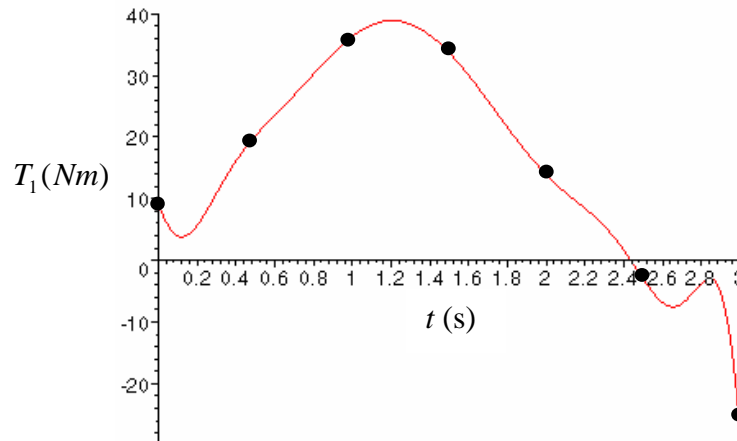


**Figure 5.9:** Optimal torque

The values and variations of torque strongly depends on the requested maneuver time  $t_f$ . As shown in Fig. 5.11, the maximum value of torque increases to about  $60 \text{ Nm}$  if  $t_f = 2\text{s}$  and is reduced to about  $18 \text{ Nm}$  for  $t_f = 20\text{s}$ . It is evident that the torque is almost always positive for a short time, and alternates for longer times.

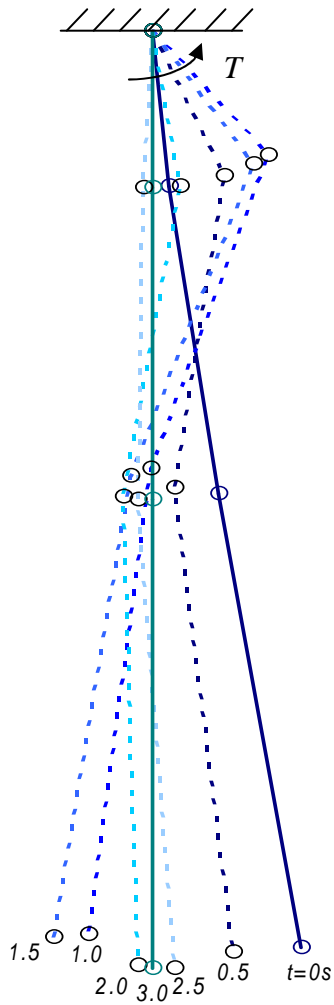


**Figure 5.10:** Pendulum configuration at different times

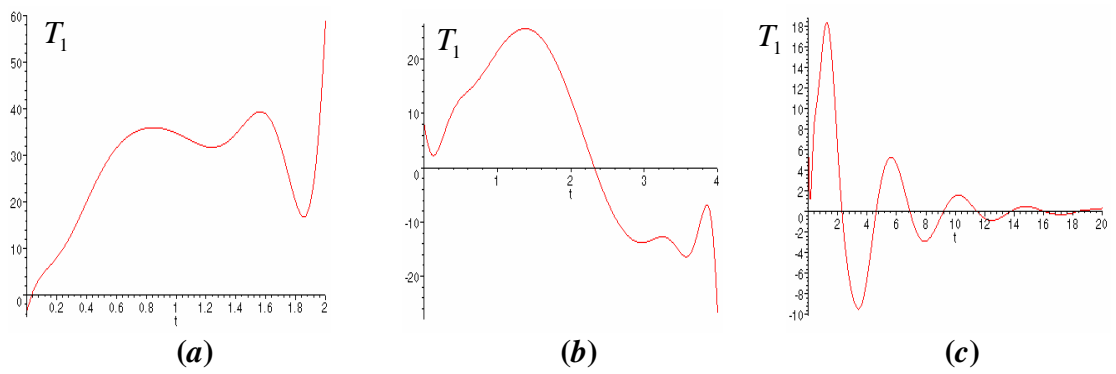


**Figure 5.11:** Plot of  $T_1$  (Nm) for (a)  $t_f = 2s$ , (b)  $t_f = 4s$ , (c)  $t_f = 20s$

Generally the variation of torque becomes unaffected if the maneuver time is sufficiently long. What is important is that, for such cases it is possible to determine constant gains that can be applied in a closed loop control, to be discussed in the next chapter.

If the triple pendulum was controlled by two actuators as shown in Fig 5.12, for example, then for such a system  $n_m = 3$ ,  $n_a = 2$ ,  $n_c = 1$ ,  $n_t = 4$ .

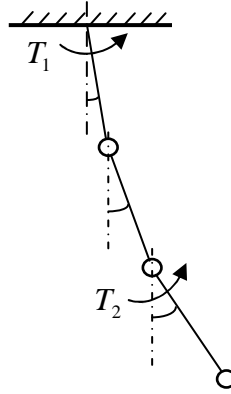


**Figure 5.12:** Triple pendulum controlled by two actuators

For this case the  $\bar{E}$  would have the form

$$\bar{E} = \begin{bmatrix} E_1 & 0 & 0 & -\hat{D}_{11} \\ 0 & E_2 & 0 & -\hat{D}_{21} \\ 0 & 0 & E_3 & -\hat{D}_{31} \\ \tilde{D}_{11} & \tilde{D}_{21} & \tilde{D}_{31} & 0 \end{bmatrix} \begin{bmatrix} \eta_1 \\ \eta_2 \\ \eta_3 \\ v_1 \end{bmatrix} = 0 \quad (5.72)$$

Each of the variables must satisfy the equation  $\tilde{E}\eta_1 = \tilde{E}\eta_2 = \tilde{E}\eta_3 = \tilde{E}v_1 = 0$  where,

$$\tilde{E} = \det \bar{E} = E_1 E_2 \tilde{D}_{31} \hat{D}_{31} + E_1 E_3 \tilde{D}_{21} \hat{D}_{21} + E_2 E_3 \tilde{D}_{11} \hat{D}_{11} \quad (5.72a)$$

The order of the above operator is again 12 (4+4+2+2 for  $E_1, E_2, \tilde{D}_{31}$  and  $\hat{D}_{31}$  respectively). For particular boundary conditions, this problem could be solved similarly as the previous one.

If the pendulum was controlled by three actuators then the problem could be solved efficiently by the *BA* method discussed in chapter IV.

Also, if one actuator was to control three lower modes of the continuous frame in Fig. 4.4 then operator  $\tilde{E}$  will take the form of Eq. (5.61a). If, in turn, these three lower modes were to be controlled by two actuators then operator  $\tilde{E}$  will take the form of Eq. (5.72a).



## 6. CLOSED LOOP CONTROL AND OPTIMAL GAINS

### 6.1 Introduction

In chapters III and V the optimal vibration's control was discussed with the application to the open loop control system problems, in which the actuator forces are calculated as functions of time. In the closed loop control systems, the actuator forces should be determined from the states that is (see Eq. (2.45))

$$F_a = -G \cdot z(t) \quad (6.1)$$

The gains  $G$  allow obtaining the current actuator forces (input) from the state of the system (output) [17]. Optimal gains  $G$  are constant if  $t_f \rightarrow \infty$  and can be obtained from the performance index written in the form

$$J = 1/2 \int_0^{\infty} [z^T Q z + F^T R F] dt \rightarrow \min \quad (6.2)$$

Such a problem is referred to as a time invariant problem. Nonlinear algebraic Riccati's equations mentioned in Chapter II can be used to calculate optimal gains. An alternative way of determining optimal gains is presented in this chapter. In the modal space, the gains relate the actuator forces to the modal variables as follows

$$F_j(t) = - \sum_{i=1}^{n_m} (G_{ijd} \eta_i(t) + G_{ijv} \dot{\eta}_i(t)) \quad j = 1..n_a \quad (6.3)$$

where  $G_{ijd}$  and  $G_{ijv}$  are  $2n_m \times n_a$  components of the gain matrix corresponding to the modal position and velocity respectively.

In the IMSC approach Eq. (6.3) simplifies to

$$u_i = -\hat{g}_{id} \eta_i - \hat{g}_{iv} \dot{\eta}_i \quad (6.4)$$

where  $\hat{g}_{id}$  and  $\hat{g}_{iv}$  are modal gains that can be determined for each mode independently. Such modal gains were calculated automatically by the BA in [11].

For overdetermined systems, because the modal controls are not independent, the actuator forces may depend on the state of all modal variables considered. Therefore all  $2n_m \times n_a$  components of the gain matrix in Eq. (6.3) have to be found simultaneously.

## 6.2 Calculation of gains by the Lagrange Multiplier method

The values of gains can be obtained by slightly modifying the flowchart of the program in Fig 5.1. Firstly one should realize that only the problems for which the roots of characteristic equation for the operator  $\tilde{E}$  (see Eq. (5.60), for example) are in the form  $\pm \alpha_k \pm i\beta_k$  with  $\alpha_k \neq 0$  can be considered. If at least one  $\alpha_k = 0$ , then the solution will contain a term  $(A_k \sin(\beta_k t) + B_k \cos(\beta_k t))$  which can not be attenuated with  $t \rightarrow \infty$  (see Eq. (6.6)). Such systems can not be treated as time-invariant ones (the gains can not be constant).

If  $\alpha_k \neq 0$  then each solution will have one set of exponentially increasing function  $e^{\alpha_k t} (\hat{A}_k \sin(\beta_k t) + \hat{B}_k \cos(\beta_k t))$ , and one set of exponentially decaying function  $e^{-\alpha_k t} (\tilde{A}_k \sin(\beta_k t) + \tilde{B}_k \cos(\beta_k t))$ . Since the exponential functions have to disappear when  $t \rightarrow \infty$ , one must set all the constants  $\hat{A}_k, \hat{B}_k$  to zero. This way all the zero boundary conditions at the target are automatically met. The remaining constants  $\tilde{A}_k, \tilde{B}_k$  can now be determined from the initial conditions only. The solution generated by the modification described above will be valid for the case of  $t_f \rightarrow \infty$ . Note that formally such a solution will have  $2n_m \times n_a$  independent functions, which equals the number of independent components of the gain matrix in Eq. (6.3).

One way of calculating the gains from the Eq. (6.3) would be to substitute the solution functions to both sides of this equations and compare terms at similar functions, which is somewhat cumbersome. A numerically simpler method is to use the solution for the modes and actuator forces in at least  $2n_m \times n_a$  time instances (test points) to form  $2n_m \times n_a$  equations to solve. This method is explained in detail on the examples next.

### 6.2.1 Example 1: Suspension system

The suspension system problem presented in section 5.3.2 become time invariant if  $t_f \rightarrow \infty$  is set in the performance index, that is

$$J = \frac{1}{2} \int_0^{\infty} (\eta^T \hat{Q}_d \eta + \dot{\eta}^T \hat{Q}_v \dot{\eta} + u^T \hat{R} u) dt \rightarrow \text{Minimize} \quad (6.5)$$

The initial boundary conditions are the same as before

$$x_1(0) = 10mm, \quad x_2(0) = 50mm, \quad \dot{x}_1(0) = 0, \quad \dot{x}_2(0) = 0$$

while the final boundary conditions are

$$x_1(\infty) = 0, \quad x_2(\infty) = 0, \quad \dot{x}_1(\infty) = 0, \quad \dot{x}_2(\infty) = 0$$

All the other parameters are the same as in section 5.3.2.

As solved in chapter V, the  $\eta_1$  and  $\eta_2$  are obtained in the form

$$\begin{aligned} \eta_1 = & e^{\alpha_2 t} [A_1 \cos(\beta_2 t) + A_2 \sin(\beta_2 t)] + e^{-\alpha_2 t} [A_3 \cos(\beta_2 t) + A_4 \sin(\beta_2 t)] \\ & + e^{\alpha_1 t} [A_5 \cos(\beta_1 t) + A_6 \sin(\beta_1 t)] + e^{-\alpha_1 t} [A_7 \cos(\beta_1 t) + A_8 \sin(\beta_1 t)] \end{aligned} \quad (6.6)$$

$$\begin{aligned} \eta_2 = & e^{\alpha_2 t} [B_1 \cos(\beta_2 t) + B_2 \sin(\beta_2 t)] + e^{-\alpha_2 t} [B_3 \cos(\beta_2 t) + B_4 \sin(\beta_2 t)] \\ & + e^{\alpha_1 t} [B_5 \cos(\beta_1 t) + B_6 \sin(\beta_1 t)] + e^{-\alpha_1 t} [B_7 \cos(\beta_1 t) + B_8 \sin(\beta_1 t)] \end{aligned} \quad (6.7)$$

where  $\alpha$  and  $\beta$  are given by Eq. (5.48-a).

The steps of generating optimal solutions for  $t_f \rightarrow \infty$  using the flowchart in Fig. 5.1 are explained first. All the constants by the increasing functions are set to zero, that is  $A_1 = A_2 = A_5 = A_6 = 0$  and  $B_1 = B_2 = B_5 = B_6 = 0$  in order to satisfy the boundary conditions at  $t_f \rightarrow \infty$ . It leaves only eight other constants to calculate from four initial boundary conditions and four equations obtained by grouping similar terms in Eq. (5.47-c), rewritten below.

$$g_1(\ddot{\eta}_1 + \omega_1^2 \eta_1) + g_2(\ddot{\eta}_2 + \omega_2^2 \eta_2) = 0$$

The new integration constants are

$$\begin{aligned} A_3 &= -0.002451673 & B_3 &= 0.364448 \times 10^{-2} \\ A_4 &= -0.268617 \times 10^{-3} & B_4 &= 0.0123056 \\ A_7 &= 0.712185 & B_7 &= 0.0132690 \end{aligned} \quad (6.8)$$

$$A_8 = 0.418277$$

$$B_8 = -0.065358$$

It can be noted that these values are very close to those obtained in section 5.3.2. The difference is that, in the previous case the constants  $A_1, A_2, A_5, A_6$  and  $B_1, B_2, B_5, B_6$  were very small, but now all these constants are exactly zero.

The actuator force is plotted in Fig 6.1. The plot is visually indistinguishable from the plot (5.4-c). The points indicate various time instances used for calculating gains.

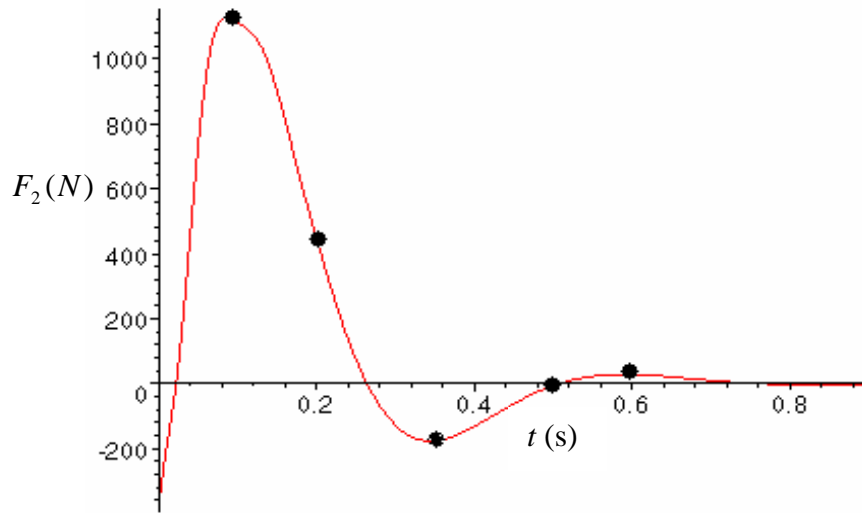


**Figure 6.1:** Actuator force plot indicating various time instances selected

For this case, Eq. (6.2) can be written as

$$F_2 = -[G_1 \quad G_2 \quad G_3 \quad G_4] \begin{bmatrix} \eta_1 \\ \dot{\eta}_1 \\ \eta_2 \\ \dot{\eta}_2 \end{bmatrix} \quad (6.9)$$

Eq. (6.9) can be solved for gains by substituting values of  $F_2$ ,  $\eta$ 's and  $\dot{\eta}$ 's for four different time instances selected randomly as indicated in Fig. 6.1. All these values are available from the *MAPLE* program with sixteen digits accuracy. For testing purposes, five different times (test points) are selected randomly and the corresponding values are listed in the table below.

SR.	$t$	$F_2$	$\eta_1$	$\dot{\eta}_1$	$\eta_2$	$\dot{\eta}_2$
1	0.1	1196.05158	0.3012712	-5.551997	0.0257316	-0.219607
2	0.2	464.85082	-0.0748636	-1.607054	0.0107910	-0.182946
3	0.35	-176.83143	-0.0429322	0.855884	-0.0042958	0.005366
4	0.5	-9.644264	0.0172252	-0.023326	-0.0001871	0.021118
5	0.6	27.446471	0.0060576	-0.130806	0.0006648	-0.001331

**Table 6.1:** Values of force and  $\eta$ 's for different times

It occurs that solving any four of the above five sets give the values of gains as follows

$$G_1 = 683.2957, G_2 = 275.11804, G_3 = 7154.0438, G_4 = 266.56303$$

with seven digits accuracy. The gains remain the same for the system regardless of any four test points selected from the Table 6.1. It assures that all the points are acceptable and the calculated gains are correct (the issue to be discussed next). It should be noted that Eq. (6.9) represents a system's trajectory that must be on a hyperplane in 5-D space with  $\eta_1, \dot{\eta}_1, \eta_2, \dot{\eta}_2$  and  $F_2$  as the dimensions. In order to visualize this trajectory in 3-D space, the Eq. (6.9) can be written in the following form

$$\hat{F}_2 = F_2 + G_3\eta_2 + G_4\dot{\eta}_2 = -G_1\eta_1 - G_2\dot{\eta}_1$$

The plot of  $\hat{F}_2$  in terms of  $\eta_1$  and  $\dot{\eta}_1$  is presented in Fig. 6.2.

A line representing  $\hat{F}_2(t)$  as a function of  $\eta_1(t)$  and  $\dot{\eta}_1(t)$  is referred to as a modal trajectory. Such a line will generally have the spiral shape converging to the origin as shown in Fig. 6.2. According to Eq. (6.2) the modal trajectory must be completely flat and entirely on a certain plane  $S$ . The gains  $G_1$  and  $G_2$  can be obtained from the orientation of  $S$  in the coordinates  $\eta_i, \dot{\eta}_i$  and  $\hat{F}_2$ . Note that in order to obtain the plane  $S$  in 3-D space, only two test points ( $t=0.1$  and  $t=0.2$  for example) are needed (the third point is always at the origin). Therefore in 5-D space considered in the example, only four points were sufficient to determine a hyperplane  $S$ .

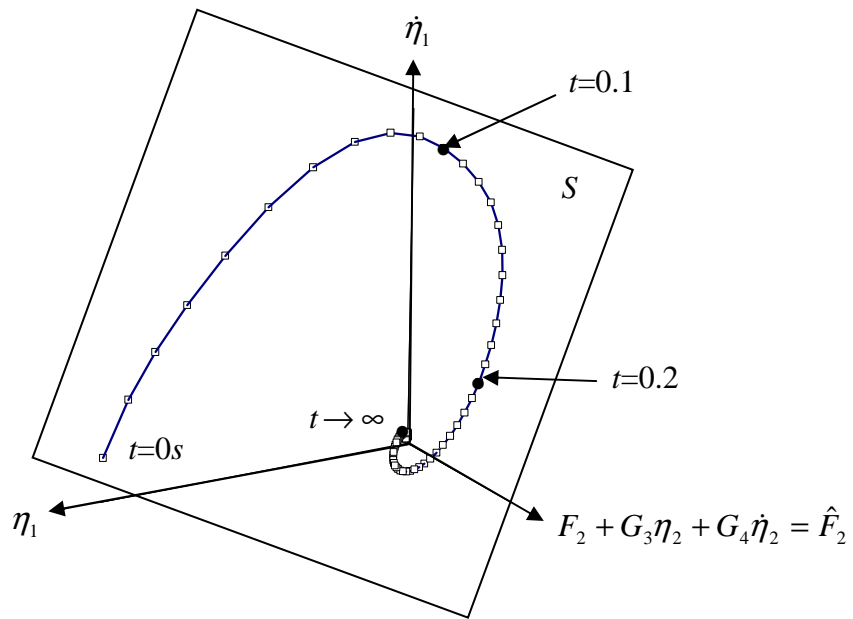


**Figure 6.2:** Modal trajectory

In general the problem of determining the gains from Eq. (6.9) is purely geometrical. The time instances must be selected in such a pattern that the calculated points define a hyperplane. Therefore a pattern with *spread* test points indicated in Fig. 6.3-*a* should give good results, while the pattern indicated in Fig. 6.3-*b* with the points concentrated about a hyperline might not be acceptable. This problem is addressed in detail in the next section.

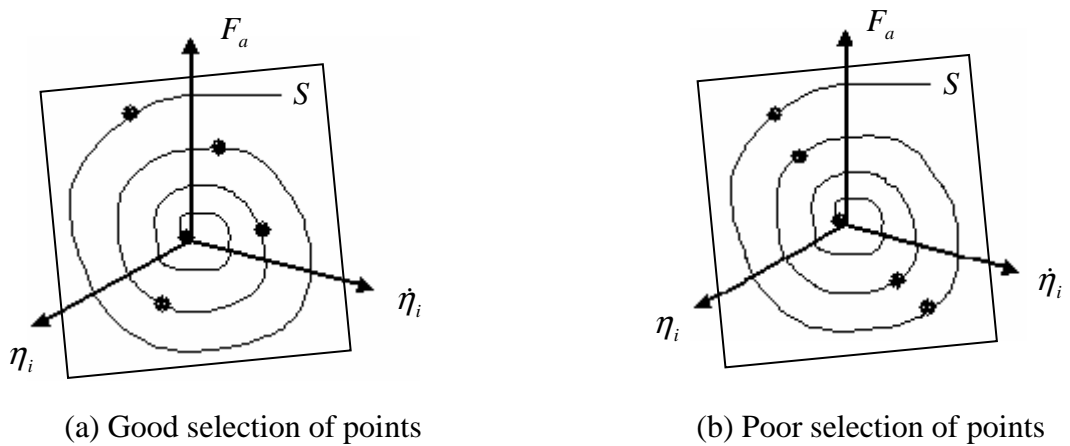


**Figure 6.3:** Selection of points on hyperplane  $S$

Another problem arises when the values of  $\hat{F}_2$ ,  $\eta_i$  and  $\dot{\eta}_i$  are not calculated *exactly* as it would be the case if the results for  $t_f = 2$  obtained in section 5.3.2 were used instead of the results for  $t_f \rightarrow \infty$  (as already mentioned, the lines representing these two solutions are indistinguishable on the graphs). Then the selected test points will not be exactly on the hyperplane. This problem is also addressed in the next section.

### 6.2.2 Example 2: Pendulum

The pendulum problem defined in section (5.4.2) is solved for  $t_f \rightarrow \infty$  using the same procedure as in example 1. The optimal torque is plotted in Fig. 6.4.

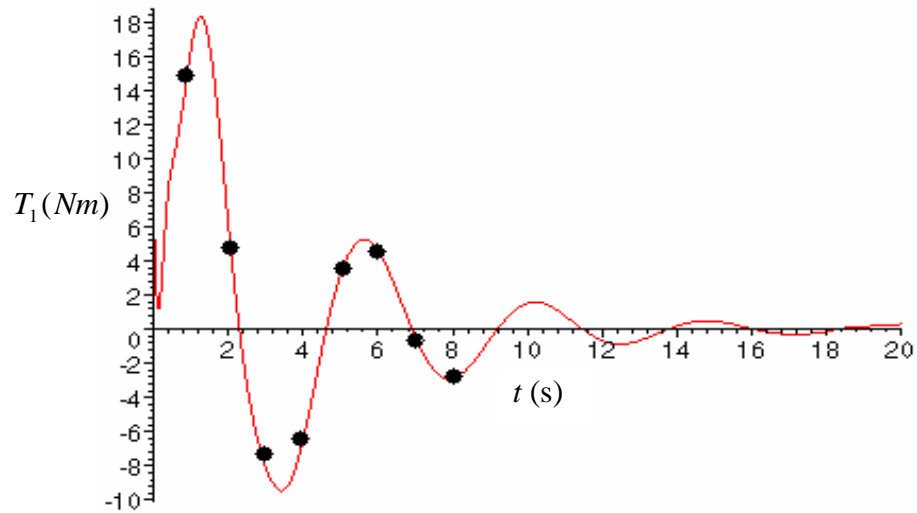


**Figure 6.4:** Actuator torque plot indicating various time instances selected

The plot is similar to the one presented in Fig. 5.10-c for  $t_f = 20s$ . The gains are calculated for this case from following equation

$$T_1 = -[G_1 \quad G_2 \quad G_3 \quad G_4 \quad G_5 \quad G_6] \begin{bmatrix} \eta_1 \\ \dot{\eta}_1 \\ \eta_2 \\ \dot{\eta}_2 \\ \eta_3 \\ \dot{\eta}_3 \end{bmatrix} \quad (6.10)$$

Several time instances are selected randomly as indicated in Fig. 6.4 to solve the Eq. (6.10) to obtain  $G$ 's. The corresponding values of the variables involved are tabulated in Table 6.2.

CASE	$t(s)$	$T_1(Nm)$	$\eta_1$	$\eta_2$	$\eta_3$	$\dot{\eta}_1$	$\dot{\eta}_2$	$\dot{\eta}_3$
1	1	16.37910	0.629546	0.41662	0.1873	-2.45506	0.1347	0.17212
2	2	6.228144	-1.1403	0.06426	0.0674	-0.64579	-0.2973	-0.270
3	3	-8.13662	-0.69937	-0.15225	-0.0916	1.214807	-0.1738	-0.0685
4	4	-6.53243	0.46522	-0.11067	-0.0737	0.755111	0.2045	0.1076
5	5	3.227427	0.547128	0.06221	0.0370	-0.49696	0.1110	0.0726
6	6	4.640630	-0.11186	0.08498	0.0523	-0.59074	-0.0684	-0.0369
7	7	-0.49757	-0.35513	-0.01353	-0.0060	0.119419	-0.0889	-0.057
8	8	-2.87283	-0.03867	-0.053	-0.0324	0.382158	0.0129	0.0062

**Table 6.2:**  $T_1$  and  $\eta$ 's for time instances indicated in Fig 6.4

The gains obtained for set (a):  $t=1, 2, 3, 4, 5, 6$  are

$$\begin{aligned} G_1 &= -2.8152, G_2 = -2.0425, G_3 = 49.7101 \\ G_4 &= 10.6546, G_5 = 10.8365, G_6 = 9.4619 \end{aligned} \quad (6.11-a)$$

However, the gain values for another set (b):  $t= 2, 3, 4, 5, 6, 8$  are

$$\begin{aligned} G_1 &= -2.8173, G_2 = -1.7596, G_3 = 51.1029 \\ G_4 &= 10.8088, G_5 = 10.9829, G_6 = 9.3559 \end{aligned} \quad (6.11-b)$$

It can be noted that the different sets of test points give slightly different values of gains (compare  $G_2$  and  $G_3$  in particular), which means that the points are not selected properly to define the hyperplane  $S$ . The question arises about the accuracy of the above results. This is discussed with the help of condition number in the coming section.

A 3-D modal trajectory plot for set (a), similar to the plot shown in Fig 6.2, is presented in Fig. 6.5. This plot is for illustrative purposes only, the real trajectory is in 7-D space, impossible to visualize.



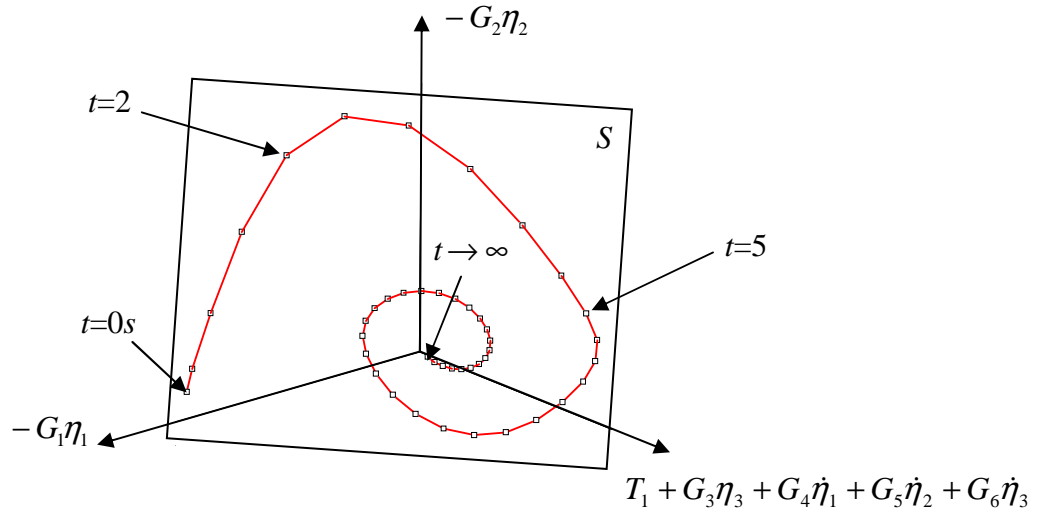


**Figure 6.5:** Modal trajectory

### 6.3 Estimation of errors in calculating gains

An error in calculating gains can be attributed to two sources namely due to a poor selection of test points and due to some inaccuracies in calculating the trajectories. These two error types and the means to evaluate them are briefly discussed below.

#### 6.3.1 Error due to the selection of test points

This error occurs because of the improper selection of the test points as indicated in Fig 6.3-*b*. It is important that these six points (the seventh point is at the origin) should be selected in such a way that they represent a seven dimensional hyperplane  $S$ . Generally, the selection of such points becomes more difficult with the increase of problem dimensionality.

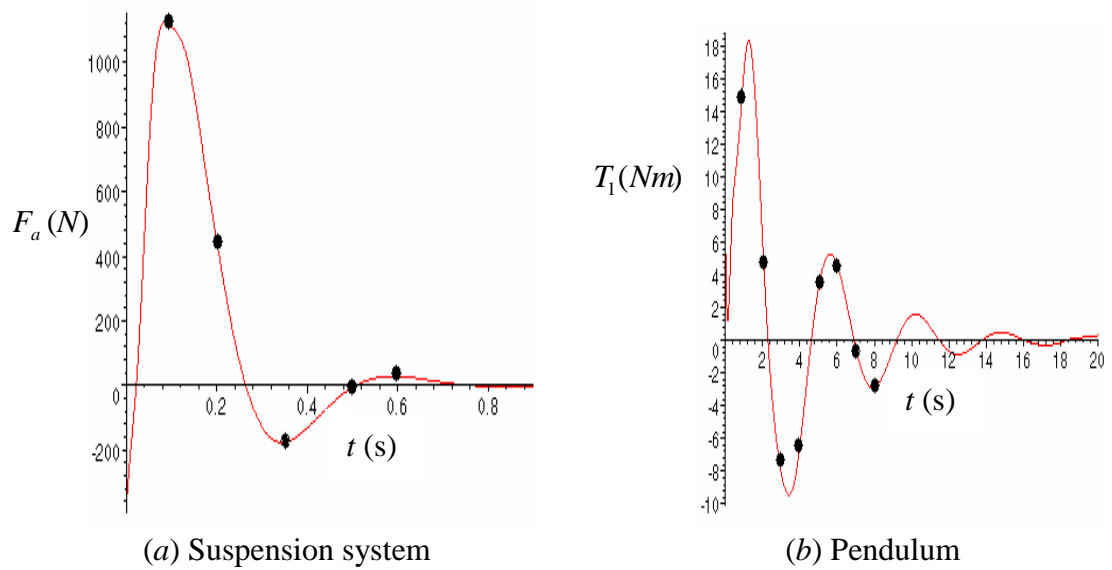


**Figure 6.6:** Force and torque plot

Also, it becomes more difficult when, the number of cycles increases (as in the *Torque* plot shown in Fig 6.6-*b*). The possibility of selected test points to form a hyperline instead of defining a hyperplane increases because there are more revolutions in the gain plot, making it difficult to choose sufficiently separated points to define the hyperplane precisely. It can be seen that the number of cycles in case (*a*) is less than that of case (*b*) resulting in less numerical complications and increased accuracy for case (*a*).

### 6.3.2 Error due to the assumption of a finite time

As mentioned before, the plots representing the pendulum problem for  $t_f = 20s$  and for  $t_f \rightarrow \infty$  are practically indistinguishable. It indicates that sufficiently long finite time may be selected to represent the infinite time case. This makes the use of MAPLE program (refer to flowchart in Fig 5.1) more convenient. The assumption of finite time always incorporates some errors. These errors were less important while calculating the modal gains in the IMSC approach [18] for which the sufficient finite time  $t_f$  values were possible to define in a closed form. However, estimating a sufficient finite time  $t_f$  and the corresponding trajectory errors are more difficult to handle for overdetermined

problems. To illustrate the problem, the case of pendulum which was solved before for infinite time (by substituting the constants corresponding to the positive exponential terms in the solution equal to zero and omitting the final boundary conditions) was solved again by assuming  $t_f = 40s$ . It is found that these two solutions differ marginally (the results change by around  $10^{-5}$ ). The error is not visible in the initial time span (up to around 20s), though can be seen if the plot scale is magnified in the latter stage as shown in Fig. 6.7.

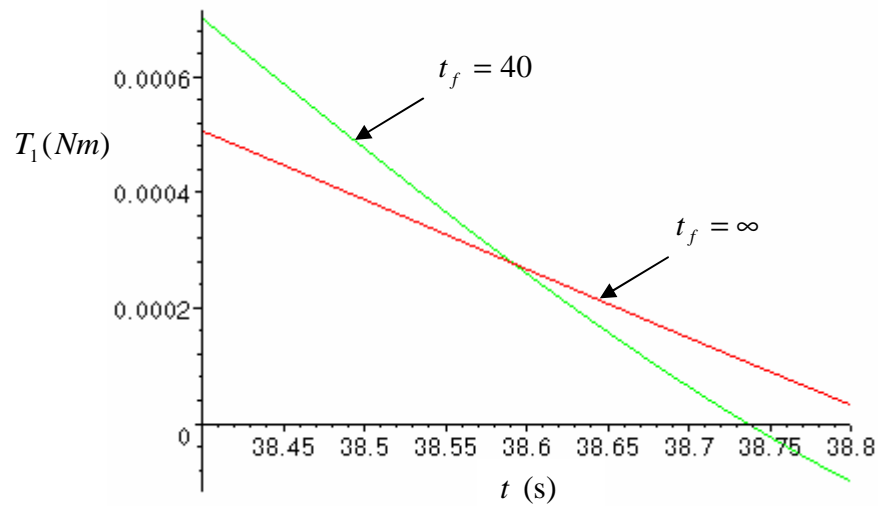


**Figure 6.7:** Magnified torque plots for pendulum

The error shown in Fig. 6.7 indicates that for a finite  $t_f$  the trajectory is not exactly plane and that hyperplane  $S$  does not exist. A deviation from a plane trajectory will be referred to as a trajectory error. Consequently, one can only try to determine a hyperplane  $\bar{S}$  that minimizes this deviation. The orientation of  $\bar{S}$  defines approximate values of the gains.

Both sources of the errors i.e. poor selection of points and trajectory error can be monitored by calculating the condition number, which is discussed next.

### 6.3.3 Condition Number

The errors due to the assumption of finite time can be estimated by inspecting the system's response or eliminated by using a more cumbersome procedure for  $t_f \rightarrow \infty$ . However, the error due to the selection of points is more difficult to control and eliminate. Anyway, in both cases, the condition number helps to select the best solution. The gains are calculated by solving the linear equations in the form  $Ax = b$ . For poor selection of points, matrix  $A$  becomes ill-conditioned (almost singular). For the trajectory error, matrix  $A$  and vector  $b$  contain some errors. The condition number is basically a measure of how ill-conditioned and sensitive to any errors is the problem of finding  $x$  (which represents the gains).

If  $\tilde{x}$  is an approximation to the solution  $x$  of  $Ax = b$ , then the condition number ( $\|A\| \|A^{-1}\|$ ) gives the idea about how close are  $\tilde{x}$  to the  $x$ . Smaller the condition number closer the  $\tilde{x}$  with  $x$  [19]. The condition number also measures the sensitivity of the solution of  $Ax = b$  to the perturbations of  $A$  or  $b$ . As mentioned the values of  $A$  and  $b$  may not be correctly determined if finite time  $t_f$  is used instead of  $t_f \rightarrow \infty$ .

The condition numbers for the cases of Eq. (6.11-*a*) and (6.11-*b*), where  $t_f \rightarrow \infty$ , are  $4.2711 \times 10^7$  and  $1.238 \times 10^9$  respectively, while for the similar cases with  $t_f = 40$  the condition numbers are  $4.32752 \times 10^7$  and  $1.367 \times 10^9$  (sets 1 and 2 in Table 6.3). The condition numbers are slightly bigger for  $t_f = 40$  as compared to  $t_f \rightarrow \infty$  which means that the error is mainly because of the selection of test points. For the pendulum case with  $t_f \rightarrow 40$ , various sets of test points are tried (test times are not tabulated) and the resulting gains along with the condition number are presented in Table 6.3.

Set No	Condition Number	G1	G2	G3	G4	G5	G6	% Error
1	1.36E+09	-2.6351	-25.6161	-66.460	-2.2055	-1.3768	18.2985	1192
2	4.32E+07	-2.8255	-2.35221	48.8038	10.5347	10.7314	9.60809	15.40
3	1.76E+08	-2.6500	-2.29395	40.4923	9.88598	9.99354	9.16999	54.781
4	8.85E+07	-2.8206	-2.20851	49.2219	10.5901	10.7799	9.54019	11.233
5	7.89E+07	-2.8203	-2.19635	49.2595	10.5950	10.7842	9.53455	10.405
6	5.45E+07	-2.8216	-2.03256	50.0712	10.6847	10.8695	9.47337	2.1689
7	4.23E+07	-2.8255	-2.35221	48.8031	10.5347	10.7314	9.60809	20.967
8	2.87E+07	-2.8282	-2.02225	50.4386	10.7154	10.9031	9.4848	4.3648
9	7.38E+05	-2.8153	-2.03959	49.7298	10.6566	10.8385	9.46113	0.2546
10	3.87E+05	-2.8152	-2.04250	49.7101	10.6546	10.8365	9.46190	0.0187
11	2.48E+05	-2.8152	-2.04361	49.7072	10.6542	10.8361	9.46254	0.0521
12	2.44E+05	-2.8152	-2.04360	49.7072	10.6542	10.8361	9.46253	0.0510
13	2.36E+05	-2.8152	-2.04362	49.7082	10.6543	10.836	9.46259	0.0503
14	1.49E+05	-2.8152	-2.04297	49.7090	10.6544	10.8363	9.46223	0.0085
15	1.40E+05	-2.8152	-2.04337	49.7089	10.6543	10.8363	9.46247	0.0335
16	1.30E+05	-2.8152	-2.04341	49.7087	10.6543	10.8363	9.46248	0.0360
17	4.44E+04	-2.8152	-2.04283	49.7091	10.6545	10.8364	9.46215	0

**Table 6.3:** Condition numbers and gains for various time sets

As can be seen, the gain values differ very little if the condition number is smaller than about  $10^6$ . Smallest condition number is 44381 for test times set:  $t = 0, 1, 1.5, 1.7, 2.2, 4$

The errors in the gains in Table 6.3 are obtained by assuming smallest condition number as a zero error case. The plot of error versus condition number is presented in Fig. 6.8.

The graph shows that for the case of pendulum the error increases as the condition number increases. The error remains insignificant if the condition number is smaller than about  $10^6$ . In this case, either the choice of test points or the choice of finite maneuver time  $t_f < \infty$  is acceptable if the condition number is smaller than the above limit. The condition number for the case of suspension system discussed in section 6.2.1 for which the gains obtained were acceptable is  $7.55 \times 10^6$ .

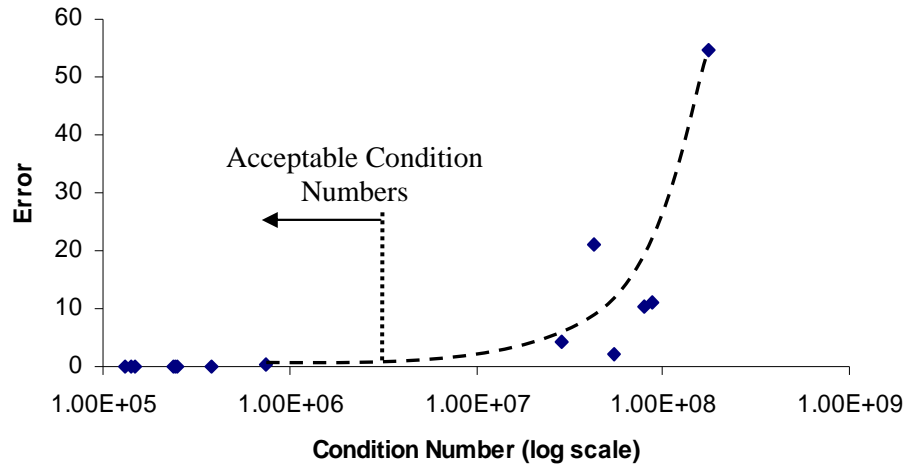


**Figure 6.8:** Error versus condition number plot

As presented, the condition number gives a better idea for selecting the test points to obtain an acceptable solution. The gains values remain almost constant if the condition numbers stay below a certain limit, which can be determined by numerical experimentations.

## 7. CONCLUSIONS AND FUTURE WORK

This thesis focuses on various techniques to solve optimal vibration control problem, in particular it tries to handle overdetermined optimal control problems more efficiently. The parametric optimization technique can theoretically solve any overdetermined problem but is not recommended. This technique is difficult to converge and mostly consumes lot of time. Also, the accuracy of this technique is poor.

The optimality equations technique was found to be more efficient as compared to other techniques. The modal space can be used to simplify the complex problems by converting a large number of DOFs formulation into a corresponding few modes formulation. This technique is efficient for the determined problems (IMSC approach), but it is difficult to apply for the overdetermined problems.

The Beam Analogy (BA), which can solve complicated optimal control cases with high numerical efficiency, applies only to IMSC problems. BA handles the optimality equations technique by constructing analogous differential equations for the static beams and solving these beams by FEM. One independent fictitious analogous FEM beam is created for each mode to control. An attempt has been made to modify BA to solve the overdetermined problems too. As compared to IMSC problems, there are extra constraints in overdetermined problems which couples the modes involved. The idea was to construct analogous fictitious beams which would have those extra constraints built in.

The BA for determined problems solves the optimality equations in the form (Eq. (4.9))

$$\hat{R}\ddot{\eta} + (2\Omega\hat{R} - \hat{Q}_v - \hat{R}\Delta^2)\dot{\eta} + (\hat{R}\Omega^2 + \hat{Q}_d)\eta = 0 \quad (7.1)$$

The optimality equations for overdetermined problems has the form (Eq. 5.55)

$$\hat{R}\ddot{\eta} + (2\Omega\hat{R} - \hat{Q}_v - \hat{R}\Delta^2)\dot{\eta} + (\hat{R}\Omega^2 + \hat{Q}_d)\eta = (A\ddot{v} - \Delta A\dot{v} + \Omega Av) = \hat{q} \quad (7.2)$$

Eq. (7.1) permit constructing the independent analogous beam solved efficiently by FEM as presented in Chapter IV. Eq. (7.2) could also describe some beams but there should be some fictitious loads  $\hat{q}$  exerted on these beams. Also, the load  $\hat{q}$  introduces some coupling between particular modes. For example, two analogous independent beams were used to solve the IMSC problem of the frame with two actuators shown in Fig. 4.4. If two modes were to be controlled by one actuator only (as in overdetermined problem solved in example 1 and 2 in chapter V) then the two analogous beams would have to be extra loaded and interconnected as illustrated in Fig. 7.1. Such a modified set of fictitious beams would be easily solved by the FEM if  $\hat{q}$  and the property of interconnection were known.

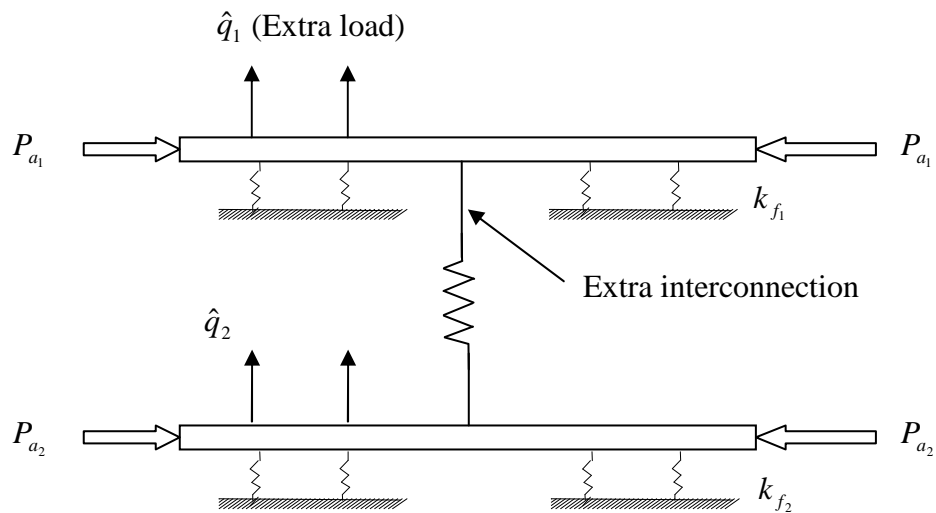


**Figure 7.1:** Conceptual design for solving overdetermined problems by BA

Unfortunately, the attempts to determine workable details of such extra loads and interconnection have not been successful. Work should be done in the future to find these modifications, so that the BA technique could be applied to the overdetermined problems.

In this thesis, the overdetermined problem has been formulated by using time dependant Lagrange multipliers. The extra constraints generated in such problems (the number of which is equal to the difference between the number of modes to control and the number of actuators) are handled by equal number of Lagrange multipliers. This



technique generates high order of differential equations (twelfth order in the cases solved in this thesis), which makes the problem mathematically challenging. The differential operators are used in order to formalize the whole procedure, which makes the problem rather easily solvable by applying the Maple programming. The results obtained are accurate.

It should be noted that solutions to overdetermined or determined problems can be verified by ANSYS software, which can be used to run the dynamic response once the actuator forces are found.

For closed loop control problems the gains are obtained without solving Riccati's equations. By assuming infinite maneuver time ( $t_f \rightarrow \infty$ ), constant gains are derived by setting selected integration constants as zero and then selecting sufficient number of test points on the optimal trajectories. However, it is found that as the number of modes to control increases, the precision of calculating gains decreases. The error in determining gains is addressed with the help of condition number. The limiting magnitude of the condition number to secure sufficient accuracy was determined by numerical experiments. The future work may attempt to determine such a limit analytically, that is based only on the characteristics of the optimal control problem.

## REFERENCES

- [1] Takayoshi, K., Takafumi, F., Takayoshi, H., Takeo, A., Nobuyoshi, M., Satoru, A. and Kohtaro, T., “Active vibration control of frame structures with smart structures using piezoelectric actuators”, *Journal of Smart Material Structures*, 1997, v 6, pp 448-456
- [2] Neelon Crawford, [www.PolarFineArts.com](http://www.PolarFineArts.com), 1999
- [3] Douglas, A. S., Fred, C. G., McGonegal, R. J., Gemini instrumentation program overview, *SPIE Proceedings*, 1997, v 2871, pp 1070-1081
- [4] <http://www.astrosurf.com/astrospace/satellitesartificiels.htm>
- [5] Jassemi-Zargani, R., Simard, J. F., Blacow, R. G. , Waechter, D. F. and Prasad, S. E., “Utilization of smart structures in enhanced satellites”, *Second CanSmart Workshop*, St-Hubert, Quebec, Canada, 1999, pp 157-167
- [6] Canfield, R. A. and Meirovitch, L., “Integrated structural design and vibration suppression using independent modal space control”, *AIAA Journal*, 1994, v 32/10, pp 2053-2060
- [7] Karihaloo, B. L. and Parbery, R. D., “Optimal control of a dynamic system representing a gantry crane”, *Journal of Optimization Theory and Applications*, 1982, v 36(3), pp 409-417
- [8] Rao, S. S., “Mechanical vibrations”, Addison-Wesley Publishing Company, 1986
- [9] Pinch, E. R., “Optimal control and the calculus of variables”, Oxford University Press, 1993, Oxford
- [10] Tadjbaksh, I. G. and Su, Y.A., “Optimal coupled-modal control of distributed parameter systems with discrete actuators”, *ASME Journal of Applied Mechanics*, 1989, v 56, pp941-946
- [11] Szyszkowski, W. and Grewal, I. S., “Optimal vibration control of continuous structures by FEM: Part I – the optimality equations”, *Journal of Communications in Numerical Methods in Engineering*, 2002, v 18, pp 861-868
- [12] Hetenyi, M., “Beams on elastic foundation”, The University of Michigan Press, Ninth printing, 1971

- [13] Grewal, I. S., "Beam analogy for optimal vibration control of linear dynamic systems by FEM", Thesis, 2000, Mechanical Engineering, University of Saskatchewan
- [14] Baweja, M., "The finite element simulation of active vibration attenuation in structures", Thesis, 2004, Mechanical Engineering, University of Saskatchewan
- [15] Baumal, A.E., McPhee, J.J., and Calamai, P.H., "Application of genetic algorithms to the optimization of an active vehicle suspension design", *Journal of Computer Methods in Applied Mechanics and Engineering*, 1998, v 163, pp.87-94
- [16] Polyanin, A. D., Zaitsev, V. F., "Handbook of exact solutions for ordinary differential equations", Chapman and Hall//CRC publication, Third Edition, 2003
- [17] Breakwell, J. A., "Optimal feedback slewing of flexible spacecraft", *Journal of Guidance and Control*, 1981, v 4/5, pp 472-479
- [18] Szyszkowski, W., Baweja, M., "Optimal gains for active vibration control by the beam analogy", *Journal of Computational Mechanics*, 2004, v 34, pp 15-26
- [19] Golub and Loan, V., "Matrix Computations", Johns Hopkins University Press, Third edition, 1996
- [20] Arora, J. S., "Introduction to optimum design", McGraw-Hill Book Company, International Edition, 1989
- [21] Hetenyi, M., "Beams on elastic foundation", The University of Michigan Press, Ninth printing, 1971
- [22] Haftka, R. T. and Gurdal, Z., "Elements of Structural optimization", Kluwer Academic Publishers, Third Edition, 1992
- [23] He, Y., McPhee, J., "Design optimization of rail vehicles with passive and active suspensions: A combined approach using genetic algorithms and multibody dynamics", *Vehicle Systems Dynamics Supplement*, 2002, v 37, pp 397-408
- [24] Beards, C. F., "Vibrations and Control Systems", Ellis Horwood Series in Mechanical Engineering, 1988

## APPENDIX A: MAPLE PROGRAM

Maple program codes to solve suspension system problem defined in Section 5.3.2 are presented below

```

> # Maple program for Suspension System (Solution by Lagrange
Multipliers)
>
> restart;
> w1:=12.94105; w2:=83.040527; g1:=1; g2:= -0.37089;
>
> # Substituting above values, roots of E (refer Eq. 5.39) are
obtained as follows
> eq1:=
.9664107135e-3*D^8+12.51434472*D^6+55131.83018*D^4+11823909.10*D^2
+2577686986.=0;
eq1 := .0009664107135 D8 + 12.51434472 D6 + 55131.83018 D4 + .1182390910 108 D2
+ .2577686986 1010 = 0
> solve( { eq1}, {D} );
{D = -22.35445833 + 82.86993856 I}, {D = 22.35445833 - 82.86993856 I},
{D = -22.35445833 - 82.86993856 I}, {D = 22.35445833 + 82.86993856 I},
{D = -7.574228032 + 12.81855288 I}, {D = 7.574228032 - 12.81855288 I},
{D = -7.574228032 - 12.81855288 I}, {D = 7.574228032 + 12.81855288 I}
>
> # Let P1:=22.35445834; P2:=82.86993855; P3:=7.574228031;
P4:=12.81855288;
> # eta1, eta2, v can be written using Eq. (5.49) in the following
form

```

**- eta1**

```

> eta1:=exp(P1*t)*(A1*cos(P2*t)+A2*sin(P2*t)) +
exp(-P1*t)*(A3*cos(P2*t)+A4*sin(P2*t)) +
exp(P3*t)*(A5*cos(P4*t)+A6*sin(P4*t)) +
exp(-P3*t)*(A7*cos(P4*t)+A8*sin(P4*t));
η1 := e(P1 t) (A1 cos(P2 t) + A2 sin(P2 t)) + e(-P1 t) (A3 cos(P2 t) + A4 sin(P2 t))
+ e(P3 t) (A5 cos(P4 t) + A6 sin(P4 t)) + e(-P3 t) (A7 cos(P4 t) + A8 sin(P4 t))
>
> # Differentiation can be done easily by following commands (e.g.
eta1)

```

**- eta11**

```

> f := t -> exp(P1*t)*(A1*cos(P2*t)+A2*sin(P2*t)) +
exp(-P1*t)*(A3*cos(P2*t)+A4*sin(P2*t)) +
exp(P3*t)*(A5*cos(P4*t)+A6*sin(P4*t)) +
exp(-P3*t)*(A7*cos(P4*t)+A8*sin(P4*t));

```

```

f:=t -> e^(P1 t) (A1 cos(P2 t) + A2 sin(P2 t)) + e^(-P1 t) (A3 cos(P2 t) + A4 sin(P2 t))
      + e^(P3 t) (A5 cos(P4 t) + A6 sin(P4 t)) + e^(-P3 t) (A7 cos(P4 t) + A8 sin(P4 t))
> Diff( f(t), t );
∂
  (e^(P1 t) (A1 cos(P2 t) + A2 sin(P2 t)) + e^(-P1 t) (A3 cos(P2 t) + A4 sin(P2 t))
  + e^(P3 t) (A5 cos(P4 t) + A6 sin(P4 t)) + e^(-P3 t) (A7 cos(P4 t) + A8 sin(P4 t)))
> etal1 := value(%);
f_prime := P1 e^(P1 t) (A1 cos(P2 t) + A2 sin(P2 t))
          + e^(P1 t) (-A1 sin(P2 t) P2 + A2 cos(P2 t) P2) - P1 e^(-P1 t) (A3 cos(P2 t) + A4 sin(P2 t))
          + e^(-P1 t) (-A3 sin(P2 t) P2 + A4 cos(P2 t) P2) + P3 e^(P3 t) (A5 cos(P4 t) + A6 sin(P4 t))
          + e^(P3 t) (-A5 sin(P4 t) P4 + A6 cos(P4 t) P4) - P3 e^(-P3 t) (A7 cos(P4 t) + A8 sin(P4 t))
          + e^(-P3 t) (-A7 sin(P4 t) P4 + A8 cos(P4 t) P4)

```

>

> # Second and fourth derivatives of etal1, etal2, v are obtained using above command

> # Second derivative of etal1:

```

η12 := (P1^2 e^(P1 t) A2 - P1 e^(P1 t) A1 P2 + P1^2 e^(-P1 t) A4 + P1 e^(-P1 t) A3 P2
        - (P1 e^(P1 t) A1 + e^(P1 t) A2 P2 - P1 e^(-P1 t) A3 + e^(-P1 t) A4 P2) P2) sin(P2 t) + (
        - (e^(-P3 t) A8 P4 + P3 e^(P3 t) A5 + e^(P3 t) A6 P4 - P3 e^(-P3 t) A7) P4 + P3 e^(-P3 t) A7 P4
        + P3^2 e^(P3 t) A6 - P3 e^(P3 t) A5 P4 + P3^2 e^(-P3 t) A8) sin(P4 t) + P1^2 e^(P1 t) A1 + P1 e^(P1 t) A2 P2
        + P1^2 e^(-P1 t) A3 - P1 e^(-P1 t) A4 P2
        + (P1 e^(P1 t) A2 - e^(P1 t) A1 P2 - P1 e^(-P1 t) A4 - e^(-P1 t) A3 P2) P2 cos(P2 t) + (-P3 e^(-P3 t) A8 P4
        + P3^2 e^(P3 t) A5 + P3 e^(P3 t) A6 P4 + P3^2 e^(-P3 t) A7
        + (-e^(-P3 t) A7 P4 + P3 e^(P3 t) A6 - e^(P3 t) A5 P4 - P3 e^(-P3 t) A8) P4) cos(P4 t)

```

> # Fourth derivative of etal1

## - etal4

```

> η14 := (P1^4 e^(P1 t) A1 + P1^3 e^(P1 t) A2 P2 + P1^4 e^(-P1 t) A3 - P1^3 e^(-P1 t) A4 P2
          + (P1^3 e^(P1 t) A2 - P1^2 e^(P1 t) A1 P2 - P1^3 e^(-P1 t) A4 - P1^2 e^(-P1 t) A3 P2) P2 + (P1^3 e^(P1 t) A2
          - P1^2 e^(P1 t) A1 P2 - P1^3 e^(-P1 t) A4 - P1^2 e^(-P1 t) A3 P2
          - (P1^2 e^(P1 t) A1 + P1 e^(P1 t) A2 P2 + P1^2 e^(-P1 t) A3 - P1 e^(-P1 t) A4 P2) P2) P2 + (
          P1^3 e^(P1 t) A2 - P1^2 e^(P1 t) A1 P2 - P1^3 e^(-P1 t) A4 - P1^2 e^(-P1 t) A3 P2
          - (P1^2 e^(P1 t) A1 + P1 e^(P1 t) A2 P2 + P1^2 e^(-P1 t) A3 - P1 e^(-P1 t) A4 P2) P2 - (P1^2 e^(P1 t) A1
          + P1 e^(P1 t) A2 P2 + P1^2 e^(-P1 t) A3 - P1 e^(-P1 t) A4 P2
          + (P1 e^(P1 t) A2 - e^(P1 t) A1 P2 - P1 e^(-P1 t) A4 - e^(-P1 t) A3 P2) P2) P2) cos(P2 t) + ((
          - (-P3 e^(-P3 t) A8 P4 + P3^2 e^(P3 t) A5 + P3 e^(P3 t) A6 P4 + P3^2 e^(-P3 t) A7) P4 - P3^2 e^(-P3 t) A7 P4
          + P3^3 e^(P3 t) A6 - P3^2 e^(P3 t) A5 P4 - P3^3 e^(-P3 t) A8) P4 - P3^3 e^(-P3 t) A8 P4 + P3^4 e^(P3 t) A5
          + P3^3 e^(P3 t) A6 P4 + P3^4 e^(-P3 t) A7

```

$$\begin{aligned}
& + (-P3^2 e^{(-P3 t)} A7 P4 + P3^3 e^{(P3 t)} A6 - P3^2 e^{(P3 t)} A5 P4 - P3^3 e^{(-P3 t)} A8) P4 + ( \\
& - (-P3 e^{(-P3 t)} A8 P4 + P3^2 e^{(P3 t)} A5 + P3 e^{(P3 t)} A6 P4 + P3^2 e^{(-P3 t)} A7) P4 - P3^2 e^{(-P3 t)} A7 P4 \\
& + P3^3 e^{(P3 t)} A6 - P3^2 e^{(P3 t)} A5 P4 - P3^3 e^{(-P3 t)} A8 - (-P3 e^{(-P3 t)} A8 P4 + P3^2 e^{(P3 t)} A5 \\
& + P3 e^{(P3 t)} A6 P4 + P3^2 e^{(-P3 t)} A7 \\
& + (-e^{(-P3 t)} A7 P4 + P3 e^{(P3 t)} A6 - e^{(P3 t)} A5 P4 - P3 e^{(-P3 t)} A8) P4) P4) \cos(P4 t) + ( \\
& P1^4 e^{(P1 t)} A2 - P1^3 e^{(P1 t)} A1 P2 + P1^4 e^{(-P1 t)} A4 + P1^3 e^{(-P1 t)} A3 P2 \\
& - (P1^3 e^{(P1 t)} A1 + P1^2 e^{(P1 t)} A2 P2 - P1^3 e^{(-P1 t)} A3 + P1^2 e^{(-P1 t)} A4 P2) P2 - (P1^3 e^{(P1 t)} A1 \\
& + P1^2 e^{(P1 t)} A2 P2 - P1^3 e^{(-P1 t)} A3 + P1^2 e^{(-P1 t)} A4 P2 \\
& + (P1^2 e^{(P1 t)} A2 - P1 e^{(P1 t)} A1 P2 + P1^2 e^{(-P1 t)} A4 + P1 e^{(-P1 t)} A3 P2) P2) P2 - ( \\
& P1^3 e^{(P1 t)} A1 + P1^2 e^{(P1 t)} A2 P2 - P1^3 e^{(-P1 t)} A3 + P1^2 e^{(-P1 t)} A4 P2 \\
& + (P1^2 e^{(P1 t)} A2 - P1 e^{(P1 t)} A1 P2 + P1^2 e^{(-P1 t)} A4 + P1 e^{(-P1 t)} A3 P2) P2 + (P1^2 e^{(P1 t)} A2 \\
& - P1 e^{(P1 t)} A1 P2 + P1^2 e^{(-P1 t)} A4 + P1 e^{(-P1 t)} A3 P2 \\
& - (P1 e^{(P1 t)} A1 + e^{(P1 t)} A2 P2 - P1 e^{(-P1 t)} A3 + e^{(-P1 t)} A4 P2) P2) P2) \sin(P2 t) + (-(( \\
& - (e^{(-P3 t)} A8 P4 + P3 e^{(P3 t)} A5 + e^{(P3 t)} A6 P4 - P3 e^{(-P3 t)} A7) P4 + P3 e^{(-P3 t)} A7 P4 \\
& + P3^2 e^{(P3 t)} A6 - P3 e^{(P3 t)} A5 P4 + P3^2 e^{(-P3 t)} A8) P4 + P3^2 e^{(-P3 t)} A8 P4 + P3^3 e^{(P3 t)} A5 \\
& + P3^2 e^{(P3 t)} A6 P4 - P3^3 e^{(-P3 t)} A7 \\
& + (P3 e^{(-P3 t)} A7 P4 + P3^2 e^{(P3 t)} A6 - P3 e^{(P3 t)} A5 P4 + P3^2 e^{(-P3 t)} A8) P4) P4 \\
& - (P3^2 e^{(-P3 t)} A8 P4 + P3^3 e^{(P3 t)} A5 + P3^2 e^{(P3 t)} A6 P4 - P3^3 e^{(-P3 t)} A7) P4 \\
& + P3^3 e^{(-P3 t)} A7 P4 + P3^4 e^{(P3 t)} A6 - P3^3 e^{(P3 t)} A5 P4 + P3^4 e^{(-P3 t)} A8 - (P3^2 e^{(-P3 t)} A8 P4 \\
& + P3^3 e^{(P3 t)} A5 + P3^2 e^{(P3 t)} A6 P4 - P3^3 e^{(-P3 t)} A7 \\
& + (P3 e^{(-P3 t)} A7 P4 + P3^2 e^{(P3 t)} A6 - P3 e^{(P3 t)} A5 P4 + P3^2 e^{(-P3 t)} A8) P4) P4) \sin(P4 t)
\end{aligned}$$

```

>
> # Equation (5.47-a) can be written as
> eq100:= (1/w1^2)*eta14 + eta12 + 2*w1^2*eta1 = v2 + w1^2*v;
>
> # Following command allows to collect the similar terms of the
> above equation
> collect(eq100,exp(-P3*t));

```



```

>
> # Modifying above command with 'exp(P3*t)' and then by
> 'exp(+/-P1*t)' four equations can be obtained. Again same command
> (with sin(P2*t), cos(P2*t), sin(P4*t) and cos(P4*t)) is used for
> these four equations. In all 16 equations can be obtained from
> (5.47-a,b,c)
>
> # Boundary Conditions gives remaining 8 equations (for example
> eta1(0) is shown)
> #IBC
> t:=0;

```

## - etal(0)

```
> etal:=exp(P1*t)*(A1*cos(P2*t)+A2*sin(P2*t)) +  
exp(-P1*t)*(A3*cos(P2*t)+A4*sin(P2*t)) +  
exp(P3*t)*(A5*cos(P4*t)+A6*sin(P4*t)) +  
exp(-P3*t)*(A7*cos(P4*t)+A8*sin(P4*t)) = 0.709734;
```

$$\eta_1 := A1 + A3 + A5 + A7 = .709734$$

```
>
```

```
> # The equations are solved simultaneously to obtain the  
integration constants
```

## - solve

```
> solve( { eq12, eq22,eq32, eq42,eq52, eq62,eq72, eq82,eq13,  
eq23,eq33, eq43,eq53, eq63,eq73, eq83},  
{A1,A2,A3,A4,A5,A6,A7,A8, B1,B2,B3,B4,B5,B6,B7,B8} );
```

```
{B5 = -.5486532439 10-15, A1 = .1356215634 10-27, A2 = .7172285038 10-28,  
B8 = -.06535815634, A4 = -.0002686174641, A3 = -.002451673850, B6 = -.7474072826 10-14,  
B7 = .01326901521, A7 = .7121856739, B2 = .5064939884 10-27, B4 = .01230566876,  
B3 = .003644484794, A8 = .4182774153, B1 = -.6170973743 10-27, A5 = -.8533845802 10-13,  
A6 = .3648544695 10-13}
```

```
>
```

```
> # Substituting back all these constants gives equations for etal  
and eta2.
```

```
>
```

```
> etal:=exp(P1*t)*(A1*cos(P2*t)+A2*sin(P2*t)) +  
exp(-P1*t)*(A3*cos(P2*t)+A4*sin(P2*t)) +  
exp(P3*t)*(A5*cos(P4*t)+A6*sin(P4*t)) +  
exp(-P3*t)*(A7*cos(P4*t)+A8*sin(P4*t));
```

```
 $\eta_1 :=$ 
```

$$e^{(-22.35445834 t)} (-.002451673850 \cos(82.86993855 t) - .0002686174641 \sin(82.86993855 t)) \\ + e^{(-7.574228031 t)} (.7121856739 \cos(12.81855288 t) + .4182774153 \sin(12.81855288 t))$$

```
>
```

```
eta2:=exp(P1*t)*(B1*cos(P2*t)+B2*sin(P2*t)) +  
exp(-P1*t)*(B3*cos(P2*t)+B4*sin(P2*t)) +  
exp(P3*t)*(B5*cos(P4*t)+B6*sin(P4*t)) +
```

```

exp(-P3*t)*(B7*cos(P4*t)+B8*sin(P4*t));
η2 := e(-22.35445834 t) (.003644484794 cos(82.86993855 t) + .01230566876 sin(82.86993855 t))
      + e(-7.574228031 t) (.01326901521 cos(12.81855288 t) - .06535815634 sin(12.81855288 t))
>
> # Substituting eta1 and eta2 in Eq. (5.26), modal forces are
obtained as
> u1:= eta12 + w1^2*eta1;
u1 := -7.373036598 e(-22.35445834 t) sin(82.86993855 t)
      + 93.55987913 e(-7.574228031 t) sin(12.81855288 t)
      + 16.60677007 e(-22.35445834 t) cos(82.86993855 t)
      - 157.3873170 e(-7.574228031 t) cos(12.81855288 t) + 167.4707751
      e(-22.35445834 t) (-.002451673850 cos(82.86993855 t) - .0002686174641 sin(82.86993855 t)) +
      167.4707751
      e(-7.574228031 t) (.7121856739 cos(12.81855288 t) + .4182774153 sin(12.81855288 t))
> u2:= eta22 + w2^2*eta2;
u2 := -64.85595943 e(-22.35445834 t) sin(82.86993855 t)
      + 9.566411838 e(-7.574228031 t) sin(12.81855288 t)
      - 68.79981629 e(-22.35445834 t) cos(82.86993855 t)
      + 11.27225781 e(-7.574228031 t) cos(12.81855288 t) + 6895.729124
      e(-22.35445834 t) (.003644484794 cos(82.86993855 t) + .01230566876 sin(82.86993855 t)) +
      6895.729124
      e(-7.574228031 t) (.01326901521 cos(12.81855288 t) - .06535815634 sin(12.81855288 t))
>
> # DOFs are obtained from Eq. (2.2)
>
> x1:=0.01033*eta1 + 0.15777*eta2;
x1 := .01033
      e(-22.35445834 t) (-.002451673850 cos(82.86993855 t) - .0002686174641 sin(82.86993855 t))
      + .01033 e(-7.574228031 t) (.7121856739 cos(12.81855288 t) + .4182774153 sin(12.81855288 t))
      + .15777
      e(-22.35445834 t) (.003644484794 cos(82.86993855 t) + .01230566876 sin(82.86993855 t))
      + .15777 e(-7.574228031 t) (.01326901521 cos(12.81855288 t) - .06535815634 sin(12.81855288 t))
> x2:=0.070559*eta1 - 0.00462*eta2;
x2 :=
      .070559 e(-22.35445834 t) (-.002451673850 cos(82.86993855 t) - .0002686174641 sin(82.86993855 t))
      + .070559 e(-7.574228031 t) (.7121856739 cos(12.81855288 t) + .4182774153 sin(12.81855288 t))

```



```

- .00462 e(-22.35445834 t) (.003644484794 cos(82.86993855 t) + .01230566876 sin(82.86993855 t))
- .00462 e(-7.574228031 t) (.01326901521 cos(12.81855288 t) - .06535815634 sin(12.81855288 t))
>
> # Force from Eq. (2.2)
> F:=u1/(-0.01033 + 0.070559);
F := -122.4167195 e(-22.35445834 t) sin(82.86993855 t)
      + 1553.402499 e(-7.574228031 t) sin(12.81855288 t)
      + 275.7271425 e(-22.35445834 t) cos(82.86993855 t)
      - 2613.148433 e(-7.574228031 t) cos(12.81855288 t) + 2780.567086
      e(-22.35445834 t) (-.002451673850 cos(82.86993855 t) - .0002686174641 sin(82.86993855 t)) +
      2780.567086
      e(-7.574228031 t) (.7121856739 cos(12.81855288 t) + .4182774153 sin(12.81855288 t))
>
> # Condition number for matrix A can be calculated by following
comand
> with(linalg):
Warning, new definition for norm
Warning, new definition for trace
>
> A:=array([[-2.202367892, .1200043874, .3899848721e-1, 0, 0, 0],
[-.4652204013, .1106658118, .7372750458e-1, -.7551109287,
-.2045576259, -.1076912991], [.4992283769, -.2783282042,
-.1915691137, 1.879292657, .5060470028, .1623041989],
[.8301209063, -.1790695734, -.1490457534, 1.416989486,
.4661927501, .2525944389], [1.017882645, .9132181482e-1,
.6500686767e-1, -.8700474389, .2164650948, .1104806161],
[1.218607715, -.1327499055e-1, -.1721585754e-1, .1425909564,
.2220704759, .2278514995] 1]);
A :=
[ -2.202367892,      .1200043874,      .03899848721,      0,      0,      0
  -.4652204013, .1106658118, .07372750458, -.7551109287, -.2045576259, -.1076912991
  .4992283769, -.2783282042, -.1915691137, 1.879292657, .5060470028, .1623041989
  .8301209063, -.1790695734, -.1490457534, 1.416989486, .4661927501, .2525944389
  1.017882645, .09132181482, .06500686767, -.8700474389, .2164650948, .1104806161
  1.218607715, -.01327499055, -.01721585754, .1425909564, .2220704759, .2278514995 ]
>
> cond(A, infinity);
51404.40672

```